

# **Investigation of alternative supplementary cementitious materials and a new method to produce them**

Von der Fakultät für Maschinenbau, Verfahrens- und Energietechnik  
der Technischen Universität Bergakademie Freiberg

genehmigte

## **DISSERTATION**

zur Erlangung des akademischen Grades

Doktor-Ingenieur (Dr.-Ing.)

vorgelegt

von Dipl.-Ing. Michael Weihrauch

geboren am 09.09.1969 in Freiberg, Deutschland

Gutachter.: Prof. Dr. Thomas Bier, Technische Universität Bergakademie Freiberg  
Prof. Dr. Alexandros Charitos, Technische Universität Bergakademie Freiberg  
Dr. Peter Kruspan, Holcim AG, Würenlingen/Schweiz (gutachterliche Stellungnahme)

Tag der Verleihung: 04.07.2022

## **Versicherung**

Hiermit versichere ich, dass ich die vorliegende Arbeit ohne unzulässige Hilfe Dritter und ohne Benutzung anderer als der angegebenen Hilfsmittel angefertigt habe; die aus fremden Quellen direkt oder indirekt übernommenen Gedanken sind als solche kenntlich gemacht.

Bei der Auswahl und Auswertung des Materials sowie bei der Herstellung des Manuskripts habe ich Unterstützungsleistungen von folgenden Personen erhalten:

Prof. Dr.-Ing. Thomas A. Bier

Dr. sc. nat. ETH Peter Kruspan

Weitere Personen waren an der Abfassung der vorliegenden Arbeit nicht beteiligt. Die Hilfe eines Promotionsberaters habe ich nicht in Anspruch genommen. Weitere Personen haben von mir keine geldwerten Leistungen für Arbeiten erhalten, die nicht als solche kenntlich gemacht worden sind.

Die Arbeit wurde bisher weder im Inland noch im Ausland in gleicher oder ähnlicher Form einer anderen Prüfungsbehörde vorgelegt.

Wo kämen wir hin,  
wenn alle sagten,  
wo kämen wir hin,  
und keiner ginge,  
um zu sehen,  
wohin man käme,  
wenn man ginge.

Originaltext:

Wo chiente mer hi  
wenn alli seite  
wo chiente mer hi  
und niemer giengti  
fur einisch z'luege  
wohi dass me chiem  
we me gieng.

*Kurt Marti*

*(1921 – 2017), Schweizer Pfarrer, Schriftsteller und Lyriker*

# Acknowledgements

I first thank my employer, **Holcim**, a global leader in innovative and sustainable building solutions. Thank you for the exciting workplace and the opportunity to write and publish this thesis.

I had strong support during the study, and I thank the **Technical University Freiberg** and especially **Prof. Dr. Thomas Bier**, my doctoral supervisor, for fruitful and inspiring discussions and for giving me the opportunity to submit this thesis.

My sincere gratitude is extended to **Dr. Peter Kruspan**, who has opened the world of product design, mineralogy and cement chemistry to me. Thank you so much for our priceless discussions and your valuable support.

Special thanks to **Prof. Dr. Alexandros Charitos**, with whom I had inspiring and motivating exchanges and who shares similar professional interests in carbon-capturing technologies.

I greatly appreciate my supervisor, **Rudy Blum**, and my colleague, **Ernst Bucher**, for their innovative spirit, great feedback, excellent encouragement and guidance.

Thank you to my parents, who consistently taught me the value of education, and especially to my father, **Dr. Fritz Weihrauch**, who motivated me to write this thesis.

Finally, I am extremely grateful to my wife **Katrin**, not only for her valuable input and support in correcting my grammar and spelling but especially for her love and patience shown to me every day of our marriage. My thanks also to my children **Peter, Eric and Lisa**, who are my greatest motivation to maintain the peaceful and beautiful world I used to live in.

## Abstract

The main contributor to CO<sub>2</sub> emissions in the cement industry is cement clinker, which produces CO<sub>2</sub> mainly through the burning of limestone in a kiln at approximately 1'450 °C. The impact of cement on CO<sub>2</sub> emissions was reduced significantly in recent decades by substituting cement clinker with reactive industrial by-products such as fly ash or granulated blast furnace slag. However, due to the closure of coal power plants and steel furnaces, especially in Europe and North America, a substantial source of the so called supplementary cementitious materials (SCMs) will diminish in the next few years and require urgent replacement.

The cement industry is investigating alternatives such as thermally activated kaolinitic clay or metakaolin. However, suitable clay deposits are rare in many regions of the world and their exploitation could be critical for the environment. One aim of this research is thus to investigate locally available materials that can be sourced from various waste streams. Hence, at least one waste material should be selected from aggregate washing sludge. Other waste materials could be road cleaning sludge or deconstruction gypsum. These three waste material streams are currently mostly deposited in quarries or landfills and could therefore be turned into circular economy products. The waste materials are locally available in sufficient quantities. If a suitable mineralogical composition can be achieved, such materials could be thermally activated and could develop the desired hydraulic, latent hydraulic or pozzolanic properties required for the strength development of composite cements. However, because these materials are often contaminated, conventional methods for the thermal activation at temperatures of 700 °C - 850 °C would not be suitable to meet the emission restrictions without additional measures. Therefore, a second aim of this research is the development of a new method to dry, thermally activate and grind critical and partly contaminated materials in an energy-efficient way.

## Table of Contents

<b>List of Tables .....</b>	<b>IX</b>
<b>List of Figures.....</b>	<b>XI</b>
<b>List of Abbreviations .....</b>	<b>XIV</b>
<b>Glossary .....</b>	<b>XVI</b>
<b>Chapter 1: Introduction .....</b>	<b>1</b>
1.1 Motivation.....	3
1.2 Research hypotheses and objectives .....	4
1.3 Research methodology.....	5
1.4 Thesis outline .....	6
<b>Chapter 2: State of the art in SCM production .....</b>	<b>7</b>
2.1 Supplementary cementitious materials .....	7
2.2 Classification of SCMs .....	8
2.2.1 Classification according to origin.....	8
2.2.2 Classification according to reaction behaviour.....	10
2.3 Chemical composition of SCMs .....	16
2.4 Formation of hydraulic or pozzolanic minerals in thermal processes .....	17
2.4.1 Cement clinker.....	17
2.4.2 Burnt oil shale.....	18
2.4.3 Fly ash .....	19
2.4.4 Calcined clay .....	20
2.5 Performance of composite cements .....	23
2.6 Calcining technologies.....	24
2.6.1 Flash calciner.....	25
2.6.2 Rotary calciner.....	27
2.7 Comparison of process technologies.....	28
2.8 Summary of Chapter 2 .....	29
<b>Chapter 3: Alternative SCMs and a new method for activation .....</b>	<b>30</b>
3.1 Introduction.....	30
3.2 Target of alternative SCM.....	31
3.3 Waste materials .....	32
3.3.1 Aggregate washing sludge.....	32
3.3.2 Road cleaning sludge.....	33
3.3.3 Deconstruction gypsum .....	34
3.4 Producing alternative SCMs .....	35
3.5 Thermal activation of alternative SCMs .....	36
3.6 Limitations in current calcining technology .....	37
3.6.1 Difficult emission control .....	37
3.6.1.1 Particulate emission .....	37
3.6.1.2 Gaseous emission .....	37
3.6.2 Challenging material preparation .....	38
3.6.3 Demand for noble fuels .....	39
3.6.4 Difficult colour control.....	40
3.6.5 Strict temperature control .....	41
3.6.6 CO <sub>2</sub> footprint of calciners .....	41
3.7 Proposed new method of calcination .....	42
3.7.1 Feed material handling .....	45
3.7.2 Thermal heat-exchange system .....	45
3.7.3 Clay calciner design.....	47
3.7.4 Grinding.....	48
3.8 Summary Chapter 3 .....	49

<b>Chapter 4: Theoretical Considerations.....</b>	<b>50</b>
4.1 Material considerations .....	50
4.1.1 Composition of alternative SCM .....	50
4.1.2 Anticipated products and characteristics .....	51
4.2 Process considerations .....	53
4.2.1 System capacity .....	54
4.2.2 Material characteristics.....	54
4.2.3 Material receiving, crushing and handling .....	55
4.2.4 Thermodynamic modelling.....	55
4.2.4.1 Mass balance .....	56
4.2.4.2 Drying and cooling heat balance .....	58
4.2.4.3 Calcination heat balance.....	62
4.2.4.4 Gas balance .....	65
4.2.4.5 Impact on clinker kiln line .....	68
4.2.4.6 Impact of calcite on the gas balance.....	69
4.2.5 Calciner design .....	69
4.2.6 Colour control.....	70
4.2.7 Emission prediction.....	72
4.2.7.1 Emission during drying .....	73
4.2.7.2 Emission during calcination .....	73
4.2.8 CO <sub>2</sub> footprint of produced material .....	74
4.2.9 Grinding requirements.....	77
4.3 Summary of Chapter 4 .....	78
<b>Chapter 5: Experimental tests and proof of concept.....</b>	<b>79</b>
5.1 Introduction.....	79
5.2 Sampling and characterization .....	80
5.2.1 Kaolinitic AWS from France.....	80
5.2.2 Non-kaolinitic AWS from Switzerland .....	84
5.2.3 Road cleaning sludges from Switzerland .....	87
5.2.4 Deconstruction gypsum from Switzerland .....	89
5.2.5 Sample preparation and shipping .....	91
5.3 Drying screw conveyor testing .....	93
5.4 Calcination testing.....	97
5.4.1 Mineralogy of activated products .....	100
5.4.1.1 Non-kaolinitic SCM.....	100
5.4.1.2 Kaolinitic AWS from France .....	101
5.4.2 Colour.....	102
5.5 Crushing tests.....	103
5.6 Grinding tests .....	103
5.7 Mortar compressive strength testing .....	109
5.8 Water demand testing.....	109
5.9 Summary of Chapter 5 .....	110
<b>Chapter 6: Experimental results .....</b>	<b>111</b>
6.1 Characteristics of activated materials .....	111
6.2 Concrete performance and colour .....	113
6.2.1 Thermally activated kaolinitic AWS from France.....	113
6.2.2 Thermally activated non-kaolinitic alternative SCM from Switzerland.....	116
6.3 Equipment dimensioning .....	119
6.3.1 Process mass flow.....	119
6.3.2 Heat-exchanging screws and thermal oil system.....	120
6.3.3 Rotary calciner dimensioning.....	123
6.3.4 Ball mill dimensioning .....	124
6.4 CO <sub>2</sub> reduction.....	125
6.5 Summary of Chapter 6 .....	127
<b>Chapter 7: Conclusion and outlook .....</b>	<b>129</b>

---

7.1	Conclusions.....	129
7.2	Outlook.....	131
	<b>Literature.....</b>	<b>134</b>



## List of Tables

Table 2-1:	Typical chemical compositions and reaction behaviour of SCMs and OPC.....	16
Table 2-2:	Influence of SCMs on the performance of concrete mixtures.....	24
Table 2-3:	Selection criteria for available calcining technologies .....	28
Table 3-1:	Net CO <sub>2</sub> emission per t of calcined clay depending on calcining technology (Based on net CO <sub>2</sub> contribution of 96 kg CO <sub>2</sub> /GJ for coal and 0 kg CO <sub>2</sub> /GJ for Biomass) .....	42
Table 4-1:	Maximum allowable clinker replacement in cement according to EN 197-1 .....	52
Table 4-2:	Mechanical and physical requirements given as characteristic values (European Committee for Standardization, 2011, S. 1-38).....	53
Table 4-3:	Heat balance of heat-exchanging circuit, based on a production rate of 15 tph.....	61
Table 4-4:	Heat balance of the calciner circuit based on a production rate of 15 tph and reference temperature of 20 °C .....	63
Table 4-5:	Net CO <sub>2</sub> contribution depending on product (clinker or calcined clay) and the manufacturing method of calcined clay .....	76
Table 4-6:	Impact of material and calcining method on the CO <sub>2</sub> production and potential CO <sub>2</sub> taxes .....	77
Table 5-1:	Moisture of samples from AWS deposit near Rennes, France.....	81
Table 5-2:	Chemical composition of kaolinitic AWS sample, Rennes (France) according to XRF .....	82
Table 5-3:	Mineralogical composition of kaolinitic AWS sample, Rennes (France) according to XRD .....	83
Table 5-4:	Average moisture and density of selected non-kaolinitic AWS samples, Switzerland .....	85
Table 5-5:	Chemical composition of selected non-kaolinitic AWS sample, Switzerland, according to XRF .....	86
Table 5-6:	Mineralogical composition of non-kaolinitic AWS sample, Switzerland, according to XRD.....	86
Table 5-7:	Chemical composition of investigated RCS Switzerland, according to XRF .....	88
Table 5-8:	Environmentally relevant characteristics of investigated RCS .....	89
Table 5-9:	Moisture of investigated RCS .....	89
Table 5-10:	DCG particle size distribution.....	90
Table 5-11:	Material composition of DCG excluding metals.....	90
Table 5-12:	Mineralogical composition of gypsum part of DCG after removal of solid contaminants, according to XRD .....	91
Table 5-13:	Mineralogical composition of mix of AWS, RCS and DCG according to XRD .....	92

---

Table 5-14:	Calculated heat from thermal oil heating system .....	95
Table 5-15:	Heat from thermal oil heating system .....	96
Table 5-16:	Calculation of specific heat transfer area .....	96
Table 5-17:	Technical Parameters of IBU-tec kiln .....	98
Table 5-18:	Mineralogical composition of product of non-kaolinitic SCM sample at different temperatures, according to XRD .....	100
Table 5-19:	Mineralogical composition of product of kaolinitic AWS sample under oxidizing and reducing condition at different temperatures; Rennes, France according to XRD .....	102
Table 5-20:	PSD parameters of grinding trials .....	107
Table 5-21:	Power consumption of the different trials .....	107
Table 6-1:	Selected thermal oil volume of heat-exchanging screws.....	122
Table 6-2:	Design parameters of rotary calciner .....	124
Table 6-3:	Net CO <sub>2</sub> contribution related to materials tested with the new calcining technology .....	126
Table 6-4:	Composition and net CO <sub>2</sub> contribution of the produced cement.....	127

## List of Figures

Figure 1-1:	Global CO <sub>2</sub> emissions from cement production; 95 % confidence interval (Andrew, 2018).....	1
Figure 1-2:	Global average estimate of cement composition (IEA et al., 2018, p. 34).....	2
Figure 2-1:	Classification of SCMs according to their origin .....	8
Figure 2-2:	Classification of OPC and SCMs according to their reaction behaviour .....	11
Figure 2-3:	Zones of SCM and OPC shown in a ternary CAS phase diagram .....	12
Figure 2-4:	Mineralogical changes as a function of temperature during clinker formation .....	18
Figure 2-5:	Scanning electron microscopy (SEM) picture of an oil shale burnt at 750 °C displaying mostly irregular particles (Külaots et al., 2010).....	19
Figure 2-6:	SEM particle characterization of a fly ash with mostly spherical and some angular particles (Faheem et al., 2021) .....	20
Figure 2-7:	Structures and ideal formulas of kaolinite, illite and montmorillonite (adapted from Fernandez, Martirena & Scrivener, 2011) .....	21
Figure 2-8:	Layered structure of kaolinite shown SEM (Wang, Li, Peng & Zhang, 2011).....	21
Figure 2-9:	Simplified illustration of results of derivative thermogravimetry (DTG) mass change analysis during the transformation of kaolinite to metakaolin, spinel and mullite.....	22
Figure 2-10:	Simplified process for flash calcination technology.....	26
Figure 2-11:	Simplified process for rotary calcination technology.....	27
Figure 3-1:	Kaolinite content in soil and main kaolin deposits (Copyright Esri; Esri and the Esri logo are licensed trademarks of Environmental Systems Research Institute, Inc.).....	31
Figure 3-2:	Typical disposal of AWS in ponds (Schmitz, Röhling & Dohrmann, 2011).....	32
Figure 3-3:	Mineralogical composition of 28 AWS samples in Germany (Schmitz, Röhling & Dohrmann, 2011) .....	33
Figure 3-4:	Left: Road cleaning truck (Kanton Luzern, 2013); Right: cleaning of road drainage (Cahans, 2017) .....	34
Figure 3-5:	DCS in a construction waste recycling plant.....	34
Figure 3-6:	Possible mixture to produce an SCM without sufficient kaolinitic clay. Left to right: DCG, AWS, RCS, a mixture of materials .....	36
Figure 3-7:	Tests conducted with different oxygen levels from (left) fully oxidizing to (right) reducing conditions .....	40
Figure 3-8:	Creating a reducing atmosphere during cooling in a rotary calciner (Martirena Hernández et al., 2020) .....	40

Figure 3-9:	Formation of mullite balls due to high burning zone temperature in a rotary calciner .....	41
Figure 3-10:	Simplified model of the integrated SCM calciner .....	43
Figure 3-11:	Simplified flow diagram of heat-exchange system .....	46
Figure 3-12:	Simplified scheme for connecting the integrated calciner system with the cement clinker kiln .....	47
Figure 4-1:	Target area to produce alternative SCM shown in a ternary CAS phase diagram. ....	50
Figure 4-2:	Interaction of hydraulic and pozzolanic reactions.....	51
Figure 4-3:	Simplified process flow diagram and boundary limits of subsystems for 1) drying and cooling and 2) calcination .....	56
Figure 4-4:	Mass balance of drying and calcining process .....	57
Figure 4-5:	Boundary of material drying heat balance.....	60
Figure 4-6:	Boundary of calcination heat and mass balance .....	62
Figure 4-7:	Gas volumes of rotary calciner gases extracted from and returned into the clinker kiln system .....	66
Figure 4-8:	Summary of design parameters of heat-exchanging and calciner system .....	70
Figure 4-9:	Influencing product colour by controlling the oxygen level during calcining and cooling .....	71
Figure 4-10:	Colour control by preventing oxygen intake into the cooling screw .....	72
Figure 4-11:	Emission behaviour of integrated rotary calciner .....	73
Figure 5-1:	Sampling at AWS pond near Rennes, France .....	80
Figure 5-2:	Particle size distribution of AWS deposit near Rennes, France .....	81
Figure 5-3:	TG, DTG and Heat Flow analysis of kaolinitic AWS, Rennes, France .....	84
Figure 5-4:	Images of received AWS sample as delivered .....	85
Figure 5-5:	PSD in tested non-kaolinitic AWS sample from Kirchberg (left) and Bretonnieres (right), Switzerland.....	85
Figure 5-6:	TG analysis of AWS sample from Kirchberg, Switzerland .....	87
Figure 5-7:	Investigated Road Cleaning Sludge.....	88
Figure 5-8:	Receiving and storage of pre-sorted gypsum boards.....	89
Figure 5-9:	left: Mix of AWS, RCS, DCG from Switzerland, Right: Kaolinitic AWS, Rennes, France.....	93
Figure 5-10:	Koelmann testing facility with drying screw.....	93
Figure 5-11:	Schematic picture of Koelmann heat-exchanging screw conveyor (Köllemann, 2020).....	94
Figure 5-12:	Thermal oil temperature progression with EC-2020-06-SYM.....	95
Figure 5-13:	Mixture of AWS, RCS and DCG before (left) and after (right) drying (test EC-2020-06-SYM).....	97

Figure 5-14:	Kaolinitic AWS (SL-2020-06-CH) before (left) and after drying (right).....	97
Figure 5-15:	Flowsheet of IBU-tec kiln testing facility (IBU-tec, 2020).....	99
Figure 5-16:	IBU-tec testing kiln installation (IBU-tec, 2020).....	99
Figure 5-17:	Schematic of mineral sizer.....	103
Figure 5-18:	VDZ grinding installation (VDZ, 2021).....	104
Figure 5-19:	PSD of fresh feed without particles above 4 mm.....	105
Figure 5-20:	View inside the testing ball mill (Trial 1).....	106
Figure 5-21:	PSD of mill and cyclone product with Trial 1 with 40 kg/h feed.....	106
Figure 5-22:	D50 and D90 value in correlation to power input.....	108
Figure 5-23:	Empty mill during pre-trials with air velocities of > 1m/s above the ball filling.....	108
Figure 6-1:	Reaction behaviour of investigated kaolinitic AWS and non-kaolinitic alternative SCM shown in a ternary CAS phase diagram.....	112
Figure 6-2:	2-Day compressive strength of different mortars ( <sup>1</sup> According to EN196-1).....	113
Figure 6-3:	28-Day compressive strength of different mortars ( <sup>1</sup> According to EN196-1).....	114
Figure 6-4:	Mortar spread of different mixtures.....	115
Figure 6-5:	Influencing the product colour by varying the calcination conditions of the kaolinitic AWS sample from Rennes/France (SL-2020-06-CH).....	116
Figure 6-6:	Examples of concrete colour in calcined clay cements. Left, calcination under oxidizing conditions; right, calcination under reducing conditions.....	116
Figure 6-7:	2 Day compressive strength of different mortars ( <sup>1</sup> According to EN196-1).....	117
Figure 6-8:	28 Day compressive strength of different mortars ( <sup>1</sup> According to EN196-1).....	118
Figure 6-9:	Colours of products.....	119
Figure 6-10:	Simplified overall massflow diagram of calcining process.....	120
Figure 6-11:	Critical oil temperature before (left) and after design modification (right) of the cooling screw.....	122
Figure 7-1:	3D view of the pilot installation.....	132

## List of Abbreviations

ASTM	American Society for Testing and Materials. This is an international standards organization
AWS	Aggregate washing sludge
AS	Aluminium silicate (such as metakaolin)
BAF	Bergakademie Freiberg
BAT	Best available techniques
BOS	Burnt oil shale
CA	Monocalcium aluminate
CA2	Dicalcium aluminate
CA3	Tricalcium aluminate
CAD	Computer-aided design
CAS	Ternary phase diagram of CaO-Al <sub>2</sub> O <sub>3</sub> -SiO <sub>2</sub>
CAPEX	Capital expenditure
CEMTECH	Conference event in the global cement sector
CFD	Computational fluid dynamics
CH	Calcium hydroxide
CO <sub>2</sub>	Carbon dioxide
CR	Conversion rate
CSH	Calcium silicate hydrate
CSHA	Calcium silicate hydrate aluminate
C2S	Belite
C3S	Alite
DCG	Deconstruction gypsum
DTG	Derivative thermogravimetry
EN	European Standards. These are technical standards drafted and maintained by the European Committee for Standardization (CEN)
EPFL	École polytechnique fédérale de Lausanne
FA	Fly ash

---

GGBFS	Ground granulated blast furnace slag
IED	European Industrial Emission Directive
ISO	International Organization for Standardization
LC3	Limestone calcined clay cement
LOI	Loss of ignition
OPC	Ordinary portland cement
OPEX	Operational expenditure
PSD	Particle size distribution
RCS	Road cleaning sludge
R&D	Research and development
SCM	Supplementary cementitious materials
SynMic	Synthetic mineral component
TGA	Thermogravimetric analysis
TOC	Total amount of organic carbon
VDZ	Verein Deutscher Zementwerke eV
VOC	Volatile organic compounds
XRD	X-ray diffraction analyser
XRF	X-ray fluorescence analyser

## Glossary

**Aggregate:** Material used in construction, including sand, gravel and crushed stone.

**Alternative fuels:** Products of full or partial biogenic origin or from fossil fuel origin, not classified as a traditional fossil fuel; used as a source of thermal energy.

**Calcination of clay:** Thermal activation of clay minerals at temperatures of 700–850 °C; the aim is to obtain a reactive supplementary cementitious material (SCM)

**Cement:** A building material made by grinding clinker together with various mineral components (e.g. gypsum, limestone, blast furnace slag, coal fly ash and natural volcanic material). Cement acts as a binding agent when mixed with sand, gravel or crushed stone and water to make concrete.

**Cementitious products:** All cements and clinker produced by a cement company. The category excludes clinker purchased from another company and used to make cement.

**Clay:** Fine-grained natural rock or soil with a complex layered aluminosilicate structure. Common types are kaolinite, illite and montmorillonite.

**Clinker:** An intermediate product in cement manufacturing; the main substance in cement. It is formed by calcination of limestone in the kiln and subsequent reactions caused by burning.

**Clinker-to-cement ratio:** Total clinker consumed divided by total amount of cement produced.

**Comminution:** A process in which solid materials are reduced in size by natural or industrial forces, including crushing and grinding; or a process in which useful materials are freed from embedded matrix materials. It is used to increase the surface area of solids in industrial processes.

**Composite cement:** Ordinary Portland cement mixed with other supplementary cementitious materials.

**Concrete:** Material comprising cement, sand and gravel or other fine and coarse aggregate.

**Co-processing:** The use of waste materials in industrial processes (e.g. cement) as substitutes for fossil fuels or raw materials.

**Dehydroxylation:** Loss of structural water.

**Dry kiln:** equipment that produces clinker without using a water/limestone slurry mix as the feedstock.

**Illite:** Clay mineral with the least potential for thermal activation.

**Kaolinite:** Clay mineral with the highest potential for thermal activation.

**Metakaolinite:** Reactive pozzolanic product of thermal treatment of kaolinite; can be used as an SCM.

**Ordinary Portland cement (OPC):** Most common type of cement; consists of more than 90 % clinker and about 5 % gypsum.

**Pozzolana:** A material that exhibits cementitious properties when combined with calcium hydroxide.

**Precalciner:** A system that precedes the rotary kiln in the cement manufacturing process. Most of the limestone calcination is accomplished here, making the process more energy efficient.

**Process CO<sub>2</sub> emissions:** CO<sub>2</sub> generated as a result of chemical reactions from carbon in raw materials.

**Supplementary cementitious materials (SCMs):** Materials used in conjunction with OPC or blended cement to enhance the properties of concrete. The enhancement occurs by hydraulic or pozzolanic activity, or both.

**Thermal energy intensity of clinker:** Total heat consumption of a kiln, divided by the clinker production.

**Traditional fuels:** Fossil fuels as defined by the guidelines of the Intergovernmental Panel on Climate Change. They include mainly coal, petroleum coke, lignite, shale petroleum products and natural gas.



## Chapter 1: Introduction

The cement industry currently faces three main challenges. The first is that this industry depletes natural resources – such as limestone, gypsum, clay, sand and water – and thus adversely affects nature. Second, the industry is one of the largest industrial contributors to global CO<sub>2</sub> emissions. Third, it is facing a significant decrease in the availability of cementitious industrial by-products such as fly ash and granulated blast furnace slag. These materials are used to substitute cement clinker and lessen the environmental footprint of cement.

Each year, over 10 billion tons of concrete are used globally. According to some sources, this makes concrete the second most consumed substance on earth after water (Lehne & Preston, 2018). Vast quantities of raw materials are required to produce this volume of concrete, depleting important natural resources (Beiser, 2019).

Besides depleting large volumes of natural resources, the cement industry is one of the biggest emitters of CO<sub>2</sub>. Each year, more than 4 billion tons of cement are produced, accounting for around 8 % of annual global CO<sub>2</sub> emissions (Lehne & Preston, 2018, S. V). If the cement industry were a country, it would be the third largest emitter in the world after China and the United States. The cement industry contributes more CO<sub>2</sub> than aviation fuel (2.5 %) and is not far behind global agriculture (12 %) (Rodgers, 2018).

Some decline in CO<sub>2</sub> emissions has been evident during the last few years (Figure 1-1). However, there is still a long way to go to reduce CO<sub>2</sub> emissions in the cement industry in a sustainable way.

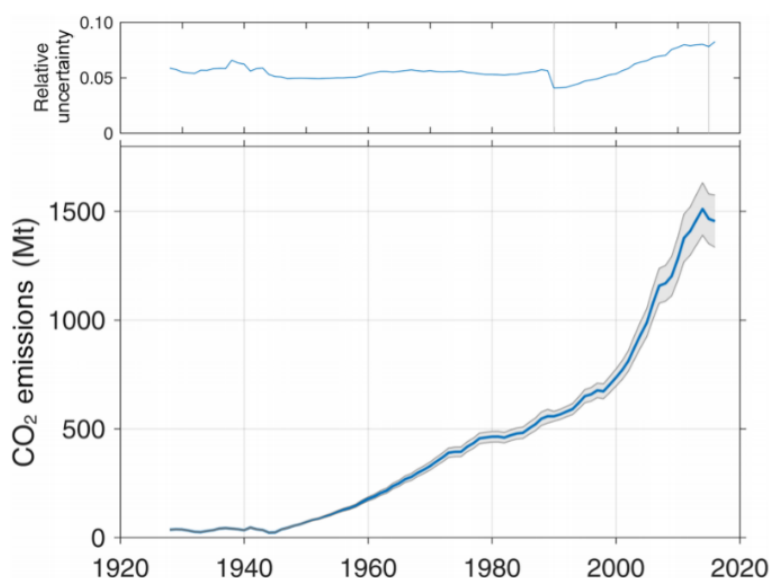


Figure 1-1: Global CO<sub>2</sub> emissions from cement production; 95 % confidence interval (Andrew, 2018)

The main contributor to CO<sub>2</sub> emissions is cement clinker, which is the main ingredient of cement. Clinker produces CO<sub>2</sub> through mainly calcium carbonate being burned in a kiln at approximately 1'450 °C. Approximately 55 % of the CO<sub>2</sub> development is associated with the decarbonization of calcium carbonate and consequent release of CO<sub>2</sub> ( $\text{CaCO}_3 \rightarrow \text{CaO} + \text{CO}_2$ ). The remaining 45 % of CO<sub>2</sub> is associated with burning fuels, heat losses and the electrical energy required to produce clinker (European Commission, 2019b).

The energy efficiency of the cement production process was gradually improved, and cement clinker was substituted with supplementary cementitious materials (SCMs) such as fly ash or granulated blast furnace slag. This approach reduced the impact of cement on CO<sub>2</sub> emissions significantly, from approximately 800 kg CO<sub>2</sub> per ton of cement in 1990 to approximately 600 kg CO<sub>2</sub> per ton of cement in 2019 (LafargeHolcim, 2020). Cement that consists of cement clinker and SCMs is called “composite cement”.

Given the low cost of cement and its large volumes, long transport distances are usually avoided. Therefore, cement is a product that is generally produced in locations relatively close to where it is consumed. For composite cements, production ideally requires the local availability of a source of an SCM, whether natural or industrial. However, such local sources are not guaranteed in all regions where cement is produced, mainly because of the decreasing availability of certain resources. For instance, the closure of coal power plants and steel furnaces in Europe and North America means that a significant source of SCM will diminish in the next few years (Businesswire 2017). The reduction of the content of clinker during the coming decades and the shift to using calcined clay and limestone instead are presented in the IEA Roadmap towards low carbon transition in the cement industry. Figure 1-2 shows the proportions of cement ingredients in 2014 versus in the near future.

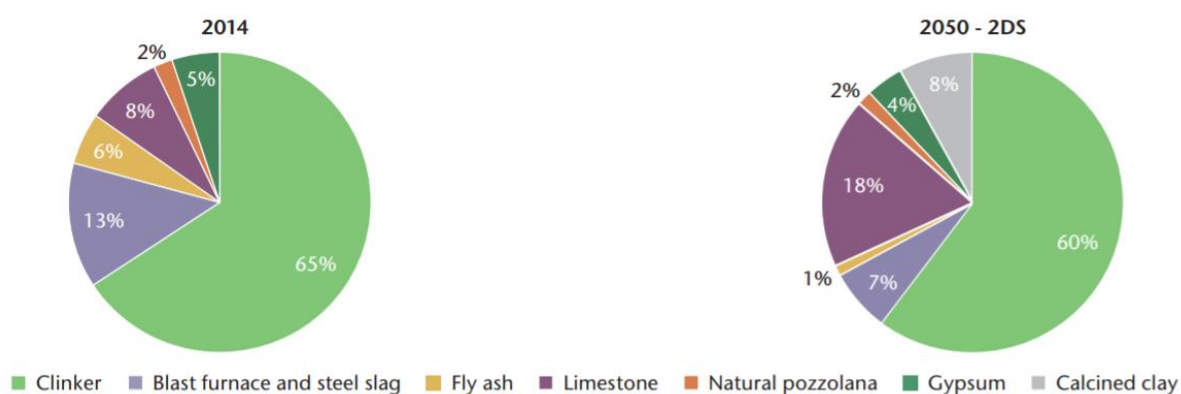


Figure 1-2: Global average estimate of cement composition (IEA et al., 2018, p. 34)

Currently, the most promising alternative in the industry is considered to be the calcination of clay. Kaolinitic clays are calcined at 700 °C–850 °C, approximately half the temperature required for clinker production. This calcination leads to the formation of a new mineralogical phase called “calcined clay” or “metakaolin”. In limestone calcined clay cement (LC3), calcined clay is mixed in a proportion of up to 30 % with 55 % ordinary Portland cement (OPC) and 15 % limestone. In this way, a similar concrete strength is achieved with a significantly lower CO<sub>2</sub> footprint (Scrivener, Zunino, Avet & Hangpongpun, 2018).

## 1.1 Motivation

Despite of the notable positive results from substituting cement clinker by calcined clay, only a few applications for producing calcined clay cements have been developed in the cement industry. The main reasons are as follows:

- There is insufficient availability of deposits having large quantities of suitable kaolinitic clays in many parts of the world; this is especially true for regions that already face a scarcity of fly ash and granulated blast furnace slag, such as Europe.
- There is often a long distance between the deposits and a manufacturing facility (i.e. cement plant or grinding station), which increases the production cost.
- There is insufficient market acceptance due to the altered cement quality parameters, such as a changed colour of the concrete.
- There is no cement standard framework for extensively using calcined clays.
- Exploiting large quantities of clay is contrary to the efforts of the European Green Deal to (1) decouple economic growth from resource use and (2) move to a clean and circular economy and using anthropogenic materials while restoring biodiversity (European Commission, 2019a).

Another critical element is the development of calcination technology. Currently, clay calcination in a rotary kiln or a flash calciner is the most widely studied production technology. However, both types of this technology have yet to overcome several challenges:

- the emission of greenhouse gases through using mainly noble fossil fuels, such as coal and petcoke
- difficulty in controlling the emission of other volatile environment-relevant components in the clay
- insufficient payback due to high investment and operating costs

- the complex preparation of clays, which usually possess insufficient particle sizes as well as high abrasiveness, high humidity and stickiness
- challenges in the process that result from the typical high and inert crystalline quartz content

These drawbacks mean that substituting cement with thermally activated and calcined clay obtained from natural clay deposits is an interesting but limited alternative. In addition, this alternative has a significant negative impact on nature.

## 1.2 Research hypotheses and objectives

Given the current scenario, one objective of this thesis is to investigate alternative SCMs which could replace cement clinker and provide an alternative to the depleting sources of fly ash and granulated blast furnace slag. It is a hypothesis of this research that materials can be sourced from various waste streams providing at least one waste material selected from aggregate washing sludge. Other ideally anthropogenic waste materials which shall be considered could be road cleaning sludge or deconstruction gypsum. These three types of waste material are currently mostly deposited in quarries or landfills and could therefore be turned into circular economy products.

Once thermally activated, the product would be similar in mineralogy, chemistry and performance to known SCMs. Examples of these current SCMs are metakaolin, fly ash, burned oil shale and natural pozzolana.

To test the hypothesis, this work investigates the properties of locally available material sources that display have a promising mineralogy and can be thermally activated. The product would be a new SCM with either pozzolanic, hydraulic or latent hydraulic reaction properties or a mixture thereof. Finally, concrete testing explores the suitability of the activated product to replace cement clinker.

Existing state of the art technologies, such as rotary or flash calciners, have distinct disadvantages for thermally activating materials. Therefore, a second objective of this study was to design and test a new production method which fulfils the following purposes:

1. Produce cement clinker and an SCM in one integrated system.
2. Use excess thermal energy from the clinker production process.
3. Dry the material sufficiently before it enters the calcination process, to avoid elevated air flows and disturbances in the cement clinker production.

4. Recycle highly contaminated materials in an ecologically friendly way.
5. Recover most of the cooling energy for drying, using heat-exchanging screws connected to a thermal oil system.
6. Control the colour of the SCM by reducing iron oxidation and thus limiting the red colour of the product.
7. Reduce the CO<sub>2</sub> footprint of composite cements.

The new production system is modelled in this thesis. Additional semi-industrial tests to dry, calcine and grind the materials are then conducted to confirm the patented technology (WO2021/124261, 2021) in the framework of this thesis.

### 1.3 Research methodology

The first step of this study was a comprehensive literature review to discover existing SCMs and their composition and reaction behaviour. The results were essential to define the chemical and mineralogical targets for the investigated waste materials. Additionally, state of the art calcining technologies that are currently available were analysed based on the literature and information from the suppliers.

As a second step, theoretic mass and heat balance calculations were performed. The aim here was to evaluate the limitations of the production system regarding its cooling and drying capacity, fuel demand and impact on the integrated cement clinker kiln. Additionally, theoretical evaluations were conducted to assess the impact of the calciner on the cement kiln emission as well as the expected CO<sub>2</sub> footprint of the newly designed plant. The results of the theoretical process simulation served as the basis for further semi-industrial testing, mainly of the rotary calciner and screw heat-exchanging system.

In preparation of the semi-industrial testing, samples from several aggregate washing sludge deposits were collected and analysed in terms of their physical, chemical and mineralogical properties. The samples were thermally activated in a laboratory and target reaction temperatures were defined for the semi-industrial testing. Additionally, other waste materials, such as deconstruction gypsum and road cleaning sludges, were analysed.

The prepared bulk samples were then shipped to the company Koellermann in Adenau, Gemany for thermal screw drying testing; this testing took place in July 2020. The dried material was shipped to the company Ibutec in Weimar, Germany, where calcination tests were conducted in August 2020. Thereafter, the calcined material was ground at the VDZ laboratory mill in

Düsseldorf, Germany and shipped to the Holcim test centre in Switzerland and Lafarge laboratory in France for mortar testing.

Additional tests for sludge mechanical dewatering, grinding with different mill systems and pneumatic conveying systems were also conducted. However, these are not part of the current research outcomes.

## 1.4 Thesis outline

The thesis is organized into seven chapters, as follows:

- Chapter 1 describes the background, motivation and main objectives of the study.
- Chapter 2 summarizes the literature review on SCMs and their origin and characteristics; it also provides an overview of state-of-the-art calcining technologies.
- Chapter 3 provides an overview of potential waste materials and describes the limitations of existing calcining systems. The chapter also presents an initial description of a new calcining technology.
- Chapter 4 discusses the targeted product quality and presents the results of the thermodynamic modelling and expected performance of the new calciner.
- Chapter 5 describes the characteristics of the various samples and the testing set up for drying, calcining and grinding.
- Chapter 6 analyses the performance results of the various types of concrete produced and finalizes the modelling of the new calciner system.
- Chapter 7 summarizes the main findings of this work and provides perspectives for the future.

## Chapter 2: State of the art in SCM production

*Chapter 2 explores available SCMs, including their origins, properties and reaction behaviours. The chapter also describes the state of the art technologies used to thermally activate minerals such as clay.*

### 2.1 Supplementary cementitious materials

SCMs are materials that can substantially substitute Portland cement. They contribute to improving the ecological footprint and properties of concrete through hydraulic, latent hydraulic or pozzolanic activity (Kosmatka, Kerkhoff & Panarese, 1979).

The use of SCMs has increased steadily in the past few decades, and pure Portland cement is no longer the dominant type. It has been replaced by many composite cements, including a wide range of different SCMs with differing chemical, mineralogical and physical characteristics. The SCM improves the performance of concrete in terms of the following characteristics, among others:

- strength development
- resistance to chemical attack
- compatibility with reactive aggregates
- suitable for use at high temperatures
- hydration heat

Possible disadvantages sometimes include limited early strength and a high water demand. However, these are largely offset by the advantages gained in the overall performance.

Several additional factors make the replacement of clinker and the substitution by SCMs particularly attractive in today's world. These include:

- an improved ecological footprint for cement production through
  - a. conservation of fossil fuels and mineral resources
  - b. use of by-products from other industries
  - c. reduction of CO<sub>2</sub> and heat emission and reduction of the impact of the cement industry on global warming
- differentiation of products and applications through

- a. producing tailored products
- b. improving cement properties for special applications
- c. improving the durability of concrete
- reduction and optimization of production cost through
  - a. improving the clinker factor
  - b. saving on thermal and electrical energy
  - c. increasing the cement output

As discussed in Chapter 1, the cement industry is willing to replace greater proportions of clinker with SCMs. However, many areas of the world already face scarcity due to depleted natural deposits or the reduced availability of industrial by-products.

## 2.2 Classification of SCMs

Different SCMs have diverse chemical and mineralogical compositions. In addition, the literature mainly differentiates SCMs in terms of their origin and reaction behaviour (Locher, 2000; Snellings, Mertens, & Elsen, 2012; Regourd 1986).

### 2.2.1 Classification according to origin

SCMs can be classified into natural or artificial materials based on their origin (Figure 2-1).

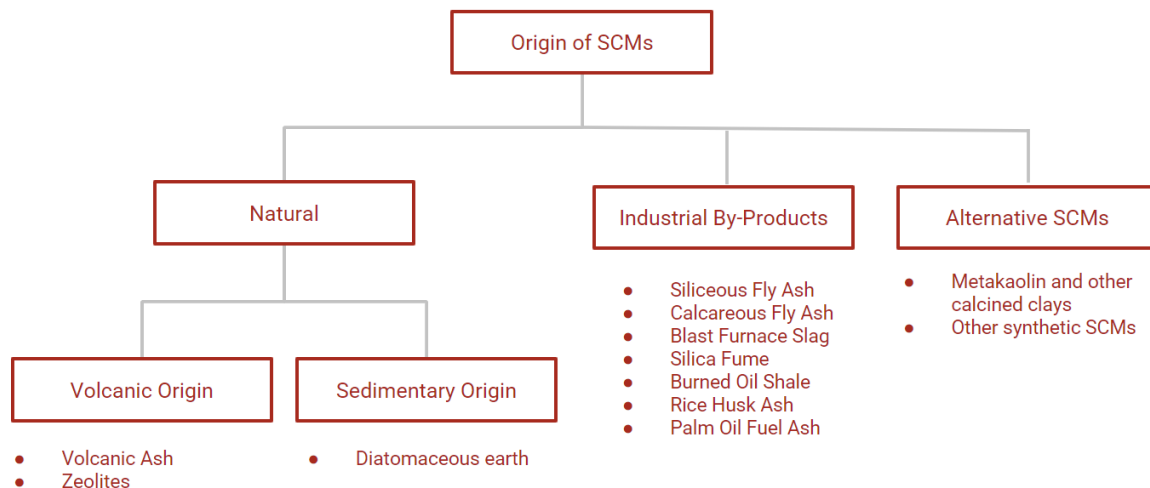


Figure 2-1: Classification of SCMs according to their origin



SCMs of natural origin can be used in their naturally occurring form. In most cases, these materials only need some preparation, such as drying or grinding, either separately from or together with cement clinker, to develop the desired cementitious properties. Generally, naturally occurring SCMs are of volcanic or sedimentary origin. SCMs of volcanic origin are typically pyroclastic materials in the form of volcanic ashes or tuff.

SCMs of sedimentary origin generally comprise amorphous silica. The silica is accumulated by the circulation of hydrothermal fluids or the biochemical sedimentation of – for example diatom fossils.

Due to their limited availability, natural SCMs are rarely used in the cement industry. Instead, by-products of industrial processes, such as fly ash and granulated blast furnace slag, constitute most SCMs currently used in the cement industry.

Fly ash is a by-product of coal combustion in power plants and is currently the most widely used SCM in concrete. It can partially replace Portland cement clinker by up to 60 % in terms of mass. China, India and the United States together generated more than 75 % of the global fly ash production in 2008, at about 777 million tons (Sakir, Raman, Safiuddin, Kaish, & Mutalib, 2020). During the burning process, incombustible impurities of coal – such as clay, shale, feldspar and quartz – fuse, cool and solidify into glassy particles (Kosmatka et al., 1979). The properties of fly ash depend on the type of coal burnt and can be classified as follows:

- siliceous fly ash
- calcareous fly ash

Apart from the composition of coal ashes, originating from combustion, calcium carbonate (limestone or dolomite) is often introduced into the coal-fired boiler. The purpose is to control sulphur emissions, which can additionally impact the type of generated fly ash.

Granulated blast furnace slag is a by-product of iron and steel production. It is obtained by quenching molten iron slag from a blast furnace in water or steam to produce a granular product that is high in reactive calcium silicate hydrates (CSH). The chemical composition of slag varies depending on the composition of raw materials in the iron production process and the cooling methodology.

Other by-products used in the cement industry as SCMs in lesser quantities are as follows:

- Silica fume or microsilica: this ultrafine powder is obtained as a by-product of silicon and ferrosilicon production. Silica fume is mainly applied to high-performance cements.
- Burnt oil shale is produced from shales with organic matter in the range of 5 %–65 %. It is produced by the combustion of oil shales in bottom or fluidized bed furnaces used for steam or electricity generation. The resulting ash has a highly variable composition, depending on the characteristics of the original shale and the temperature at which it is produced (Global Cement and Concrete Association, n.d.).
- Rice husk ash is an agricultural by-product from burning the coating on rice husks at a controlled temperature below 800 °C. The process produces approximately 25 % ash containing 85 %–90 % amorphous silica, plus approximately 5 % alumina (Zareei, Ameri, Dorostkar, & Ahmadi, 2017).
- Palm oil fuel ash is an agricultural by-product, similar to rice husk ash. It is obtained from burning waste materials such as palm kernel shell, palm oil fibre and palm oil husk. The ash can be used to partially replace cement in a concrete mix (Shehu & Awal, 2012).

As previously mentioned, the anticipated scarcity of almost all of the currently easily available SCMs means that the cement industry must find other alternative SCMs. These alternatives can be produced by thermally activating available materials, such as clays, or by developing and thermally activating synthetic mixtures with a similar composition to that of the current SCMs. The resulting SCMs are of synthetic origin and are expected to play an important role in the future of cement production.

### **2.2.2 Classification according to reaction behaviour**

In terms of their reaction behaviour, SCMs can be classified as follows:

- hydraulic
- latent hydraulic
- pozzolanic
- inert

Hydraulic, latent hydraulic and pozzolanic reactions contribute directly to the strength and durability of concrete. Inert materials do not develop their own strength, but they may react with hydraulic or pozzolanic materials especially, and they can influence the hydration of cement.

This capacity leads to earlier strengths and improved durability of concrete, allowing higher substitution levels (Mathieu, 2013).

Figure 2 2 shows the classification of SCMs according to the reaction behaviour and most popular examples. Depending on the mineralogical composition, which is often heterogenous, some SCMs – such as burnt oil shale or fly ash – may be associated with hydraulic, latent hydraulic or pozzolanic reaction behaviour.

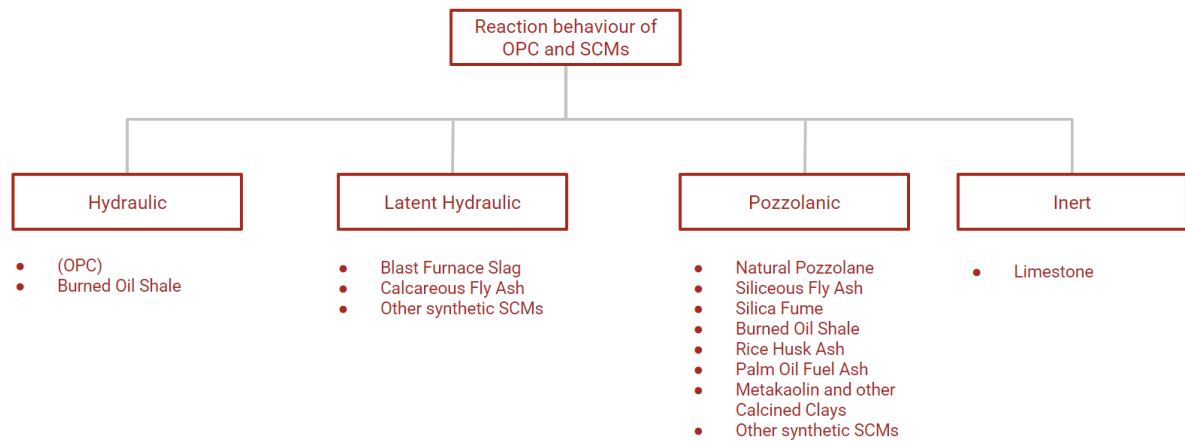


Figure 2-2: Classification of OPC and SCMs according to their reaction behaviour

The ternary phase diagram of  $\text{CaO-Al}_2\text{O}_3\text{-SiO}_2$ , referred to as the “CAS” phase diagram, is shown in Figure 2 3. This diagram is often used for a preliminary understanding of Portland cements; it can also be used for characterizing SCMs. Wright and Rankin (1915) were the first to develop such a diagram.

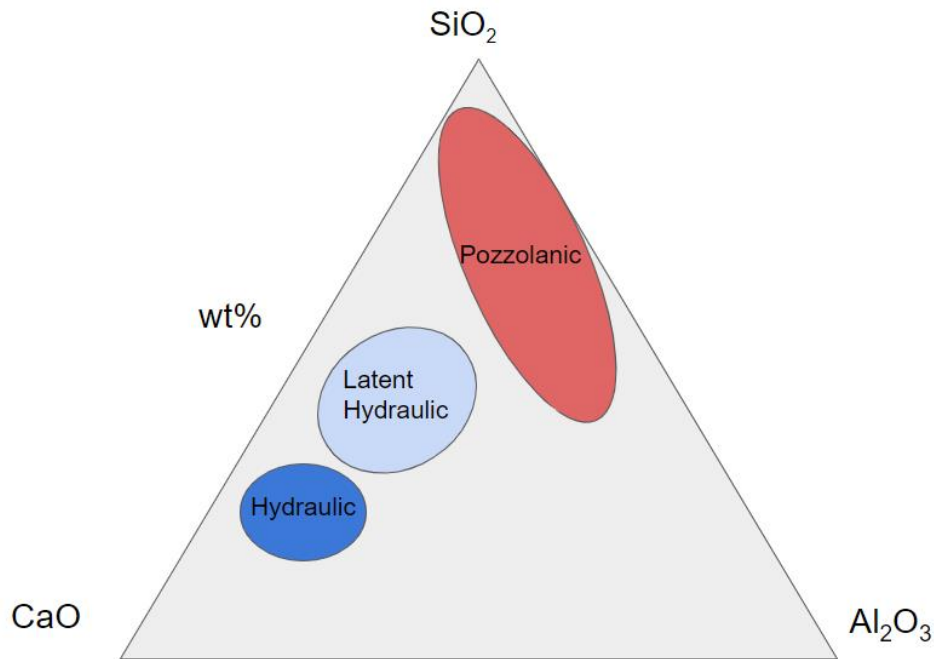


Figure 2-3: Zones of SCM and OPC shown in a ternary CAS phase diagram

The reactions of hydraulic, latent hydraulic and pozzolanic minerals in cement can be extremely complex because many minerals are usually involved. The following examples provide a brief overview of the most dominant reactions.

Hydraulic reacting minerals set and harden by hydration when water is added. The most widely known is alite ( $3\text{CaO}\cdot\text{SiO}_2$ ) or  $\text{C}_3\text{S}$ , which is the dominant mineral in cement clinker. Other minerals that are heavily present in hydraulic or latent hydraulic SCMs, such as calcareous fly ashes or burnt oil shale, are:

- belite ( $2\text{CaO}\cdot\text{SiO}_2$ ) or  $\text{C}_2\text{S}$
- calcium aluminate: several forms, including –
  - a. monocalcium aluminate ( $\text{CaAl}_2\text{O}_4$  or  $\text{CaO}\cdot\text{Al}_2\text{O}_3$ ) or CA
  - b. dicalcium aluminate ( $\text{Ca}_2\text{Al}_2\text{O}_5$  or  $2\text{CaO}\cdot\text{Al}_2\text{O}_3$ ) or  $\text{C}_2\text{A}$
  - c. tricalcium aluminate ( $\text{Ca}_3\text{Al}_2\text{O}_6$  or  $3\text{CaO}\cdot\text{Al}_2\text{O}_3$ ) or  $\text{C}_3\text{A}$
- calcium oxide ( $\text{CaO}$ )
- magnesium oxide ( $\text{MgO}$ )

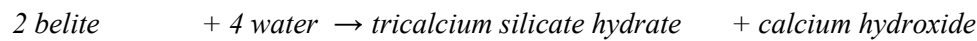
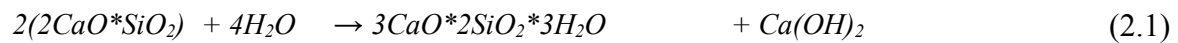
The hydration reaction involves the components of clinker and their chemical reactions with water. A few exceptions exist; however, these chemical reactions generally involve calcium,

silica and aluminium constituents, which react with water to form a whole family of calcium silicate and calcium aluminate hydrates.

The hydration reactions of the two calcium silicates in clinker are represented by the following chemical equations:

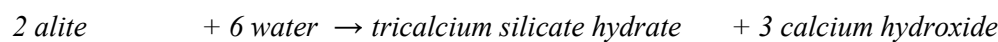
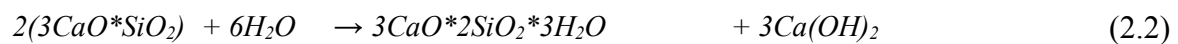
- belite reaction

The usual cement clinker comprises approximately 10 %–30 % C<sub>2</sub>S. The hydration reaction of belite can be represented by the following chemical equations shown in a regular form (Equation 2.1) and simplified as per cement industry standards (Equation 2.1a):



- alite reaction

At approximately 45 %–65 %, alite is the major phase in Portland cement and is responsible for the setting and development of early strength. The hydration reaction of alite can be represented by the following chemical equations (Equations 2.2 and 2.2a):



The reactions of both silicates are stoichiometrically similar. The main difference between the two reactions is that alite produces more than double the calcium hydroxide derived from belite.

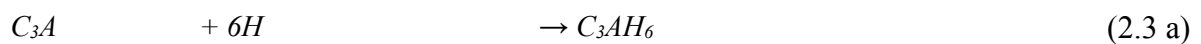
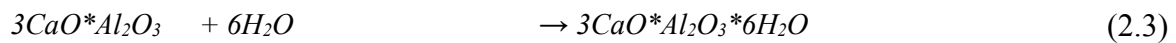
The calcium silicate hydrates (C<sub>3</sub>S<sub>2</sub>H<sub>3</sub>) developed during the alite reaction are the main contributors of strength development in the concrete.

Calcium hydroxide, Ca(OH)<sub>2</sub>, also called portlandite, has a limited or no impact on the strength development of an OPC. However, its importance is mainly related to its reaction with silica and alumina from SCMs with pozzolanic properties.

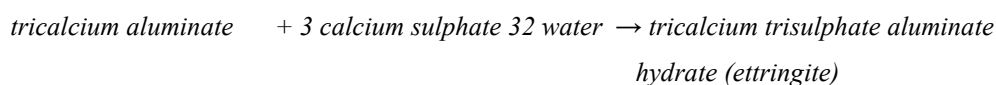
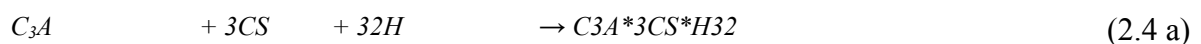
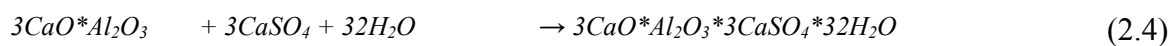
- calcium aluminate reactions

In OPC, calcium aluminates are mainly responsible for the setting behaviour.

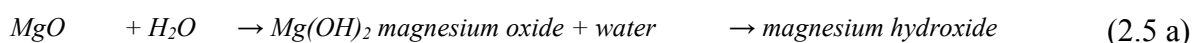
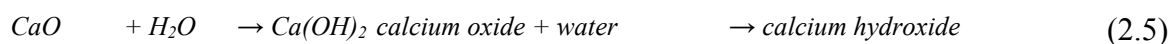
Unlike in Portland cement, which contains smaller amounts of aluminous phases, hydraulic reacting calcium aluminates are an essential part of aluminous cement (Wells & Carlson, 1956). The resulting calcium aluminate hydrates are manifold, as demonstrated by the following theoretical formulas for the reaction of tricalcium aluminate with water (Equations 2.3 and 2.3a):



The hydration of aluminates is heavily influenced by the presence of gypsum. In the absence of gypsum, the reaction of calcium silicate with water is violent, leading to immediate stiffening of the paste due to the rapid formation of calcium aluminate hydrates. This is known as “flash setting”. Conversely, too much gypsum can also negatively influence the setting behaviour by reaction of the gypsum with water, called “false setting”. When sufficient gypsum is present, the reaction continues until all available gypsum is consumed (Locher, 2000) and ettringite is formed, as shown in Equations 2.4 and 2.4a.



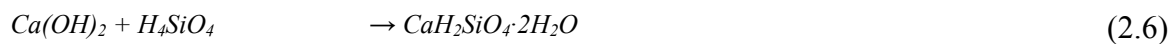
- calcium oxide and magnesium oxide reaction (Equations 2.5 and 2.5a)



The importance of the calcium and magnesium hydroxide is mainly related to its reaction with silica and alumina from SCMs with pozzolanic properties.

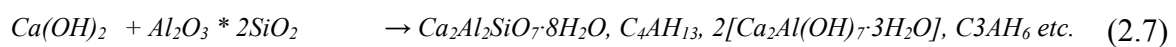
**Latent hydraulic materials** react with water and develop similar calcium silicate hydrate products, as seen in the hydraulic reactions. The main difference to hydraulic reactions is that the process is extremely slow. Therefore, additional activation is required. For the latent hydraulic granulated blast furnace slag, this activation can be achieved by adding alkaline compounds or sulphates. Due to the activation, blast furnace slag cements can be produced with up to 80 %–85 % slag, 10 %–15 % anhydrite and approximately 5 % of an alkaline activator, which is often OPC (Gruskovnjak, 2006; Locher, 2000).

**Pozzolanic materials** cannot react with water alone and require calcium hydroxide,  $\text{Ca(OH)}_2$ , which is a product of the reaction of alite, belite or calcium oxide with water. The amorphous silica, such as silicic acids  $\text{H}_4\text{SiO}_4$  or  $\text{Si(OH)}_4$ , solubilizes when in contact with water. It reacts with the  $\text{Ca}^{2+}$  ions present in  $\text{Ca(OH)}_2$  to form hydrated hydroxide silicates such as those produced in the cement hydration reactions shown in Equations 2.6 and 2.6 a (Gallego, Toro & Rojas, 2020).



*calcium hydroxide + silicic acid → calcium silicate hydrate*

Additionally, many materials that show a pozzolanic reaction contain reactive alumina, which reacts and produces several calcium alumina silicate hydrates. One example is the reaction of metakaolin, which can react to form many different CSHs shown in Equations 2.7 and 2.8 a (ŽEMLIČKA, KUZIELOVÁ, KULIFFAYOVÁ, TKACZ & PALOU, 2015).

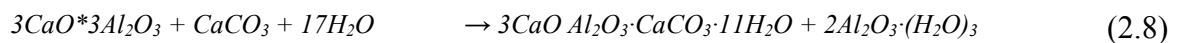


*calcium hydroxide + metakaolin → calcium silicate hydrate and calcium silicate aluminate hydrate*

The reaction of  $\text{Al}_2\text{O}_3$  from metakaolin (or other pozzolans) with sulphate-bearing compounds in a water environment containing calcium can again lead to the formation of ettringite (Equation 2.4).

The rate of the pozzolanic reaction depends on the characteristics of the pozzolan, such as the specific surface area, chemical composition and active phase content.

Studies of École Polytechnique Fédérale de Lausanne (EPFL) (Antoni, 2013; Mathieu, 2013; Zunino & Scrivener, 2021) are interesting for developing calcined clay cements. These show the positive impact of inert limestone in a ternary blend with OPC and calcined clay, where several carboaluminates are formed, contributing significantly to the strength of the composite cement. Such ternary blends are known as limestone calcined clay cements or (LC3) (Equation 2.8 and 2.8 a).



*tricalcium aluminate + calcium carbonate + calcium hydroxide + water → monocarboaluminate*

A similar reaction also develops hemicarboaluminate (Bizzozero & Scrivener, 2015).

### 2.3 Chemical composition of SCMs

A description of the chemical composition and typical reaction behaviour of selected SCMs, compared to OPC, is provided in Table 2-1. The literature describes diverse compositions of many SCMs, illustrating that these materials vary widely in their properties and reactivity.

Table 2-1: Typical chemical compositions and reaction behaviour of SCMs and OPC

Material	OPC	Limestone	Granulated blast furnace slag	Calcareous fly ash	Siliceous fly ash	Silica fume	Burnt oil shale	Me-takaolin
Typical reaction	Hydraulic	Inert	Latent hydraulic	Latent hydraulic	Pozzolanic	Pozzolanic	Hydraulic or pozzolanic	Poz-zolanic
Chemical composition (in w %)								
SiO <sub>2</sub>	16–23	0–8	28–41	40–42	50–55	85–99	10–40	49–69
CaO	49–69	45–55	37–50	20–24	4–7	0–4	20–40	0–2
Al <sub>2</sub> O <sub>3</sub>	4–7	0–3	5–14	17–20	20–26	0–6	2–10	25–44
Fe <sub>2</sub> O <sub>3</sub>	2–7	0–2	0–1	6	7	0–3	2–6	0–3
MgO	0–5	0–7	4–10	0–5	2–3	0–5	0–10	0–3
SO <sub>3</sub>	0–1	0–1	0–3	2–5	0–1	0–2	4–10	0–1
Na <sub>2</sub> O	0–1	0–1	0–3	0–2	0–2	0–2	0–1	0–1



Material	OPC	Limestone	Granulated blast furnace slag	Calcareous fly ash	Siliceous fly ash	Silica fume	Burnt oil shale	Me-takaolin
Typical reaction	Hydraulic	Inert	Latent hydraulic	Latent hydraulic	Pozzolanic	Pozzolanic	Hydraulic or pozzolanic	Poz-zolanic
Chemical composition (in w %)								
K <sub>2</sub> O	0–1	0–1	0–2	0–3	0–3	0–2	0–3	0–2
P <sub>2</sub> O <sub>5</sub>	–	0–1	–	0–2	0–2	0–1	0–1	0–1
TiO <sub>2</sub>	–	0–1	0–1	0–2	0–2	–	0–1	0–1

(Konist et al., 2020; Locher, 2000; Rutkowska, Chalecki, Wichowski, Żwirska, & Barszcz, 2016; Sakir et al., 2020; and others)

## 2.4 Formation of hydraulic or pozzolanic minerals in thermal processes

The formation of hydraulic or pozzolanic materials is relatively complex. It involves numerous minerals and requires proper preparation and the appropriate burning and cooling conditions.

### 2.4.1 Cement clinker

The formation of hydraulic minerals can best be explained based on the reactions in a cement kiln, which are described in the cement literature with minor deviations (Al-Naffakh & Jafar, 2020; Kosmatka et al., 1979; Locher, 2000). Cement clinker is produced in a kiln system at temperatures reaching 1450 °C. Since cement clinker was discovered in the mid-eighteenth century, its manufacturing conditions and chemistry have been optimized for application.

The raw materials pass through several temperature zones in the kiln system. These materials form mostly hydraulic clinker minerals, as shown in the following list and in Figure 2-4.

20 °C–300 °C	evaporation and loss of physically absorbed water
400 °C–900 °C	removal of structural H <sub>2</sub> O (H <sub>2</sub> O and OH groups) from clay mineral
>500 °C	structural changes in silicate materials
700 °C–900 °C	dissociation of carbonates, formation of free lime (CaO) and removal of CO <sub>2</sub>
>800 °C	the lime reacts with silica to form the first calcium silicates (belite – C <sub>2</sub> S), which is an endothermic reaction. The formation of belite is a solid-solid reaction requiring good mixing and intensive contact between CaO and SiO <sub>2</sub>
800 °C–1'250 °C	the lime reacts with aluminium and iron to form several intermediate products, including calcium aluminates (C <sub>3</sub> A)
>1'250 °C	upon completion of belite formation (C <sub>2</sub> S) at about 1250 °C, the calcium aluminates and ferrites reach a point where they become liquid
1'250 °C–1450 °C	within the liquid, solid belite (C <sub>2</sub> S) reacts with the residual lime to form alite (C <sub>3</sub> S) in a solid-liquid reaction. This reaction is exothermic

Once the alite ( $C_3S$ ) formation is complete, there is no value in prolonging the process at such a high temperature. The objective is then to prevent any further growth of alite and belite crystals through appropriate rapid cooling.

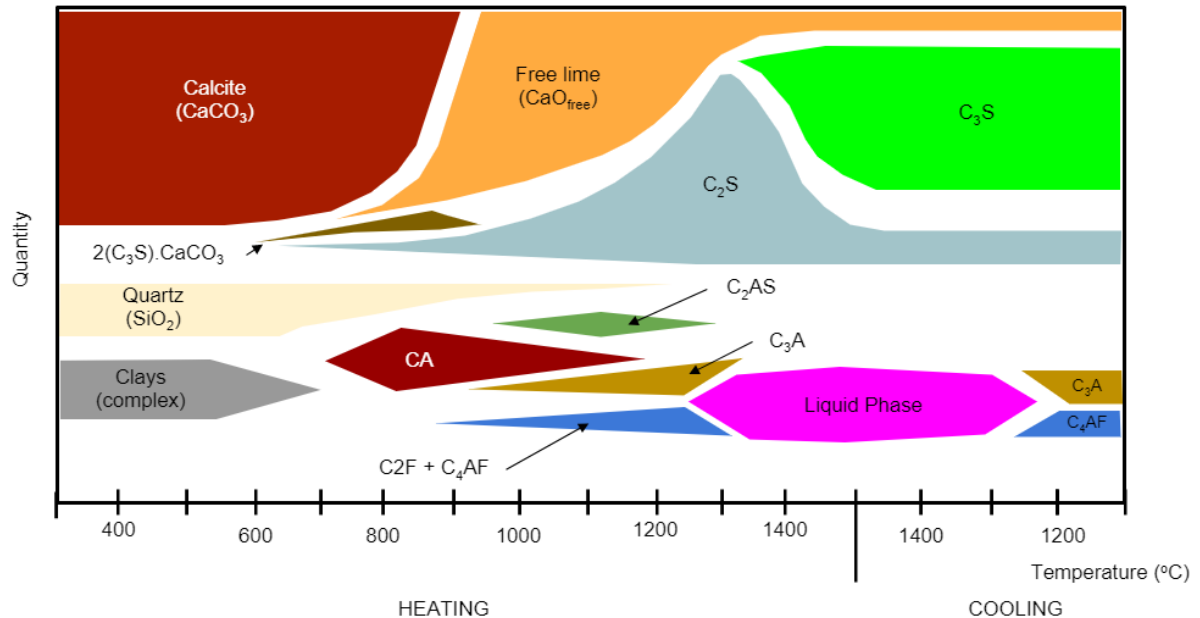


Figure 2-4: Mineralogical changes as a function of temperature during clinker formation

Reactions of hydraulic or latent hydraulic SCMs are similar to the process described above. They deviate mainly in quantity due to their different composition and burning temperatures compared to – for instance – burnt oil shale or calcareous fly ash. Additionally, many SCMs show both hydraulic and pozzolanic reaction behaviours.

## 2.4.2 Burnt oil shale

Burnt oil shale is a sedimentary rock with an organic content of 5–65 w %. Oil shale is used to produce thermal and consequently electrical energy mainly in fluid bed reactors and usually at approximately 800 °C. The resulting ashes have hydraulic and pozzolanic properties, depending on the composition (Locher, 2000).

Depending on the combustion process and temperature, the burnt oil shale contains clinker phases, mainly dicalcium silicate (belite) and monocalcium aluminat. In addition to small amounts of free calcium oxide and calcium sulphate, it contains larger proportions of pozzolanic reacting oxides, especially silicon dioxide (Raado, Tuisk, Rosenberg, & Hain, 2011).

Burnt oil shale comprises irregular and non-uniform particles of 20–100  $\mu\text{m}$ , yielding a relatively large surface area, as shown in Figure 2-5 (Külaots, Goldfarb, & Suuberg, 2010). The reason for the different microscopic appearance compared to fly ash (Figure 2-6) might be the low combustion temperature of 750  $^{\circ}\text{C}$ , at which no substantial melting phase exists.

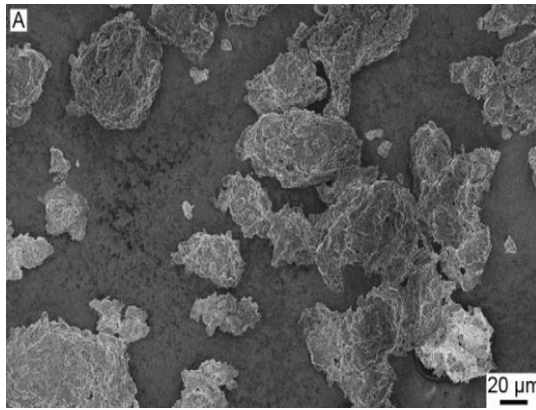


Figure 2-5: Scanning electron microscopy (SEM) picture of an oil shale burnt at 750  $^{\circ}\text{C}$  displaying mostly irregular particles (Külaots et al., 2010)

In a finely ground state, burnt shale shows pronounced hydraulic properties, such as those of Portland cement, as well as pozzolanic properties.

### 2.4.3 Fly ash

Fly ash is a secondary product of coal combustion in coal-based thermal power plants. It forms due to coal combustion at 800–1'600  $^{\circ}\text{C}$ , depending on the technology.

Coal is not exclusively composed of organic matter, which produces the energy during coal firing in power plants. It also contains a variable amount of inorganic material. This matter is transformed during combustion and defines the characteristics of fly ash, together with the burning process.

Minerals that become amorphous or react like calcium silicates during the burning process to clinker phases are interesting for the cement industry.

Depending on the base coal, the fly ash may develop latent hydraulic or pozzolanic properties. Fly ash from burning bituminous or hard coals tends to form amorphous silica minerals with pozzolanic properties, called “siliceous fly ash”. Fly ash from the combustion of soft lignite or brown coal is richer in calcium. It forms calcium silicate minerals that develop latent hydraulic properties; this type of ash is called “calcareous fly ash”.

Fly ash comprises mainly glassy and spherical particles, as shown in Figure 2-6 (Faheem, Rizwan, & Bier, 2021). These particles form through the high-temperature burning and rapid cooling of droplets, and their sizes range between 10 and 100  $\mu\text{m}$ . The small glass spheres improve the fluidity and workability of fresh concrete and contribute to the pozzolanic reactivity of fly ash.

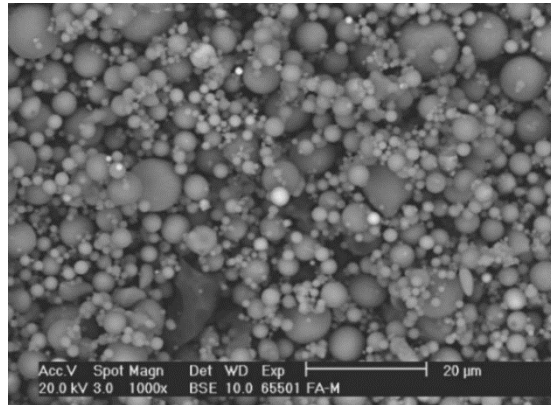


Figure 2-6: SEM particle characterization of a fly ash with mostly spherical and some angular particles (Faheem et al., 2021)

#### 2.4.4 Calcined clay

At least since the Roman era, terra cotta has been known for its binding properties in combination with lime (Hewlett & Liska, 2019). Terra cotta refers to burnt or calcined clay. Clay minerals formed by the chemical weathering or hydrothermal decomposition of silicate-bearing rock, such as granite, have a relatively heterogeneous mineral composition.

The type of clay minerals that are formed depends on the base rock composition and the hydrothermal and climatic conditions causing the decomposition. For instance, acid weathering of feldspar-rich rock, such as granite, tends to produce kaolinite in warm climates. Weathering of the same type of rock under different conditions may produce illite or montmorillonite (USGS, n.d.).

Kaolinite, illite and montmorillonite are classified as standard clay minerals with complex, layered aluminosilicates. They are differentiated by their crystalline structure, chemical composition and physical behaviour:

- |   |                        |                 |
|---|------------------------|-----------------|
| • | double-layer silicates | kaolinite       |
| • | triple-layer silicates | illite          |
| • | mixed-layer silicates  | montmorillonite |

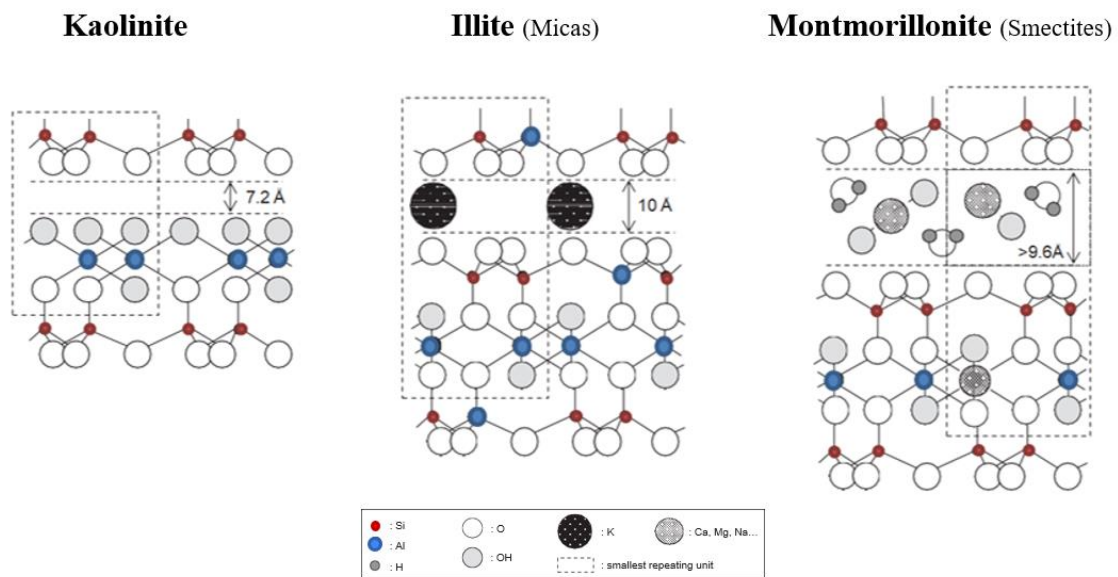


Figure 2-7: Structures and ideal formulas of kaolinite, illite and montmorillonite (adapted from Fernandez, Martirena & Scrivener, 2011)

The kaolinite structure comprises distinct interlayers of aluminate and silicate groups with hydroxyl groups (OH) in between (Figure 2-7, Figure 2-8).

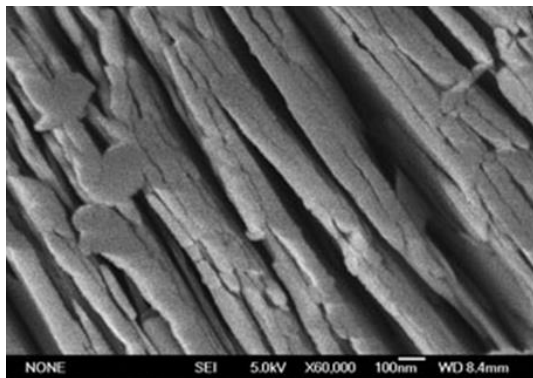
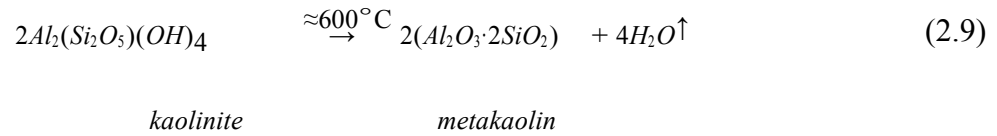


Figure 2-8: Layered structure of kaolinite shown SEM (Wang, Li, Peng & Zhang, 2011)

Both layers are linked by hydrogen bonding aluminol (Al-OH) and siloxane (Si-O) groups. Kaolinite incorporates more OH groups than the other clay minerals. The reason kaolinite has the highest potential for activation appears to be that at calcination temperatures above 600 °C, intensive dehydroxylation (loss of structural water) and disordering of the crystal structure occur. This process exposes highly reactive Al groups at the surface of the newly formed material, metakaolin (Equation 2.9).



The process governing the dehydroxylation of kaolinite and formation of metakaolin can be described in two stages:

- 1) dehydroxylation (loss of structural water)
- 2) destruction of the kaolinite sheet structure and formation of metakaolin by reorganizing Al and Si

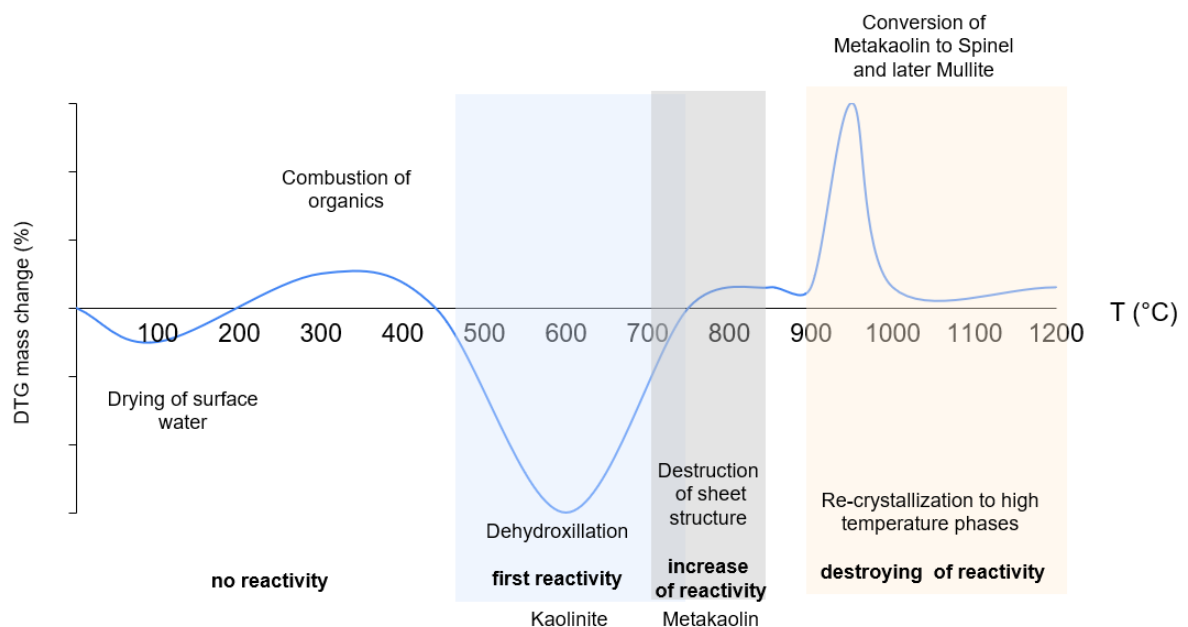


Figure 2-9: Simplified illustration of results of derivative thermogravimetry (DTG) mass change analysis during the transformation of kaolinite to metakaolin, spinel and mullite

Apart from drying and burning of organics inside the kaolinite, there is no increase in reactivity at temperatures below 450 °C (Figure 2-9). Up to 600 °C, other than some initial dehydroxylation there is typically little or no gain in reactivity. Only at 600 °C–700 °C is structural water removed. At temperatures between 700 °C and 850 °C, kaolinitic clays are activated to metakaolin with pozzolanic properties. Metakaolin is characterized by a disordered and partially amorphous structure. Exposing kaolinite to temperatures above 900 °C destroys the metakaolinite structure and its reactivity. Other phases are then formed, such as Si-Al spinel ( $Si_3Al_4O_{12}$ )

and mullite ( $3\text{Al}_2\text{O}_3 \cdot 2\text{SiO}_2$ ; Ptáček, Frajkorová, Šoukal, & Opravil, 2014, p. 443; Rowland, 1952; Scrivener, Martirena, Bishnoi, & Maity, 2018; Zuo, Wang, Zhang, Liu, & Yang, 2017).

In illite and montmorillonite, after dehydroxylation at higher temperatures (600 °C–800 °C), the Al groups are trapped between Si groups and are thus relatively unable to react. They show far less reactivity than in kaolinite (Fernandez et al., 2011).

The above general structural behaviour of the clay explains the enhanced reactivity of kaolinite. Several studies also indicate some reactivity of montmorillonite, whereas illite has shown little or no pozzolanic activity after calcination (Fernandez et al., 2011; Snellings, 2016).

Clay rarely occurs as pure kaolinite. It is instead typically a multimineral, which usually contains several clay types that influence the overall quality. Examples are quartz, feldspar, calcite, sulphates, sulphides, iron, organics and heavy metals. Quartz and feldspars occur in the coarse fraction of the clay and do not contribute to the reactivity. However, they pose a challenge for selecting the processing technology, since quartz especially contributes significantly to wear in the grinding process. It could potentially represent a health risk in the case of microcrystalline quartz.

Only a few criteria are currently available to evaluate the suitability of calcined clays for SCM. One criterion is a minimum kaolinite content of 40 % to achieve a mechanical strength performance comparable to OPC. This can be achieved by a 30 % substitution of OPC with calcined kaolinitic clay or a 50 % substitution of clinker with a calcined clay limestone addition in an LC3 cement (Díaz et al., 2020, p. 5; Scrivener, Zunino, et al., 2018).

## 2.5 Performance of composite cements

SCM is governed by chemical, physical and thermodynamic processes. Hence, SCMs partly determine the properties of concrete mixtures (Sakir et al., 2020) by

1. influencing the dispersion inside the mortar with different sizes, shapes and surface areas of the particles
2. influencing the hydration reaction of cement
3. reacting with calcium hydrate, the second product of cement hydration
4. physically filling the pore spaces in cement paste

Besides the influence of the reaction behaviour of the SCM, the influence on the performance significantly depends on the material composition, dosage, particle size and surface area. Finer particles react quickly and may influence the early strength of some SCMs, whereas coarser particles more strongly influence the late strength of a mortar. Concrete mixtures with added finer SCMs increase the water demand. Thus, an optimum composition must be determined.

The effects of SCMs on the properties of concrete mixtures, especially strength and water demand, can vary considerably even for a specific SCM. Therefore, the literature shows a rather varied impression of the impact of SCM on cement properties (Table 2-2).

Table 2-2: Influence of SCMs on the performance of concrete mixtures

Characteristic	Granulated blast furnace slag	Calcareous fly ash	Siliceous fly ash	Silica fume	Burnt oil shale	Metakaolin
Early strength	↔	↑	↓	↑	↓↑	↓
Late strength	↔	↑	↑	↑	↑	↑
Water demand	↓↑	↓↑	↓↑	↑	↑	↑
Corrosion resistance	↑	↑	↑	↑	↑	↑
Sulphate resistance	↑	↑↓	↑	↑	↓↑	↑

(Kosmatka et al., 1979; Raado et al., 2011; Sakir et al., 2020)

## 2.6 Calcining technologies

The production of calcined clay is currently the main driver in developing calcining technologies. Several process technologies are available for the thermal activation of materials at temperatures between 600 °C–900 °C. These technologies include the following:

- flash calciner
- rotary kiln
- circulating fluidized bed
- multiple hearth furnaces
- electrical calcination



In recent years, only flash calciners and rotary kilns have been favoured by the cement industry. Other technologies used in the mineral industry, such as circulating fluidized beds and multiple hearth reactors, could also be options for clay calcination. However, they are not currently considered in the cement industry and are thus not further studied here.

Cement producers are also attempting to convert existing clinker production facilities into clay kilns. However, in many cases, such conversions are difficult because

- Existing limestone preparations are unsuitable for clay. The storage, transport and dosing of sticky clay require unique solutions.
- To achieve the same capacity, clinker kiln preheater cyclones must be significantly larger than clay calciners. The former must allow higher air flows for the decarbonization of calcium carbonate.
- Moving grate coolers, which are typical for clinker manufacturing and are essential for the thermal energy efficiency of the system, are unsuitable for use with fine powders, such as calcined clay.
- In many cases, the size of the clinker kilns exceeds the need for calcination of an SCM.

Electrical calcination has not been developed to the extent that it can be used on an industrial scale. Due to the high production cost caused by the high energy demand of electrical heating, the main purpose of developing that technology is to further reduce the CO<sub>2</sub> footprint by using energy produced without fossil fuels.

### **2.6.1 Flash calciner**

“Flash calcination” generally describes a process in which a fine powder is suspended in a suitable hot gas. The powder is heated rapidly and is exposed to the target temperature for a short time (tenths of a second to a few seconds), after which it is cooled again rapidly. The flash calciner is a riser duct that provides the required short residence time (Figure 2-10). The pre-heated fine material is fed to the bottom of the calciner and entrained by the hot combustion gases. The fuel for calcination could theoretically be fired directly into the flash calciner. However, ideally, the fuel is burned externally in a combustion chamber to provide controlled ignition and complete combustion and to avoid local temperature peaks in the calciner.

Before the material enters the flash calciner, it is preheated over several cyclone stages, counter-current to the flash calciner flue gases. After flash calcining, the calcined material is cooled in a few cyclone stages, while the combustion air is simultaneously preheated.

Depending on the physical properties of the clay, mainly its particle size and moisture, the clay must either be prepared in a crusher, mill and dryer or with a combined dryer/crusher. (The latter system is known as a “hammer dryer crusher”.) Because the calcination occurs within a few seconds, the material must be well prepared and then ground into a fine powder and dried. Furthermore, the low retention time in the calciner does not allow for the application of low-volatile fuels, unless they are pre-burned in an attached hot gas generator.

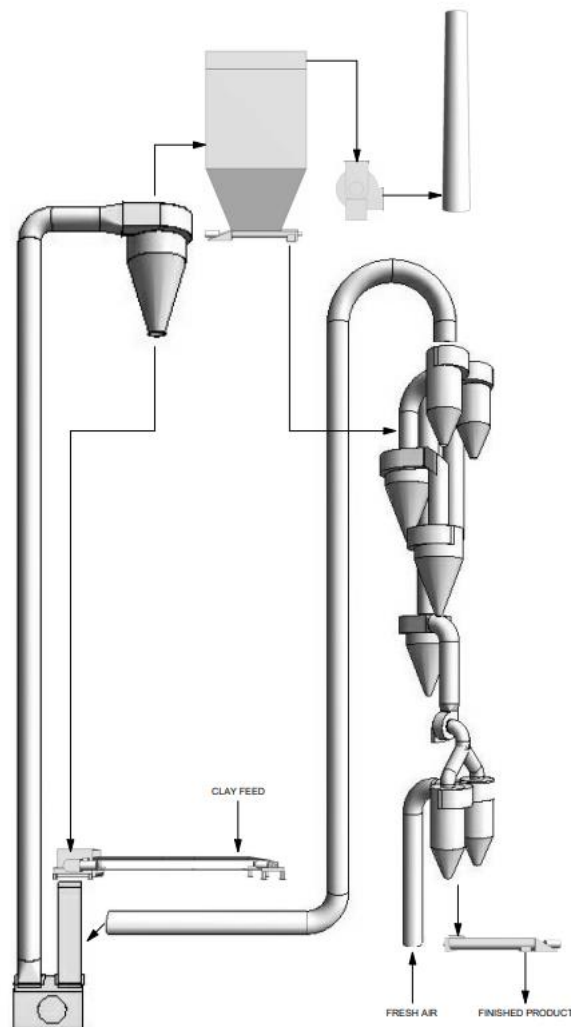


Figure 2-10: Simplified process for flash calcination technology

### 2.6.2 Rotary calciner

The rotary kiln is well known from clinker production and many other thermal processes. The kiln is fired by a burner, which provides:

- combustion gases for drying and preheating the material, through heat transfer by convection and conduction
- a so-called burning zone with an elevated temperature regime, where heat transfer occurs mainly by radiation; here, the material bed reaches the target temperature

This system is shown in Figure 2-11. The simplest set-up resembles a long dry kiln used in clinker production. The coarse and wet clay is fed directly into the kiln, counter-current to the combustion gases. In the first section of the kiln, the material is dried. Lifters installed on the inside of the kiln enhance the contact between the material and hot combustion gases. Further along in the kiln, the material is continuously heated and finally calcined in the burning zone. The residence time of the material inside the kiln is approximately 30–60 minutes and can be influenced by the slope and rotational speed of the kiln. The substantially longer residence time in a rotary calciner compared to flash calcination means that the feed material can be much coarser and does not require much preparation (unlike the flash calciner).

After the kiln, the calcined material falls into a cooler of the rotary or grate type. Energy from cooling is recovered by using, all or part of the heated up cooling air as secondary air for the calciner. The cooling air is used for fuel combustion.

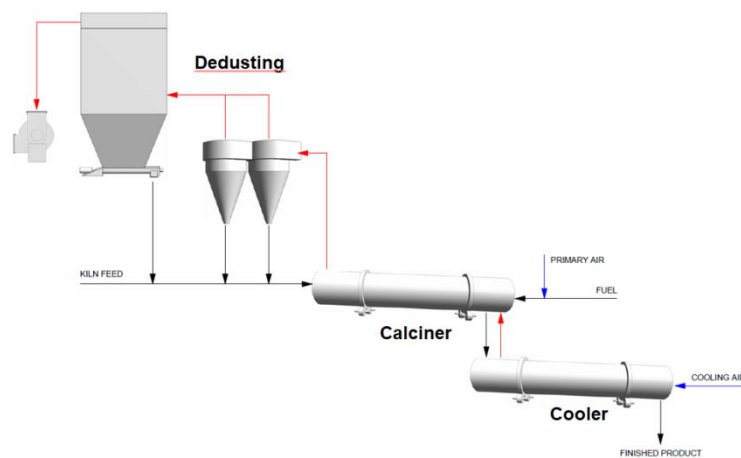


Figure 2-11: Simplified process for rotary calcination technology

## 2.7 Comparison of process technologies

In response to the growing interest in producing new SCMs, the leading technology suppliers are striving to develop process technologies specifically for clay calcination. To date, it has been difficult to identify any trends regarding the preferred technology. However, it appears that many large Western suppliers, including KHD, ThyssenKrupp and FLSmidth, prefer flash calcination over rotary calcination. The main reason might be the lower thermal energy consumption of the flash calciner and quality concerns about rotary calcination. Nonetheless, it is important to keep an open mind regarding the technology and to base the selections mainly on the parameters in Table 2-3.

Table 2-3: Selection criteria for available calcining technologies

Selection criteria	Rotary calciner	Flash calciner
Physical raw clay properties (clay preparation)	particle size: <30 mm moisture: <20 %	particle size: max. 2 mm (typically <0.2 mm) moisture: <20 % with an attached hammer dryer crusher, otherwise <2 %
Quality control	control is difficult due to varying feed size and potential over-burning at the burning zone	better due to finer feed and shorter heat exposure
Thermal energy consumption (estimated based on 15% moisture)	2'500 kJ/kg	2'000 kJ/kg
Electrical energy consumption	low	high
Retention time	typical 30 to 60 min	<5 s
Fuel availability and related firing requirements or concepts	limited potential for alternative fuels	limited potential for alternative fuels
Plant size	larger footprint	smaller footprint but significantly higher
Emissions	critical specific emission abatement equipment required	critical specific emission abatement equipment required
CO <sub>2</sub> footprint	higher due to higher thermal energy consumption	lower due to lower thermal energy consumption
Clay colour management	difficult (fuel injection in cooler)	difficult (fuel injection in cooler)
CAPEX	lower	higher

## 2.8 Summary of Chapter 2

SCMs offer an option for reducing the clinker content in cement and positively impacting the CO<sub>2</sub> footprint and cement properties.

The availability of the main SCMs, such as fly ash and clinker, will decrease significantly in the coming years. This scenario limits the hope of substituting cement and reducing CO<sub>2</sub> emission.

Calcining clay is an alternative to producing new SCMs. However, it creates other environmental challenges, such as exploiting valuable resources by opening new quarries.

Available technologies to calcine or thermally activate materials are rotary and flash calciners. Both technologies have disadvantages, which limit their use to environmentally non-critical materials.

Chapter 3 describes alternative locally available materials which have been investigated in the frame of this research. It is the intention to study if those materials can be thermally activated and can largely replace cement in the future. Additionally, in the frame of this research, the next chapter describes and investigates a new technology to thermally activate even those materials that are considered critical.

## Chapter 3: Alternative SCMs and a new method for activation

*Chapter 3 investigates possibilities for using locally available waste materials that can be thermally activated and converted to a circular economy SCM. Waste materials are often contaminated and difficult to dispose of. Once thermally activated, they should be able to develop hydraulic, latent hydraulic and pozzolanic reaction behaviour and could therefore substitute OPC substantially, reducing the CO<sub>2</sub> footprint. Calcination technologies for thermally activated materials, especially those with many volatile elements or contaminated materials, are currently unavailable. In response to this situation, Chapter 3 introduces a new ecologically friendly technology to process these materials.*

### 3.1 Introduction

In most cases, cement is used in locations relatively close to where it is manufactured. Therefore, the production of composite cements requires an available source of a pozzolanic or latent hydraulic material. This is true especially considering the steadily increasing substitution rates. The source can be either natural or synthetic. However, the local availability of such sources is not guaranteed in all regions where cement is produced, mainly because of the decreasing availability of certain sources of pozzolanic and latent hydraulic materials.

One suggested solution for providing a local SCM source is clay calcination and the production of LC3 cement. This cement comprises 30 % metakaolin, 15 % limestone, 5 % gypsum and 50 % clinker (Markert, 2021; Scrivener et al., 2018).

Some studies indicate an almost unlimited global availability of kaolinitic clay (Scrivener, John, et al., 2018). However, reality shows that in regions where fly ash and granulated blast furnace slag is becoming scarce, sources of kaolinitic clays of sufficient quantity and quality are limited. The map shown in Figure 3-1 indicates the global distribution of kaolinite. Especially in Europe, the content of kaolinite in soil is quite low. Other regions such as China, USA, central Africa or Brazil have a higher chance to explore kaolinitic deposits.

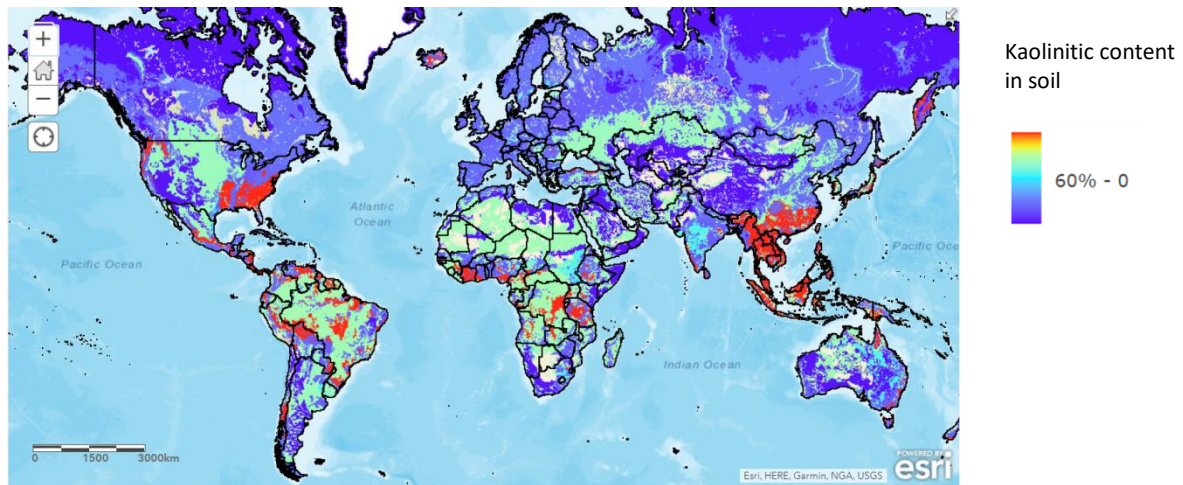


Figure 3-1: *Kaolinite content in soil and main kaolin deposits (Copyright Esri; Esri and the Esri logo are licensed trademarks of Environmental Systems Research Institute, Inc.)*

It would therefore be desirable to produce an alternative SCM predominantly based on waste products. Doing so could ensure local availability and avoid depleting natural resources. In response to this need, the current study investigates alternative SCMs produced from various waste products that are similar in chemistry and performance to metakaolin or burnt oil shale. Furthermore, it investigates a proposed process to recycle even difficult and partly contaminated waste products in an ecologically friendly way, thereby reducing the CO<sub>2</sub> footprint of composite cements.

### 3.2 Target of alternative SCM

In the burning of coal or oil shale, the main aim is to produce thermal energy and subsequently electrical energy. The produced ashes are theoretically an undesirable by-product. However, most of this ash shows latent hydraulic or pozzolanic reaction behaviour and can be used as an SCM.

During combustion of the coal and oil shale, a wide range of mineral impurities – such as lime, clay, feldspar, quartz and shale – fuse, cool and solidify as glassy particles. The resulting ashes are highly variable, depending on the composition of the original coal and oil shale impurities and the temperature at which the ashes are produced.

The objective here is to develop similar conditions regarding the composition of minerals, but to lower the activation temperature and to activate materials to produce an alternative SCM.

The anticipated raw materials may contain blends of locally available ingredients, comprising mainly

- marl
- limestone
- clay
- quartz
- calcium sulphates

One aim of this research is thus to investigate materials containing the above minerals which can be sourced from various waste streams providing at least one waste material selected from aggregate washing sludge, road cleaning sludge or deconstruction gypsum. All the above-mentioned waste material streams are currently mostly deposited in quarries or landfills and could therefore be turned into circular economy products. These waste materials are locally available in sufficient quantities. If a suitable mineralogical composition can be achieved, such materials could be thermally activated and could develop the desired hydraulic, latent hydraulic or pozzolanic properties required for the strength development of composite cements.

### 3.3 Waste materials

#### 3.3.1 Aggregate washing sludge

During the processing and washing of gravel and sand, millions of tons of clay, lime, silica or a mixture thereof are washed out annually. This material is called aggregate washing sludge (AWS) and is mainly disposed of directly into a sludge pond or lake inside the quarry (Figure 3-2).



Figure 3-2: Typical disposal of AWS in ponds (Schmitz, Röhling & Dohrmann, 2011)

In Germany alone, approximately 15 million tons of pre-processed and fine sludges are deposited annually. The volume estimated for central Europe is roughly 50 million tons (in solids). Additionally, every year approximately 150 million cubic metres of water are bound with the



clay; this water can often hardly evaporate or re-enter the ground due to the highly hygroscopic behaviour of clay (Krakow, 2012). Additionally, chemicals in the form of flocculants are introduced into the washing process to obtain better results and reduce the amount of water.

There are about 3'600 gravel and sand mining quarries in Germany alone. Hence, there is vast potential to use the locally available materials as SCMs. Schmitz, Röhling and Dohrmann (2011) analysed the AWS of 28 deposits for the brick industry and many of them included kaolinite and other clay materials that could be directly thermally activated. For instance, 16 of the analysed 28 AWS were suitable for the brick industry. The same AWS could also potentially be used as SCM (Figure 3-3).

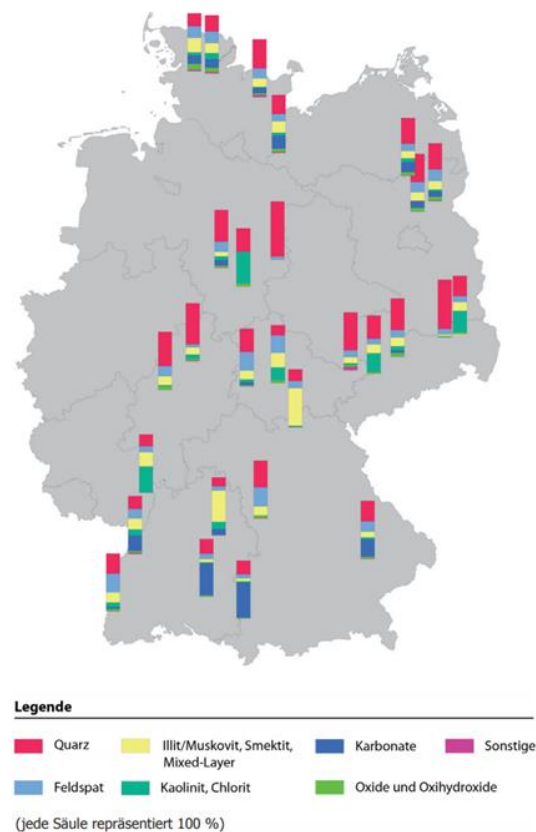


Figure 3-3: Mineralogical composition of 28 AWS samples in Germany (Schmitz, Röhling & Dohrmann, 2011)

### 3.3.2 Road cleaning sludge

Road cleaning sludge (RCS) is a waste material arising from road sweeping and road drainage (Figure 3-4). It is either collected in road cleaning trucks or special settling ponds, separating the solids from the drainage water. In many countries, the remaining sludge requires proper disposal; landfills are banned, and potential consumers of this material are urgently required.

The RCS contains many contaminants besides gravel and sand, including hydrocarbons and heavy metals, and is therefore unsuitable for most known processing technologies.



Figure 3-4: Left: Road cleaning truck (Kanton Luzern, 2013); Right: cleaning of road drainage (Cahans, 2017)

The author found no statistics describing the volume of RCS in Germany or Europe. However, considering the kilometres of roads, it can be assumed to be large. RCSs have especially been evaluated because of the high prices of CHF 200 (EUR 180) per ton in Switzerland which can be obtained for the proper disposal.

### 3.3.3 Deconstruction gypsum

Gypsum plasterboards are widely used in the construction sector, mainly for partition walls and ceiling panels in buildings. They comprise gypsum between paper linings; the boards may contain organic contaminants such as silicone, paint and impregnators or metals (screws, bolts and profiles). Their consumption has increased steadily in recent decades. According to Statista (2021), the production of gypsum plasterboards reached in Germany approximately 237 million m<sup>2</sup> in 2020, equivalent to approximately 2.4 million tons. Figure 3-5 shows typical pre-processed deconstruction gypsum (DCG), which can be obtained from a construction waste recycling plant.



Figure 3-5: DCS in a construction waste recycling plant

Against the background of a circular economy, the recycling of waste gypsum is of growing importance. For instance, in Switzerland, a regulatory framework for gypsum plasterboard recycling was introduced in legislation in 2016. It requires separating gypsum waste from general demolition and construction waste. Weimann, Adam, Buchert, and Sutter (2021) recently outlined the potential for recycling DCG boards, but most of this waste is still dumped in landfills. The reason is the low market prices for natural (new) gypsum.

### 3.4 Producing alternative SCMs

All the above-mentioned waste material streams are currently deposited mainly in quarries or landfills. The exception is RCS, which is sometimes burned inside municipal waste incinerators.

For highly contaminated waste streams, such as RCS and DCG, municipalities are urgently seeking solutions to avoid landfilling and polluting the environment.

Based on the specific waste and circular-economy material streams outlined above, two approaches were explored in this study for the production of an alternative SCM:

- 1) thermal activation of AWS with sufficient kaolinite content
- 2) thermal activation of AWS with insufficient kaolinite content; here, mainly calcite containing AWS are mixed with RCS and DCG to yield similar properties to calcareous fly ash (or other reactive products)

For AWS with a sufficiently high kaolinite content, one challenge is appropriate dewatering. The mechanical water removal of slurries that have a high clay content is generally difficult.

Due to the increasing reactivity and development of pozzolanic reaction behaviour, after dehydroxylation at 700°C–850°C, this AWS would be most suited to producing an alternative SCM. It does not require mixing with other materials to improve the reactivity if the kaolinite content is sufficiently high.

With insufficient kaolinite content or other potentially reactive clays, the investigation focused on transforming the above-mentioned waste materials into cementitious material. This was achieved by calcining AWS or RCS and increasing the reactivity of the cementitious material by adding a source of calcium sulphate, such as DCG, to the raw material mixture (Figure 3-6).

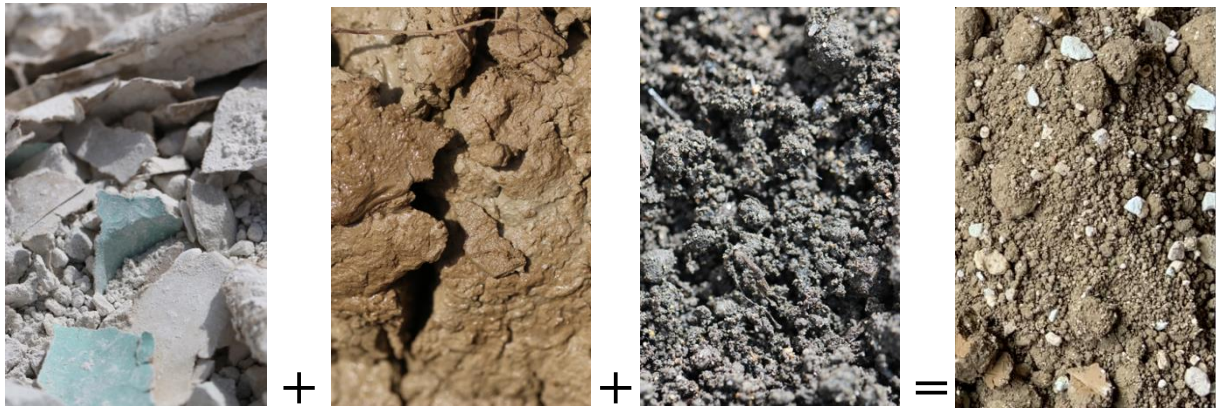


Figure 3-6: Possible mixture to produce an SCM without sufficient kaolinitic clay. Left to right: DCG, AWS, RCS, a mixture of materials

The selected source of calcium sulphate, which could be DCG, is calcined with the AWS and RCS. In this process, the sulphate source positively influences the reactivity of SCMs with latent hydraulic reaction behaviour (Gruskovnjak, 2006; Locher, 2000). Additionally, DCG was considered based on processing an anthropogenic material and the formation of calcium sulphate (anhydrite) and subsequently the substitution of natural gypsum in the final cement product. The thermal treatment of the DCG above 400 C is essential. Tests using untreated gypsum boards to replace natural gypsum in cement have been conducted, showing a significant reduction in the cement compressive strength, attributed to the high content of organics, including paraffin waxes and silicones. Mortar tests with the thermally treated DCG showed the same strength development as geogenic gypsum from a natural deposit (Kruspan, Bier & Weihrauch, 2022).

### 3.5 Thermal activation of alternative SCMs

With increasing rates of clinker substitution, SCMs are required where cement is produced. Transporting the SCM over long distances is expensive and installing stand-alone manufacturing facilities is only attractive if SCMs are produced on a large scale and can be distributed to several cement plants or grinding stations to reduce investment cost (CAPEX) and operational cost (OPEX).

The small sizes of many deposits make the integration of a calciner in an existing cement plant the most attractive solution. Currently, flash and rotary calciners are the most widely considered

technologies within the cement industry. However, these technologies have certain disadvantages, which make them unsuitable for many raw materials – unless substantial CAPEX is invested into material preparation, environmental control and colour management.

### **3.6 Limitations in current calcining technology**

The global trend should ideally be towards expanding the production capacity for SCM. In reality, new projects for calcinating clay or other SCMs are far more limited than new clinker kiln lines. The reasons for this imbalance could be limitations in the flash or rotary calciner technology, such as:

- difficulty in controlling emissions
- challenges in material preparation
- requirements for high quantities of noble fuels
- difficulties in colour control

#### **3.6.1 Difficult emission control**

##### 3.6.1.1 Particulate emission

Modern bag filters equipped with membrane bags would allow non-critical particulate emission below 10 microns, regardless of the selected calciner technology.

##### 3.6.1.2 Gaseous emission

Gaseous emissions occur from two sources:

- the feed material
- fuels

Because minerals such as clay are formed by chemical weathering or hydrothermal decomposition of silicate-bearing rock (such as granite), their compositions vary significantly. In addition to the type of base rock and its decomposition process, several other factors play a role. Clay becomes mixed with many other materials before it reaches the final deposit, and the mixture may influence the emissions once thermally treated in a calciner.

Clays are already widely used in cement clinker production to correct the quality of the limestone and yield the appropriate chemical composition of a raw material. Therefore, clays have been intensively studied globally. Often they contain high levels of volatile elements, causing emissions of SO<sub>2</sub>, CO, VOC, HCl, HF, NH<sub>3</sub>, dioxins, mercury and other heavy metals.

For weathered clays and those exposed to aerobic conditions (i.e. where free oxygen is present), emissions might be less critical. The reason is that some of the relevant volatile components could have been partly oxidized and leached off.

Apart from dust control, none of the currently available calciner technologies – such as flash or rotary calciners – are currently suitable for controlling gaseous emissions. The reason is that all the gases are used for combustion, drying and preheating. In addition, the gradual increase in the temperature of the material allows volatile elements (such as organics, sulphur and heavy metals) to evaporate and exit with the exhaust gas.

Many emissions are critical and would exceed the legal limits unless complex and expensive additional abatement measures are implemented. It is expected that the emission levels will be similar for conventional rotary and flash calciners.

Furthermore, it is unclear how clay calciners might be regulated in the future. The regulations for cement kilns that co-incinerate waste may apply under the European Industrial Emission Directive (IED) or the Ceramics covering Best Available Techniques (BAT). Such kilns mainly produce ceramic products, bricks, expanded clays and refractories. The norms are crucial since clay might include elements with low emission limits in the cement industry. Such limits might not be achievable for clay calcination where, for example, fluorides produce hydrofluoric acid (HF; Voicu, Ciobanu, Istrate, & Tudor, 2020). For calciners located in a cement production facility, such as a cement plant or grinding station, cement production emission norms are likely to apply.

### **3.6.2 Challenging material preparation**

Clay and other potential calcination materials contain several minerals that influence the physical properties (e.g. quartz, feldspar, calcite, sulphates and iron). While the rotary calciner can accept relatively larger particles of <30 mm, the flash calciner can only accept a feed of <2 mm. For a larger feed size, crushing or comminution is required.

The flowability is a challenge to be considered in the upstream processes, especially regarding the receiving, storage and transport. Moist material with higher than 15 % water content is usually highly adhesive and sticks to conveyors, chutes and bins. Lessons learned from the clay industry must be considered for the preparation stage to avoid process interruptions. Especially challenging might be the processing of clay in areas with low temperatures in winter; extremely soft clay typically becomes a hard rock once frozen.

The crystalline quartz content of clay can be as high as 50 % and the quartz usually occurs in a coarser fraction of >2 mm. Hence, abrasion should be considered, especially for selecting the crushing and grinding equipment and its wear protection measures. Many suppliers offer a high-speed hammer dryer crusher to grind feed material of up to 50 mm; however, this option might be challenging considering the wear rate.

Depending on the properties of the clay, for the flash or rotary calciner, substantial additional installations might be required to process the material before calcination.

### **3.6.3 Demand for noble fuels**

Generally, the typical process temperature for the activation of clay minerals is with 700-850 °C and short retention time in this temperature zone very critical for the proper and complete, emission-free combustion of fuels.

In flash calciner systems, “direct firing” refers to introducing the fuel directly into the calciner. Given the minimum gas retention time in a flash calciner of typically 5 seconds, only easily burnable, fast igniting noble fuels with high heating values and volatility, such as natural gas or coal, can be used. These fuels are expensive, have a high CO<sub>2</sub> footprint and require additional infrastructure – such as a gas pipeline or coal grinding system.

“Indirect firing” refers to firing via a separate hot gas generator system. In such cases, lower quality and alternative fuels can be considered but investment cost will be significantly higher.

A rotary calciner is usually fired directly by a dedicated burner system. Due to the open flame of the burner with a high flame temperature, less expensive alternative fuels with lower quality could also be burned in a rotary calciner.



Special consideration must be given to the fuel and introducing the fuel into the calcination system. Obtaining and preparing suitable fuels can significantly impact the investment and production costs of the calciner system.

### 3.6.4 Difficult colour control

A limiting factor is that many AWSs have an  $\text{Fe}_2\text{O}_3$  content of around 2 %–9 % or even higher. If calcined in an oxygen-rich atmosphere, these produced SCMs turn red. Only by creating a reducing condition with little or no oxygen, the colour of the clay can be controlled (Figure 3-7). Due to expected reduced acceptance, cement producers avoid selling cement that displays a non-traditional grey colour.



Figure 3-7: Tests conducted with different oxygen levels from (left) fully oxidizing to (right) reducing conditions

Many rotary or flash calciner manufacturers control the colour by injecting liquid fuel at the exit of a rotary kiln or the cooling cyclones of a flash calciner while the calcined material exits. This causes the material to combust, exhausting the oxygen available during the cooling process (Figure 3-8). Controlling the calcination atmosphere enables the production of a grey or black calcined clay rather than a red material. The reactivity and properties of red and black clay are similar (Martirena Hernández, Almenares-Reyes, Zunino, Alujas-Diaz, & Scrivener, 2020).

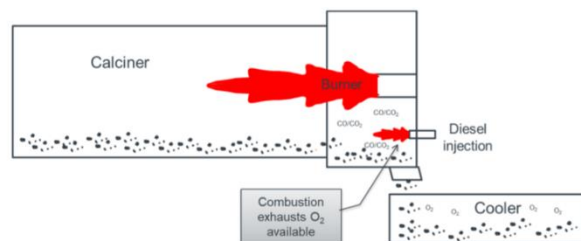


Figure 3-8: Creating a reducing atmosphere during cooling in a rotary calciner (Martirena Hernández et al., 2020)

Hence, injecting diesel or other easy-burning noble fuels during the cooling stage of a rotary or flash calciner is a possibility for controlling colour. However, it will impact production costs and emissions.



### 3.6.5 Strict temperature control

Because SCMs such as metakaolin are formed within a relatively small temperature window, between 700 °C and 850 °C, the temperature inside the calciner is critical and sometimes in conflict with the proper combustion of fuels. Peaks above 900 °C can quickly create structures such as spinel or mullite, creating melting phases and agglomerating to larger boulders (Figure 3-9). In addition to the loss of hydraulic properties due to over-burning, these large blocks are extremely difficult to handle in industrial processes. The difficulty in controlling the burning temperature and the long retention times inside the burning zone mean that a rotary calciner is more likely than a flash calciner to be affected by this issue.



Figure 3-9: Formation of mullite balls due to high burning zone temperature in a rotary calciner

### 3.6.6 CO<sub>2</sub> footprint of calciners

The main reason for increasing the volume of SCMs in cements is to lessen the CO<sub>2</sub> footprint. For each ton of cement clinker, approximately 850 kg of CO<sub>2</sub> is released into the atmosphere. Approximately 55 % of the CO<sub>2</sub> development is associated with the decarbonization of calcium carbonate and consequent release of CO<sub>2</sub> ( $\text{CaCO}_3 \rightarrow \text{CaO} + \text{CO}_2$ ). The remaining 45 % of CO<sub>2</sub> is associated with burning fuels, heat losses and electrical energy required to produce clinker.

Substituting at least part of the cement clinker with SCMs can thus have a strongly positive effect in terms of reduced CO<sub>2</sub> emission. The lowest footprint is currently achieved by substitution of clinker with fly ash or granulated blast furnace slag, since the CO<sub>2</sub> tag of these industrial by-products is counted as zero. However, with the increasing cost of CO<sub>2</sub> it is expected

that fly ash and granulated blast furnace slag will eventually be charged with a CO<sub>2</sub> tax, resulting in a more negative impact on the produced composite cement.

For clay calcination, the CO<sub>2</sub> footprint depends on the thermal efficiency of the applied calciner technology and the fuel as well as impurities in the limestone or dolomite. If no limestone or dolomite impurities are present, the flash calciner has a larger net CO<sub>2</sub> footprint than the rotary calciner. More noble fuels are required for fast combustion within a few seconds and with lower combustion temperatures inside the flash calciner. The rotary calciner, with its higher flame temperature, can probably burn more alternative fuels that have less volatility and heating value, such as biomass with no net CO<sub>2</sub> contribution. Therefore, despite a higher thermal energy consumption, the rotary calciner will emit less CO<sub>2</sub> (Table 3-1). Because of very limited industrial applications for both technologies, operational data are estimations only which were based on the discussions with several suppliers.

Table 3-1: Net CO<sub>2</sub> emission per t of calcined clay depending on calcining technology (Based on net CO<sub>2</sub> contribution of 96 kg CO<sub>2</sub>/GJ for coal and 0 kg CO<sub>2</sub>/GJ for Biomass)

	<b>Rotary calciner</b>	<b>Flash calciner</b>
Heat consumption	2'500 kJ/kg	2'000 kJ/kg
CaO/MgO in product	0 %	0 %
Fuel mix	50 % coal or other noble fuel 50 % biomass	100 % coal or other noble fuel 0 % biomass
<b>Net CO<sub>2</sub> emission per t of calcined clay (fuel only)</b>	<b>0.12 t CO<sub>2</sub>/t clay</b>	<b>0.19 t CO<sub>2</sub>/t clay</b>

### 3.7 Proposed new method of calcination

Because of the described disadvantages of existing calcining technologies, this research has investigated a new technology which will have the following objectives:

1. Develop a method for producing cement clinker and an SCM in one integrated system.
2. Partial use excess thermal energy from the clinker production process.
3. Dry the material sufficiently before it enters the calcination process, to avoid elevated air flows and disturbances in the cement clinker production.
4. Recycle highly contaminated materials in an ecologically friendly way.
5. Recover most of the cooling energy for drying, using heat-exchanging screws connected to a thermal oil system.

6. Control the colour of the SCM by reducing iron oxidation and thus limiting the red colour of the product.
7. Reduce the CO<sub>2</sub> footprint of composite cements.

The core process is illustrated in Figure 3-10. It is based on the concept of combining two production lines to 1) enable the recycling of partially contaminated waste products and 2) produce an SCM in an ecologically friendly way by combining the gas streams of both systems. In the clinker production line ①, Portland cement clinker is produced conventionally by preheating raw meal and subsequently calcining the preheated raw meal in the clinker rotary kiln (WO2021/124261, 2021).

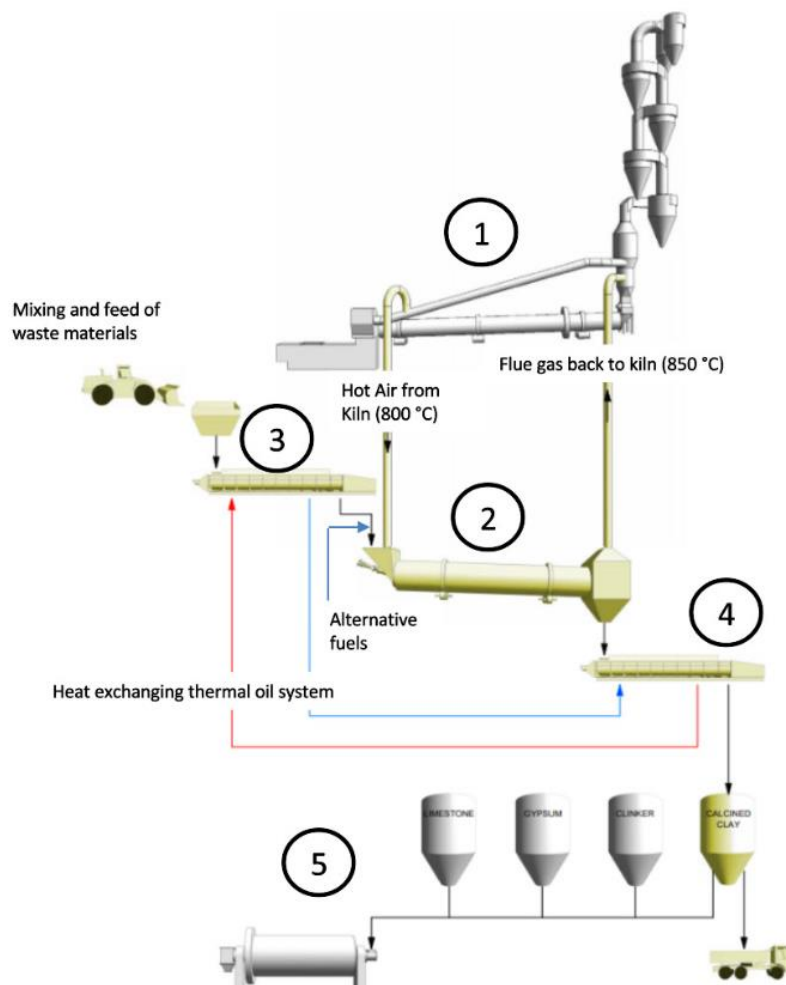


Figure 3-10: Simplified model of the integrated SCM calciner

The SCM is produced in a separate but connected production line, which comprises an integrated SCM calciner for calcining ②. The new method provides a drying step before the calcination step to process SCMs that have high water content. Synergies are exploited between the two production lines to increase energy efficiency and reduce the environmental impact.

According to the first aspect of synergies, the surplus heat of the clinker production line is used as a heat source in the calcining step to calcine the SCM. This means the external energy input for calcining the raw material can be reduced significantly.

According to the second aspect of synergies, the integrated SCM calciner ② exhaust gas originating from the calcining step is introduced into the clinker production line ① for the secondary combustion. Thus, contaminants in the exhaust gas of the calcining step can be thermally decomposed at 850-1000 °C or can be integrated into the solid material (raw meal, clinker) present in the clinker production line. These steps prevent the contaminants from escaping into the environment via the exhaust gas.

The raw feed material is dried in a set of drying screws ③ to reduce the amount of free water, from the typical <20 % to ideally <5 wt %. The water will be separated inside the drying screw is filtered and can then be condensed, treated or released into the atmosphere.

The drying screws ③ heat the feed material and remove the water via a circuit of a heat transporting liquid, such as thermal oil or water, which is circulating with the shaft and the flyers or body of the screw.

By separating excess water from the raw material, the thermal energy consumption for the thermal treatment process is minimized. In addition, the impact of the clinker production is minimized.

The dryer ③ and cooler ④ are operated in a heat-exchanging relationship. The heat drawn from the SCM during the cooling step ④ is used as a heat source for drying the raw material in the drying step ③. This process recovers the thermal energy withdrawn from the calcined SCM in the cooling step ④.

The integrated SCM calciner ② is ideally operated at approximately 700 °C–850 °C partly using excess heat derived from the clinker production line. Alternatively, the integrated calciner

comprises a burner or mechanical feeder fed with fuel, ideally 100 % alternative (renewable) fuels.

Raw material for producing the desired SCM, such as AWS and RCS, often contains iron oxide in small quantities, which may cause the final product to have a red colour. When mixed with Portland cement to produce a composite cement, red may be undesirable for mainly aesthetic reasons. The red colouring is due to the presence of iron (III) in the SCM product. The integrated SCM calciner ② and screw cooler ④ should ideally be operated in a reducing atmosphere that transforms iron (III) into iron (II) to avoid a red colour.

After calcination and cooling, the newly produced SCM is transported and stored. Ideally, it is then separately ground in a mill ⑤ before being mixed with cement to produce a composite cement.

### **3.7.1 Feed material handling**

The AWS and RCS are expected to be highly cohesive. Special measures must be taken to allow continuous and spillage-free transport, storage and operation. In addition, a moisture content of up to 25 % is considered the maximum permissible moisture for the calcination process.

Most of the feed is expected to comprise fine pieces. However, large foreign bodies of up to 200 mm like stones or wood particles can be expected. Before entering the process, the material must be deagglomerated and crushed with a mineral sizer to control the maximum feed size that enters the manufacturing process.

### **3.7.2 Thermal heat-exchange system**

The concept of the proposed drying system is to connect the cooling and drying screws to exchange heat efficiently. The following heat-exchange system was developed and is illustrated in Figure 3-11.

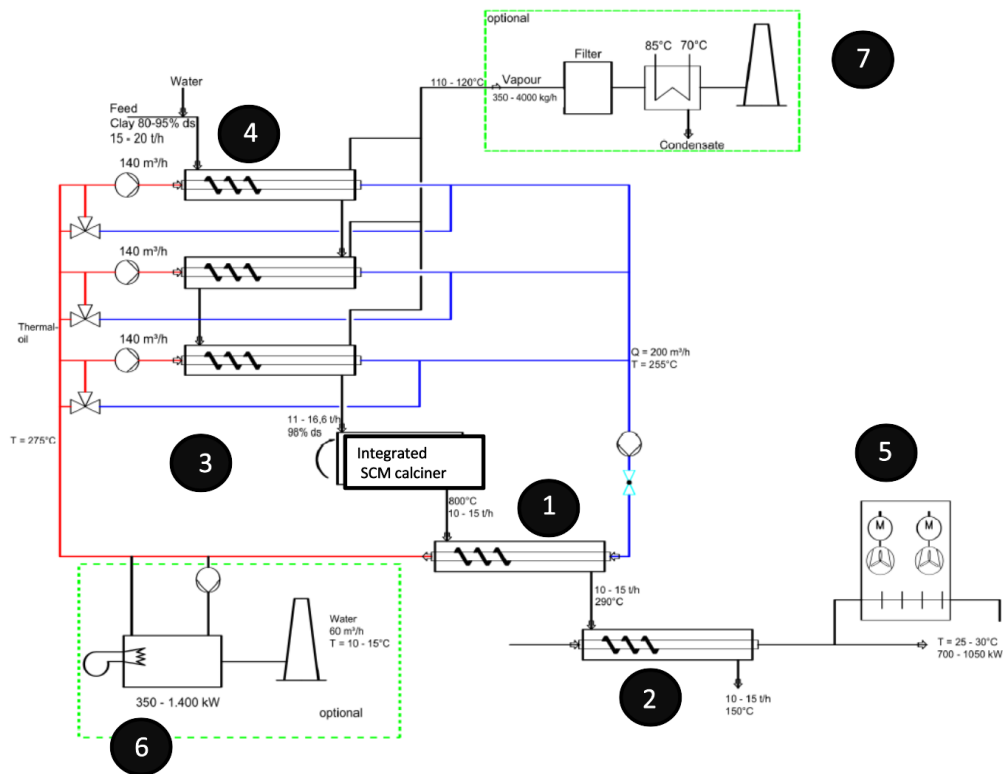


Figure 3-11: Simplified flow diagram of heat-exchange system

The thermal heat-exchange system functions as follows:

- A. Cool the thermally activated material in the first stage to approximately 290 °C with a thermal oil-operated cooling screw ①; then, in a second step with another cooling screw, cool it to <math><150\text{ }^\circ\text{C}</math>. The second cooling screw is operated with water ②. The material (“product”) is received from the integrated SCM calciner ③ and subsequently discharged by the cooling screws to the transport equipment.
- B. Dry the wet input material to an integrated SCM calciner ③ with a set of three drying screws. The drying screws ④ are arranged in a sequence. The material is heated stepwise until water is evaporated and leaves the drying screw for the next process step (intermediate storage).
- C. Heat is transferred from the first stage of the cooling to the three drying screws ④ in a closed loop via a heat transfer medium (thermal oil). The second cooling stage is operated as a closed water circuit, using an adiabatic cooling tower ⑤ to reduce the temperature in the water circuit.

D. An additional heater ⑥ in the thermal oil circuit heats the system to operating temperature. The heater remains hot in case of short production interruptions. The heater can also use waste heat sources of the connected clinker production plant.

E. A system collects, transports, filters and condenses the steam that is evaporated at the drying screws. It also removes the oil from the contaminated water ⑦.

### 3.7.3 Clay calciner design

This section focuses on the design considerations of the investigated calciner. The central focus of the new method is to connect the integrated SCM calciner to the existing kiln system.

The calciner receives hot air at approximately 800-900 °C from the cement clinker kiln tertiary air duct. The air is used for pre-heating of material and the contained oxygen is used for combustion of fuels inside the calciner. The flue gases exiting the calciner are then returned back into the cement clinker kiln process. Raw material, fuel, air and combustion gases travel through the integrated rotary calciner in co-current flow. The general set-up of the integrated SCM calciner system and its integration into the clinker kiln are illustrated in Figure 3-12:

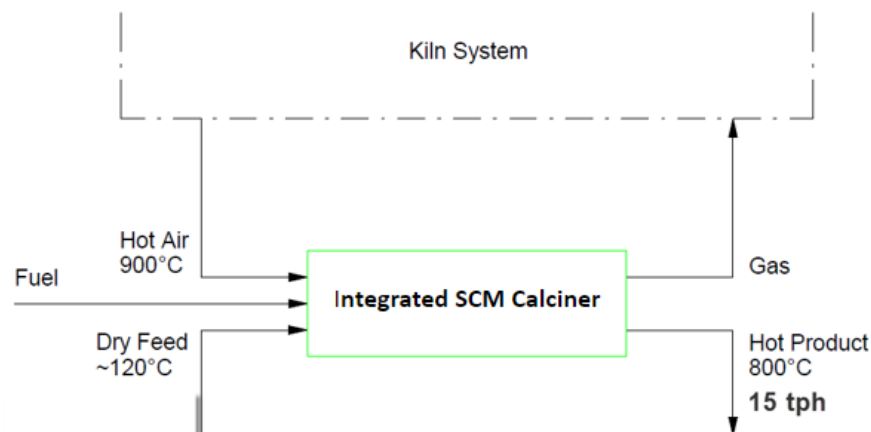


Figure 3-12: Simplified scheme for connecting the integrated calciner system with the cement clinker kiln

The integrated SCM calciner possesses lifting elements in the first approximately 40 % of its cylindrical portion. The intention is to expose material and fuel intensively to the hot air from the clinker kiln tertiary air duct; dry it completely, if required; and simultaneously start the ignition of the fuels and heat transfer to the material to start the thermal activation process. The advantage of mixing the fuel with the material is an equalized temperature distribution to avoid

temperature peaks that can cause overheating, especially of clay minerals. Combustion does not need to be rapid, and coarse fuel with a moderate net calorific value (NCV) is preferred to avoid local overheating.

The second part of the integrated SCM calciner provides sufficient temperature and residence time for the complete burnout of the fuel and thermal activation of the material. The low gas velocity enables the separation of the material from the flue gases to a large extent. The main process control parameter for the energy input is the temperature of the flue gases at the exit of the integrated SCM calciner.

The hot air from the clinker kiln (approx. 800 °C–900 °C) is theoretically sufficient to ignite the fuels. However, if required, a separately injected reactive fuel from a small burner at the kiln inlet (e.g. liquid fuel, gas, used oil) helps to elevate the temperature, removes the remaining moisture from the feed material, ignites the coarse fuel and generally controls the process and variations. The heat input from this fuel is expected to account for up to a third of the total heat input.

Unburned fuel particles are not extracted from the integrated SCM calciner by the draft passing through it. The draft is <4 m/s. Therefore, fuels with a high proportion of particles having low particle density must be avoided. It is assumed that a typical coarse calciner fuel, such as wood chips, would be suitable.

Chlorine and sulphur from the fuel and the feed material may be incorporated into the final product. Alternatively, they may potentially be transferred in considerable amounts via the flue gas of the integrated SCM calciner to the clinker kiln.

### **3.7.4 Grinding**

Grinding of the produced SCM is proposed for two main reasons:

1. To allow pneumatic transport of the calcined clay
2. Grinding the produced SCM separately optimizes the performance of the cement since clay for instance can be over-ground quite significantly if it is ground together with cement clinker



Crystalline quartz is a new mineral for cements with alternative SCMs. Because fine silica of less than 3 microns can cause health problems; this results in a challenge regarding selling the cement without specific precautions.

### **3.8 Summary Chapter 3**

The trend in the cement industry to calcine clay and produce metakaolin as an SCM is highly positive; it can reduce the clinker content and limits the CO<sub>2</sub> footprint for cement. However, the availability and quality of suitable clays are limited in many regions of the world. Additionally, exploiting clay from natural deposits should be avoided. Clay plays an important role in nature and is a fertile soil that – besides its rich mineral composition – preserves the water content.

Rather than exploiting natural deposits, the industry must consider the use of waste products and products from the circular economy. Examples are washing sludges from the aggregate industry or DCG boards. Using such sources would help to reduce the ecological footprint of the cement industry.

Thermal activation at 700 °C–850 °C is required to develop the cementitious properties of materials such as clay. Existing activation and calcination methods have limited suitability. In response to this situation, a new methodology was developed to activate difficult and contaminated materials in an energy-saving and ecologically friendly system. The system has been patented and is further investigated in the next chapters.

## Chapter 4: Theoretical Considerations

*Chapter 4 discusses the targeted mineralogical composition and cement properties and evaluates the key design parameters of the new calcination method. An industrial size calcining system is modelled and integrated into an existing clinker kiln system. The chapter explains the energy efficiency of the autonomous heat-exchange system and the positive impact of pre-drying on the performance of the cement kiln. Additionally, the theoretical background for using contaminated raw materials and fuels is discussed, and the system's capacity to eliminate major emissions is demonstrated. Finally, the positive effect on CO<sub>2</sub> emissions related to the new calcining method is outlined at the end of the chapter.*

### 4.1 Material considerations

#### 4.1.1 Composition of alternative SCM

The targeted alternative SCM covers an area of reaction behaviour in the CAS diagram that ranges from hydraulic to latent hydraulic and/or pozzolanic (Figure 4-1). Depending on the mineralogical composition, the produced alternative SCM shows specific or mixed reaction behaviours. This diversity is related to the fact that the produced materials range from calcined clay (pozzolanic) to calcareous fly ash (latent hydraulic) and materials similar to burnt oil shale (hydraulic). These points were described in Chapter 2.

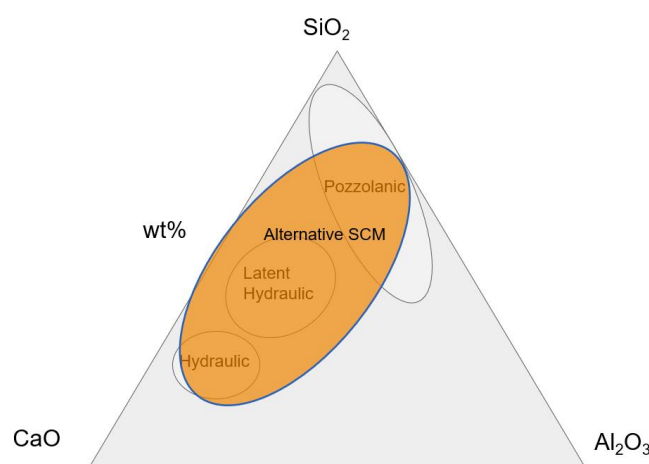


*Figure 4-1: Target area to produce alternative SCM shown in a ternary CAS phase diagram.*

In a finely ground state, the targeted materials such as kaolinitic AWS or the alternative mixture of AWS, RCS and DCG could develop pronounced pozzolanic properties like metakaolin or

hydraulic properties which are known from the reaction of clinker phases (i.e. belite) with water.

The main target of the hydraulic, latent hydraulic or pozzolanic reaction is the desired formation of calcium silicate hydrates (CSHs). These are primarily responsible for the strength in cements (Figure 4-2). Hydraulic reactions require water to produce the desired CSH.

Pozzolanic materials do not harden when mixed with water; however, when finely ground, they react with dissolved CH to form CSH and CSAH components. These compounds are similar to those formed in the hardening of hydraulic materials. Therefore, the pozzolanic reaction depends on a prior hydraulic reaction and sufficiently produced calcium hydroxide (CH) in order to react as illustrated in Figure 4-2. To make full and ideal use of the reaction and strength potentials, one need to strike the correct balance between hydraulic and pozzolanic reactions for cements.

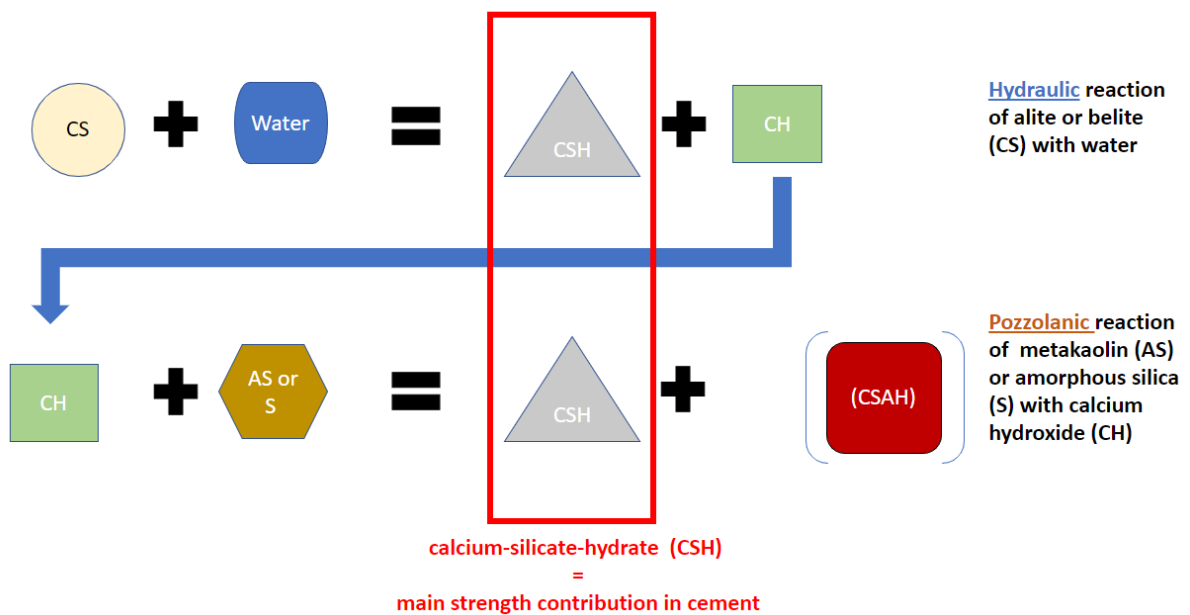


Figure 4-2: Interaction of hydraulic and pozzolanic reactions

#### 4.1.2 Anticipated products and characteristics

It was an objective of the study to develop an alternative SCM that is suitable to produce a cement that fulfils performance requirements. The composition and the mechanical and physical properties defined in the relevant cement standards were particularly important. The standard applicable for most European countries is EN 197-1.

Because the approach to thermally activate and produce SCMs from waste materials is a rather new development, the European Norm EN 197-1 does not specifically consider all alternative SCMs. For instance, LC3 cements (see Chapter 2) could together with limestone develop a strength that is superior to OPC, but the standard continues to limit the substitution of clinker to a maximum of 35 % in the case of CEM II/B. Other cement types that allow higher amounts of pozzolanic material, such as CEM IV/B, do not allow the further addition of limestone. Cement types that allow clinker substitution with pozzolanic materials and the rates are shown in Table 4-1.

Table 4-1: Maximum allowable clinker replacement in cement according to EN 197-1

Relevant cement types based on EN 197-1	Max. allowable clinker replacement in cement
CEM II/A-Q	6–20 %
CEM II/B-Q	21–35 %
CEM IV/A	11–35 %
CEM IV/B	36–55 %
CEM V/A	18–30 %, Gbfs addition required
CEM V/B	31–49 %, Gbfs addition required
CEM II/A-T	6–20 % Burnt shale
CEM II/B-T	21–35 % Burnt shale

The North American standards (ASTM) are more flexible about the composition and content of SCMs. For instance, ASTM-C618 permits an unlimited calcined pozzolana content (ASTM International, 2020). A new European standard (EN-197-5) allowing for higher substitution rates is currently in the approval phase and is expected to be released in 2022.

In terms of strength development, the standard strength of a cement is the compressive strength after 28 days, determined in accordance with EN 196-1. The strength must conform to the requirements in Table 4-2. The early strength of a cement refers to the compressive strength determined in accordance with EN 196-1 at either Day 2 or Day 7; this strength must also conform to the requirements in Table 4-2. Three classes of standard strength are included: Class 32,5, Class 42,5 and Class 52,5 (see Table 4-2; European Committee for Standardization, 2011, S. 1-38). The concrete later produced with alternative SCM and tested in the frame of this research shall comply with the EN 196-1 requirements in terms of strength.

Table 4-2: *Mechanical and physical requirements given as characteristic values (European Committee for Standardization, 2011, S. 1-38)*

Strength class	Compressive strength MPa			
	Early strength		Standard strength	
	2 days	7 days	28 days	
32,5 N	-	$\geq 16,0$	$\geq 32,5$	$\leq 52,5$
32,5 R	$\geq 10,0$	-		
42,5 N	$\geq 10,0$	-	$\geq 42,5$	$\leq 62,5$
42,5 R	$\geq 20,0$	-		
52,5 N	$\geq 20,0$	-	$\geq 52,5$	
52,5 R	$\geq 30,0$	-		

## 4.2 Process considerations

The production of alternative SCM requires similar steps to those of the production of regular cement. These steps include:

- Material receiving, crushing and handling
- Material drying
- Thermal activation or calcination
- Emission control
- Cooling
- Grinding

Additionally, as a special requirement for the proposed calcination method, the following points are investigated:

- Integration of the system into an existing clinker kiln
- Colour control of the final product

The following paragraphs discuss the requirements and theoretical background regarding the selection and sizing of equipment. The theoretical benefits of the new calcining method are also examined.

### 4.2.1 System capacity

The goal of the theoretical investigation and testing of the proposed calcining technology was to design a system that

- can produce about 100'000 t of alternative SCM per year
- resulting in about 15 tph production capacity

With a net availability index (NAI) of the cement clinker kiln of 90 % and a NAI of the calciner system of about 85%, an overall NAI of the system of approximately 75 % was assumed

The relevant calculations are shown in Equations 4.1 and 4.1a. The following theoretical considerations are therefore based on the desired design capacity of about 15 tph.

$$\text{production capacity (tph)} = \frac{\text{yearly production (tpy)}}{\frac{\text{days}}{\text{year}} \times \frac{\text{hours}}{\text{day}}} \times \frac{100 \%}{\text{NAI}} \quad (4.1)$$

$$\text{production capacity (tph)} = \frac{100'000 \text{ tpy}}{\frac{365 \text{ days}}{\text{year}} \times \frac{24 \text{ hours}}{\text{day}}} \times \frac{100 \%}{75 \%} \sim \mathbf{15 \text{ tph}} \quad (4.1a)$$

### 4.2.2 Material characteristics

For the theoretical modelling of the system, a feed material with the following characteristics was considered:

- Feed Moisture: approx. 17 %
- Granulometry: 95 % < 200 microns, 100 % < 200 mm
- Mineralogy:
  - 40 % kaolinite
  - 40 % quartz
  - 20 % others
- Fuel: wood chips 95 % < 80 mm with a heating value of 14'000 kJ/kg (14.0 MJ/kg)

Due to the character of the installation, some variations in the material characteristics and ambient conditions must be considered for the dimensioning of the industrial process.

### 4.2.3 Material receiving, crushing and handling

Once received in the production facility, the materials will be stored in a closed storage area and then crushed to a particle size of below 30 mm. Relatively large metal contaminations are removed by means of a metallic separator and metal detector. After these pre-processing activities, the feed material is fed to the drying screws, calciner and cooling screws, which are described in the following paragraphs.

### 4.2.4 Thermodynamic modelling

Proper thermodynamic modelling is important to set the basis for equipment dimensioning and energy estimation. The system's effect on the proposed integrated clinker production system must also be assessed. The mass and heat balances are essential for the future commissioning and operation of the plant since mass and heat balance will provide essential operation parameters.

The investigated rotary calciner is a complex and interconnected production system. Hence, the overall mass and energy balance must consider the following aspects:

1. Preparation of a simplified process flow diagram, including
  - a. Splitting the total system into discrete subsystems and setting the balance boundary limits
  - b. Illustration of mass and energy streams entering and leaving the subsystems
2. Calculation and simulation of individual mass and energy streams
3. Balancing the mass and energy streams, considering the following main simple rules, which are true for continuously running systems where no material and energy is being stored (Equation 4.2 and 4.3):

$$\sum \text{Heat in} = \sum \text{Heat out} \quad (4.2)$$

$$\sum \text{Mass in} = \sum \text{Mass out} \quad (4.3)$$

The preparation of a simplified process flowsheet and clear definition of the balance limits inside the production process are essential tasks. The balance limit can be considered as a black box, in which all mass and energy flows passing the defined envelopes can be highlighted; later, the values can be used in calculations to balance the mass and heat streams.

In the case of the proposed integrated rotary calciner, a simplified flow diagram is shown in Figure 4-3. The diagram considers the following two mass and energy boundaries:

1. Material drying and cooling balance
2. Calcining balance

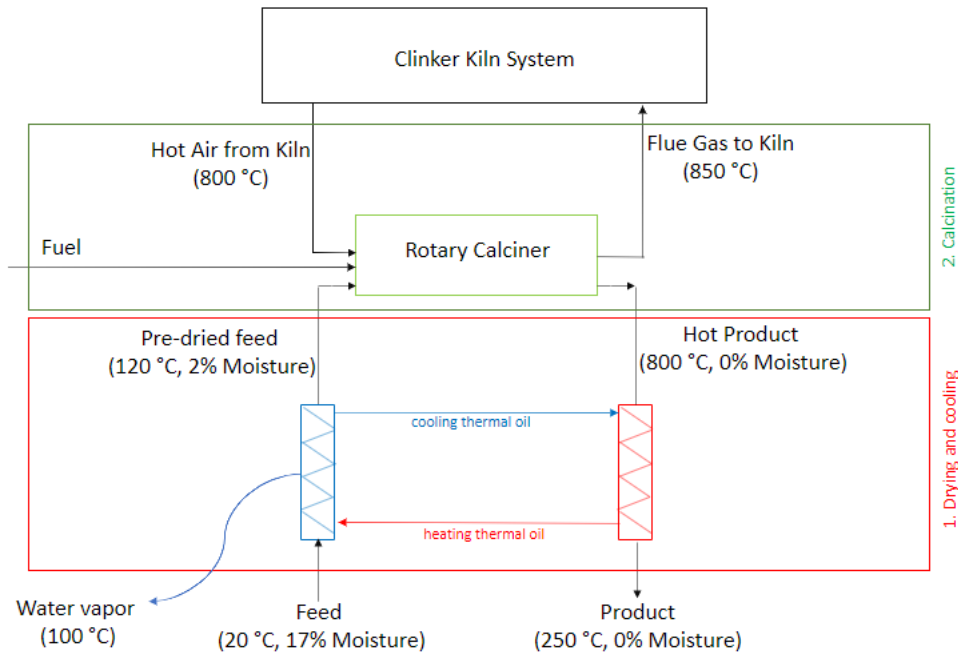


Figure 4-3: Simplified process flow diagram and boundary limits of subsystems for 1) drying and cooling and 2) calcination

The nature of an industrial process is that many uncertainties and variations exist regarding the operational conditions, such as moisture, chemical and mineralogical conditions, fuel properties and ambient conditions. Therefore, the results of the mass and gas balance calculations shown below must sufficiently consider the safety margins and must include sufficient flexibility to react to variations.

#### 4.2.4.1 Mass balance

Mass balancing is an important approach to account for a material (or mass) that enters or leaves the system. The mass balance provides the basis for heat balances; the energy required for heating, cooling and calcining; and the dimensioning of the equipment.



For the case of the integrated calcination system, a mass balance was prepared based on the targeted final production rate of about 15 tph (Figure 4-4). It considers the material flows entering or leaving the system.

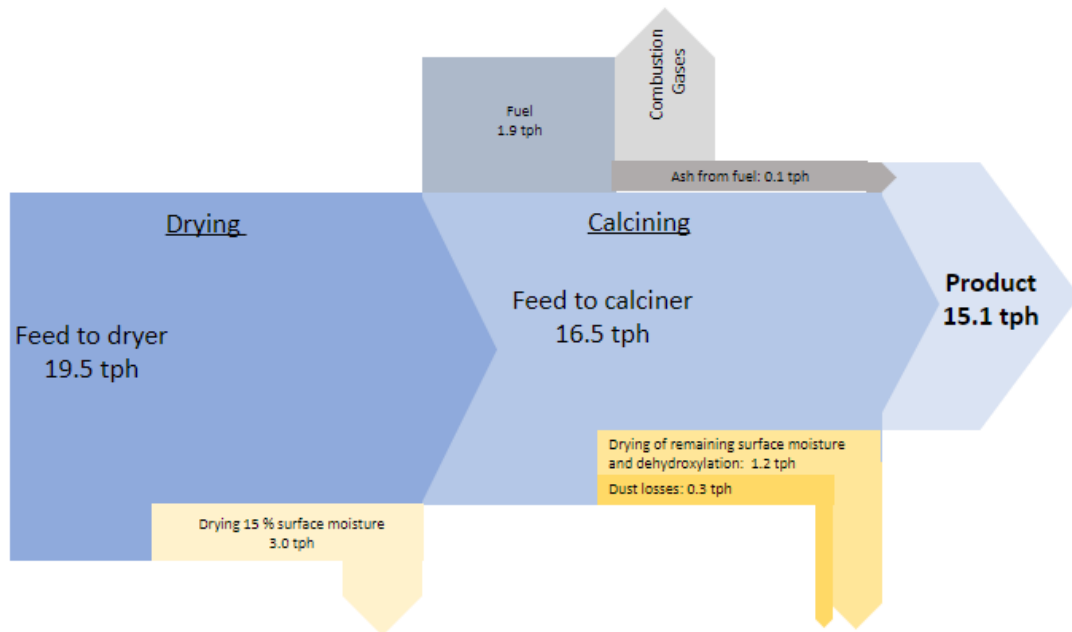


Figure 4-4: Mass balance of drying and calcining process

The mass balance is the result of numerous iteration steps and a combination with the heat balance to achieve the desired 15 tph final product capacity.

1. **Drying Process:** Based on an overall surface moisture of 17 %, it was assumed that about 15 % of the moisture is removed at the drying step. The remaining 2 % of moisture is carried with the material to the calcining step. Calculation of the required feed material into the dryer is based on Equations 4.5 and 4.5a:

$$m \text{ feed to dryer (tph)} = \frac{m \text{ feed to calciner (tph)}}{100 \% - \% \text{ moisture to be removed}} \times 100 \% \quad (4.5)$$

$$m \text{ feed to dryer (tph)} = \frac{16.5 \text{ tph}}{(100 \% - 15 \%)} \times 100 \% \sim \mathbf{19.5 \text{ tph}} \quad (4.5a)$$

Based on the above assumptions, about 3 tph moisture would leave the drying screws in the form of water vapour.

2. **Calcining Process:** During the exposure of the material and fuel to the 800 °C gases from the clinker kiln, several reactions occur. These reactions influence the final mass of the product leaving the calciner. They include:
- Removal of remaining surface moisture of about 2 % of 16.5 tph, resulting in about 0.3 tph water.
  - Dehydroxylation of kaolinite. Removal of the structural water inside the kaolinite causes a product loss due to dehydroxylation of 13.9 % (Zhou, Liu, Xu, Cheng, & Liu, 2018). Where only 40 % kaolinite exists in the dry feed material, the structural water would result in a mass loss of about 0.9 tph.
  - Ashes from fuel of approximately 4 % of 1.9 tph. Assuming that wood chips are used, about 4 % of ashes are considered in addition to the product, resulting in an ash intake into the product of 0.1 tph.
  - Dust losses due to bypassing of an assumed amount of 2 % of 15.4 tph = 0.3 tph of the product via the exhaust gases into the clinker kiln.

To obtain the desired production capacity of about  $m_{\text{product}} = 15.1 \text{ tph}$ , the calciner needs to receive about  $m_{\text{feed to calciner}} = 16.5 \text{ tph}$  of feed material from the drying stage (Equation 4.4 and 4.4a).

$$m_{\text{feed to calciner}} = m_{\text{product}} + a) + b) - c) + d) \quad (4.4)$$

$$m_{\text{feed to calciner}} = 15.1 \text{ tph} + 0.3 \text{ tph} + 0.9 \text{ tph} - 0.1 \text{ tph} + 0.3 \text{ tph} = \mathbf{16.5 \text{ tph}} \quad (4.4a)$$

Volatile elements that might also be converted into gas and leave the process via the calciner exhaust have not been considered here. The reason is that their influence on the heat and mass balance is probably limited. Those elements are analysed later during the environmental evaluation.

#### 4.2.4.2 Drying and cooling heat balance

A significant consumer of thermal energy is usually the requirements for drying. Depending on the source, free water in the material can vary significantly. In the case of washing sludges, which are a product of the washing of aggregates, the moisture content after washing can be as high as 60 %, depending on the composition. Mechanical pre-drying mainly in filter presses can reduce the moisture to below 20 %. With an increasing content of clay, mechanical drying becomes more difficult due to the material's fineness and porosity.

Remaining water needs to be dried thermally. Generally, any material that dries by evaporation of the water requires vast thermal energy. The goal of the new calcining system is to maximize the use of the energy recovered from cooling the calcined product by using the recovered heat for drying, through a heat-exchanging screw system. The equation for calculating the sensible heat of solids, liquids and gases is:

$$Q = m * cp * \Delta T \quad (4.6)$$

where:

Q is the heat content,

m is the mass of the material, which in this case could be a mixture of kaolinite, quartz and other minerals or water

cp is the specific heat capacity, which implies the amount of energy required to raise 1 kg of solid material, water or gas by 1 °C under constant pressure

$\Delta T$  refers to the temperature of the mass referred to a reference temperature (20 °C selected in this case)

The following cp values were calculated based on the chemical composition and temperature:

- Solids (clay with an assumed composition of 61 % SiO<sub>2</sub>, 22 % Al<sub>2</sub>O<sub>3</sub>, 8 % Fe<sub>2</sub>O<sub>3</sub> and 9 % others):
  - Cp = 0.74 kJ/kg °C @ 20 °C
  - Cp = 0.92 kJ/kg °C @ 150 °C
  - Cp = 1.01 kJ/kg °C @ 250 °C
  - Cp = 1.17 kJ/kg °C @ 800 °C
- Water (standard from literature)
  - Cp = 4.2 kJ/kg °C @ 25 °C

In addition to the heat required to change the temperature, more energy is required to change the water from a liquid condition to vapour. The additional heat required for vaporization is around 540 cal/g (2'260 kJ/kg) at 100 °C.

By the reduction of the temperature of 15 tph (15'000 kg/h) of the calcined material, from about 800 °C to 250 °C, the following energy amount is released. The calculation is based on a reference temperature of 20 °C (Equation 4.7):

$$Q_{usable} = Q_{total} - Q_{out} \quad (4.7)$$

$$Q_{total} = 15'000 \text{ kg/h} \times 1.17 \text{ kJ/kg } ^\circ\text{C} \times (800 \text{ } ^\circ\text{C} - 20 \text{ } ^\circ\text{C}) \div 1000 \text{ kJ/MJ} = 13'688 \text{ MJ/h} \quad (4.7a)$$

$$Q_{out} = 15'000 \text{ kg/h} \times 1.01 \text{ kJ/kg } ^\circ\text{C} \times (250 \text{ } ^\circ\text{C} - 20 \text{ } ^\circ\text{C}) \div 1000 \text{ kJ/MJ} = 3'484 \text{ MJ/h} \quad (4.7b)$$

$$Q_{usable} = Q_{total} - Q_{out} = \mathbf{10'204 \text{ MJ/h}} \quad (4.7c)$$

The calculated recovered heat of 10'204 MJ/h can be transferred to a set of drying screws (Figure 4-5) through a heat-transfer medium, such as thermal oil, to remove the surface moisture from the feed material. The use of heat-exchanging drying and cooling screws with thermal oil as a heat transfer medium is a specific element of the patented solution (WO2021/124261, 2021).

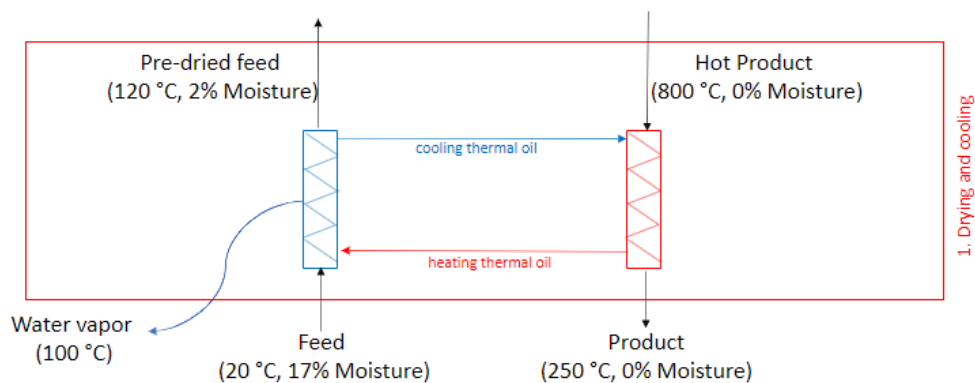


Figure 4-5: Boundary of material drying heat balance

This section demonstrates the limitations of the system in terms of drying capacity. The heat required for the drying is calculated based on several moisture levels. The calculation considers the following heat-consuming processes, as shown in Table 4-3, including:

1. Heating of feed material from approximately 20 °C to 120 °C
2. Heating the water inside the feed material from 20 °C to about 100 °C
3. Evaporation energy of water
4. Energy losses of the heat transfer system

The heat required for the base case with 17 % feed moisture is highlighted with a red box in Table 4-3.

Table 4-3: Heat balance of heat-exchanging circuit, based on a production rate of 15 tph

		Option 1 15 % Feed Moisture	BASE CASE 17 % Feed Moisture	Option 2 30 % Feed Moisture
<b>Energy available from cooling (<math>Q_{usable}</math>)</b>	<b>MJ/h</b>	<b>10'204</b>	<b>10'204</b>	<b>10'204</b>
<b>Desired production rate (dry)</b>	<b>tph</b>	<b>15</b>	<b>15</b>	<b>15</b>
<b>Moisture in wet feed material</b>	<b>%</b>	<b>15</b>	<b>17</b>	<b>30</b>
Remaining moisture after dryer	%	2	2	2
Feeding rate to calciner (based on mass balance)	tph	16.5	16.5	16.5
Moist feed material	tph	19.1	19.5	23.2
Evaporated water in drying step	tph	2.6	3.0	6.7
Energy requirement for drying				
Heating up				
Feed material from 20 °C to 120 °C	MJ/h	1'402	1'402	1'402
Water inside the feed material from 20 to about 100 °C	MJ/h	966	1'121	2'345
Evaporation energy of water (2260 kJ/kg)	MJ/h	5'716	6'755	14'950
Energy losses (5%)	MJ/h	425	488	984
<b>Total energy requirement for drying</b>	<b>MJ/h</b>	<b>8'509</b>	<b>9'766</b>	<b>19'681</b>
<b>Balance of heat available and required</b>	<b>MJ/h</b>	<b>1'695</b>	<b>438</b>	<b>-9'477</b>

The highly efficient heat-exchanging system means that about 10'204 MJ/h (~2'800 kW) of energy ( $Q_{usable}$ ) can be continuously utilized in the heat-exchanging mode between the cooling and drying screws (Equation 4.7c). Making maximum use of that energy positively influences the overall energy requirement of the new calcination technology.

To illustrate the opportunities and limitations of the investigated heat-exchanging system, this section investigates two additional options. They have a lower feed moisture of 15 % (Option 1) and a significantly higher feed moisture of 30 % (Option 2). The details are shown in Table 4-3.

In all cases, it is assumed that drying is not complete due to coarse feed material and about 2 % residual moisture remains and is carried over to the calcination process. The calculation indicates that an autonomous cooling and drying system would be feasible at moisture levels of approximately 17 %. For lower moistures of about 15 % (Option 1), excess heat of approximately 1'695 MJ/h returns to the cooling screws; this results in insufficient cooling of the calcined material and the heating of thermal oil to undesired and potentially critical temperatures. In that case, measures to cool the oil by means of a heat exchanger system or by adding feed material with a higher moisture level must be considered.

For feed materials with relatively high levels of moisture (above 17 %), additional heat sources need to be introduced. If not, the drying will be incomplete, and insufficiently dried material will be introduced into the downstream calcination process. This would result in high fuel consumption and large exhaust gas volumes. Furthermore, moisture levels of 30 %, as shown in Option 2, are undesirable. In such cases, the additional drying energy of about 9'477 MJ/h is too high to be regarded as attractive for a thermal drying process.

#### 4.2.4.3 Calcination heat balance

As outlined in Chapter 2, the dehydroxylation of kaolinite is expected to take place at temperatures between 500 °C and 700 °C. The formation of metakaolin occurs between 700 °C and 850 °C, which will be the target for testing the kaolinitic AWS. Temperatures above 900 °C are to be avoided since they destroy the metakaolin structure and its pozzolanic reactivity.

For AWS containing calcite, or for an anticipated mixture of AWS, RCS and DCG, similar temperatures are desired to produce the first clinker phases.

Due to the connection of the rotary calciner to the clinker kiln system, a portion of the hot air from the kiln is passed at 800°C to the rotary calciner and provides large part of the oxygen and heat to initiate combustion of fuels fed to the calciner. This allows flue gases to return to the kiln system at the same temperature range (800–850°C) but larger gas volumes (Figure 4-6).

The calciner is fed with pre-dried material from the drying process at temperatures of 120 °C. The material is heated and leaves the system at temperatures of about 800 °C into the cooling system (Figure 4.6).

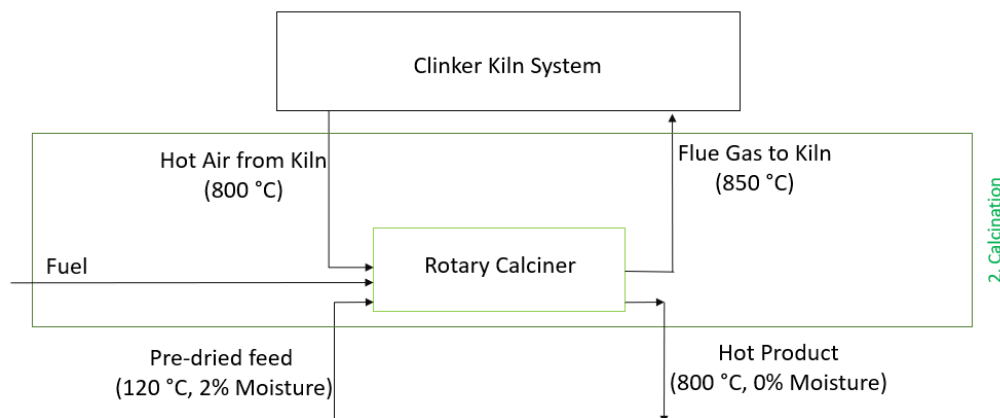


Figure 4-6: Boundary of calcination heat and mass balance

The rotary calciner interacts with the clinker production by extracting gases from the kiln system and returning hot gases back to the kiln calciner. The rotary calciner is providing heat back to the kiln system; it also decreases the efficiency of the preheater tower by adding gas volumes. The impact of additional gas volumes is investigated later in this chapter.

The heat required for calcination is calculated based on the following heat-consuming processes, as shown in Table 4-4:

1. Heating of feed material from approximately 120 °C to 800 °C
2. Heating of the structural water and potentially limited surface water inside the feed material, from 120 °C to about 850 °C
3. Heating of false air from about 20 °C to 850 °C
4. Heat of formation of metakaolin or calcination of calcite
5. Energy losses (radiation and convection)

The calculation of the heat balance (see Table 4-4) is an iterative process. It consists of numerous independent equations and iterations.

Table 4-4: Heat balance of the calciner circuit based on a production rate of 15 tph and reference temperature of 20 °C

Reference temperature is 20°C							
<b>HEAT INPUT</b>	Nm <sup>3</sup> /h	kJ/Nm <sup>3</sup> °C		MJ/h	kW	kJ/kg product	
	kg/h	kJ/kg °C	kJ/kg °C				
Hot air (from kiln system)	7'000	1.39	800	7'605	2'112	493	21.4%
Excess air	2'100	1.27	20	0	0	-	0.0%
Material feed	16'500	1.00	120	1'650	458	107	4.6%
Feed heat value (GCV)	16'500	-	-	0	0	-	0.0%
Fuel	1'875	-	14'000	26'250	7'292	<b>1'703</b>	73.9%
<b>TOTAL OF INPUTS</b>				<b>35'505</b>	<b>9'862</b>	<b>2'304</b>	<b>100.0%</b>
<b>HEAT OUTPUT</b>							
Flue gas (incl. vapour)	11'100	1.52	850	13'999	3'889	908	39.4%
Product (dust in flue gas) to kiln system	300	1.10	850	274	76	18	0.8%
Product (to cooling) sensible heat	15'100	1.10	800	12'956	3'599	841	36.5%
Heat of formation/activation Product	15'300	-	324	4'957	1'377	322	14.0%
Water evaporation (from feed moist.)	300	-	2'260	678	188	44	1.9%
Radiation & convection losses				2'160	600	140	6.1%
Balance error				481	134	31.2	<b>1.4%</b>
<b>TOTAL OF OUTPUTS</b>				<b>35'505</b>	<b>9'862</b>	<b>2'304</b>	<b>100.0%</b>

The difference between the heat input and output is balanced to the maximum extent in order to obtain equilibrium. The main variables are the fuel input and the hot air from the clinker kiln

system; these also must be balanced to obtain the required level of excess air in the combustion gas. The additional heat input to the calciner in the form of fuel was calculated with 1'703 kJ/kg product.

Main contributors of the heat input into the calciner are:

1. Hot air, which is extracted from the clinker kiln tertiary air duct at about 800 °C.
2. Heat introduced via the feed material, which is already preheated due to the initial drying process.
3. Fuel – which could be biomass such as wood chips; this fuel starts combustion immediately after coming into contact with hot air from the clinker kiln. To produce 15 tph product with the specified moisture and mineralogy, about 1'875 kg/h of such fuel is required.

Other contributions of heat input into the calciner system could be exothermic reactions. These are not considered for the anticipated processes with kaolinitic clays or other alternative SCMs.

Heat introduced with the fuel is calculated from Equation 4.8 by multiplying the introduced mass of fuel ( $m_{fuel}$ ) with the NCV or lower heating value.

$$Q = m_{fuel} * NCV \quad (4.8)$$

The heat output is calculated based on the sum of heat leaving the system or the required endothermic reactions that consume heat in the system. It includes:

1. Flue gas leaving the calciner, including stoichiometric combustion gas, water vapour from drying and dehydroxylation, and excess air after combustion. The overall volume of flue gases is reintroduced into the clinker kiln system. It is important that the volume of flue gases is kept to a minimum, since they influence the operation of the clinker kiln.
2. Limited heat losses due to small amounts of dust leaving the calciner directly to the connected kiln system.
3. Sensible heat of product leaving the calciner at temperatures of about 800 °C. Parts of that heat are used to heat the thermal oil and dry the feed material in a heat-exchanging system (described earlier in the chapter). The above-described heat sources are calculated from Equation 4.6.
4. Heat of formation



The heat of formation considers energy that is required (endothermic reactions) or released (exothermic reaction) when the raw material is transformed. According to the literature, the energy required for the dehydroxylation of kaolinite and transformation to metakaolin is roughly 200 kJ/mol, depending on the degree of crystallinity, particle size, stability of hydroxyl groups and so on (Daou et al., 2020, p. 480; Redfern, 1987, p. 451). At the first stage of dehydroxylation, a low activation energy is required because OH groups at the edges of the layers may escape without diffusion through the grain (Redfern, 1987, p. 451). Small particle sizes therefore result in lower activation energies being required (Stoch & Waclawska, 1981, p. 299). Based on a theoretical molecular weight of kaolinite of 222 g/mol, the specific energy required for activation results in 900 kJ/kg kaolinite. In the case of 40 % kaolinite in the feed material and about 90 % successful conversion into metakaolin in the product, 324 kJ/kg material (900 kJ/kg x 40 % x 90 %) must be considered for the heat balance as an additional heat input.

5. Water evaporation energy required to change the remaining 2 % water from liquid condition to vapor is around 540 cal/g (2'260 kJ/kg).
6. Heat loss through the walls by radiation and convection. The kiln shell, inlet and outlet chamber lose a certain amount of energy, which can be determined from the wall temperatures and the ambient conditions. For the theoretical heat balance, a loss due to radiation and convection of 2'160 MJ/h (600 kW) has been calculated.

#### 4.2.4.4 Gas balance

Hot air is extracted from the clinker kiln line, used for preheating and combustion and the combustion flue gases are reintroduced into the clinker kiln. The temperature of the gases leaving the calciner should be roughly 850 °C, which is slightly higher than the 800 °C of gases entering the calciner system. The flue gas contains the following volumes (Figure 4-7):

- $V_{\text{from H}_2\text{O}}$ : Water vapour from drying and dehydroxylation of the material
- $V_{\text{from combustion}}$  : Gas volume from stoichiometric combustion
- $V_{\text{excess air}}$  : Excess air

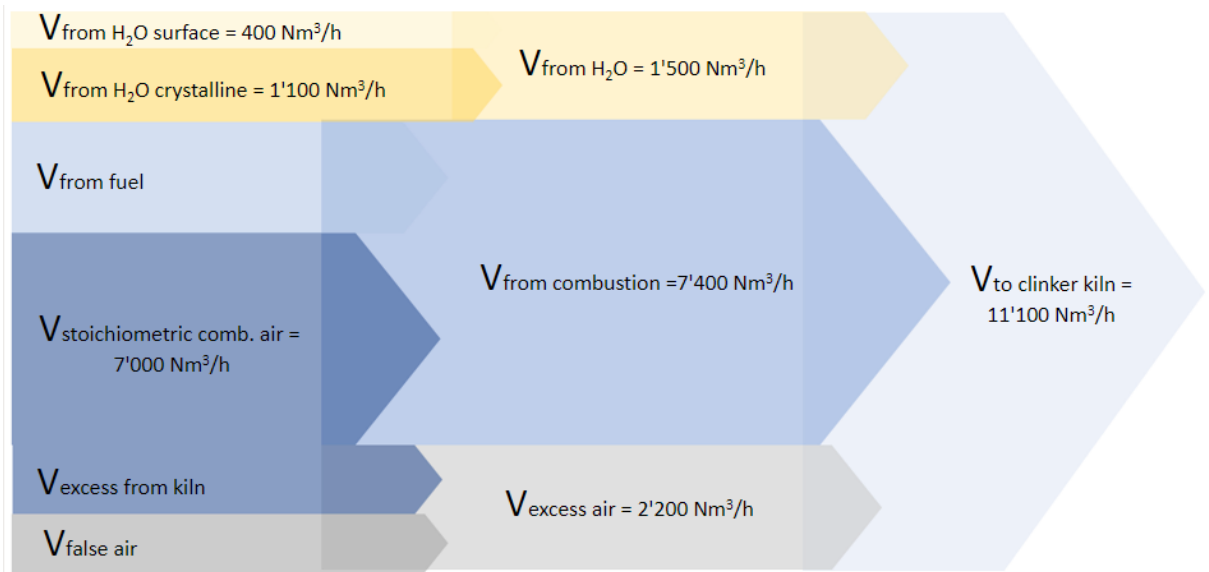


Figure 4-7: Gas volumes of rotary calciner gases extracted from and returned into the clinker kiln system

Because the feed material is pre-dried inside the drying screws, about 2 % of surface moisture must be additionally dried in the calciner. Additional water vapour is produced through dehydroxylation and removal of crystalline water inside the kaolinite at higher temperatures. As calculated earlier in the chapter, about 1.2 tph water vapour leaves the calciner, of which 0.3 tph is associated with the drying of surface water and 0.9 tph with the dehydroxylation of crystalline water in the kaolinite.

The assumption of ideal gases can be applied with reasonable tolerances compared to real gases. One mole has a volume of  $V_m = 0.0224 \text{ Nm}^3/\text{mol}$  at the nominal temperature and pressure condition of  $p = 101.3 \text{ kPa}$  and  $T = 274^\circ\text{K}$ . Based on a molar weight of water of  $M = 18.01 \text{ g/mol}$ , the following nominal air volume is calculated from the water vaporized inside the calciner (Equations 4.9 and 4.9a):

$$V_{\text{from H}_2\text{O}} = \frac{m_{\text{H}_2\text{O}}}{M} \times V_m \quad (4.9)$$

$$V_{\text{from H}_2\text{O}} = \frac{1.2 \frac{\text{t}}{\text{h}} \times 10^6 \frac{\text{g}}{\text{t}}}{18.01 \frac{\text{g}}{\text{mol}}} \times 0.0224 \frac{\text{Nm}^3}{\text{mol}} \sim 1'500 \frac{\text{Nm}^3}{\text{h}} \quad (4.9a)$$

The combustion process can be described as fuel and oxygen undergoing a chemical reaction while releasing thermal energy, combustion gases and ash.

The required specific air volume for complete combustion without any excess of oxygen (stoichiometric combustion) ( $A_{min}$ ) is for most fuels in the range of 0.26 Nm<sup>3</sup>/MJ. The NCV of the wood chips, considered as the main fuel, was specified earlier, with 14.0 MJ/kg yielding the following calculation for the air required for a stoichiometric combustion namely  $V_{stoichiometric\ comb.air}$  (Equations 4.10 and 4.10a). The calculated 7'000 Nm<sup>3</sup>/h stoichiometric combustion air is mainly received from the clinker kiln and should provide sufficient oxygen for complete combustion. Additional air for combustion could be partly obtained also from false or fresh air entering the rotary calciner system.

$$V_{stoichiometric\ comb\ air} = m_{fuel} \times NCV \times A_{min} \quad (4.10)$$

$$V_{stoichiometric\ comb\ air} = 1'875 \frac{kg}{h} \times 14.0 \frac{MJ}{kg} \times 0.26 \frac{Nm^3}{MJ} \sim 7'000 \frac{Nm^3}{h} \quad (4.10a)$$

The specific volume of all combustion gases from a stoichiometric combustion including for instance CO<sub>2</sub>, H<sub>2</sub>O, SO<sub>2</sub>, N<sub>2</sub> can be determined based on the composition of the fuel and is estimated for most fuels with  $V_{min, wet} = 0.28$  Nm<sup>3</sup>/MJ. This specific value includes the humidity of the fuel and the inert parts of the combustion air (N<sub>2</sub>, H<sub>2</sub>O). On a dry basis (excluding N<sub>2</sub> and H<sub>2</sub>O), the specific stoichiometric combustion air is estimated for most fuels with  $V_{min, dry} = 0.25$  Nm<sup>3</sup>/MJ. Together with the quantity of fuel and its NCV, the volume flow of the stoichiometric combustion gases exiting the kiln can be determined using equations 4.11 and 4.11 a.

$$V_{from\ combustion} = m_{fuel} \times NCV \times V_{min, wet} \quad (4.11)$$

$$V_{from\ combustion} = 1'875 \frac{kg}{h} \times 14.0 \frac{MJ}{kg} \times 0.28 \frac{Nm^3}{MJ} \sim 7'400 \frac{Nm^3}{h} \quad (4.11a)$$

An additional air volume passing through the calciner and returning to the cement clinker kiln is excess air ( $V_{excess}$ ), which originates from excess hot air coming from the kiln as well as false air. Excess air is not used in the combustion process. The amount of excess air is defined by the amount of Oxygen (dry) after combustion. In the case of an assumed amount of excess oxygen of 4.75 %, excess air in the amount of 2'200 Nm<sup>3</sup>/h was calculated in equation 4.12. Ideal conditions need to be tested at a semi-industrial scale or during future operations. Potentially, the operation of the clay calciner under a reducing atmosphere (i.e. no excess air and potentially insufficient oxygen for complete combustion) can be considered and might have a positive impact on the energy balance of the clinker kiln. This would be due to secondary combustion of carbon monoxide (CO) inside the clinker kiln calciner. Additionally, a reducing atmosphere in

the clay calciner might positively influence the colour of the calcined clay product by avoiding the formation of  $\text{Fe}_2\text{O}_3$  and a red colour of the calcined clay product. This point is described in detail later in this chapter.

$$V_{\text{excess air}} = (V_{\text{from combustion}}) \times \frac{\%O_2}{21\% - \%O_2} \quad (4.12)$$

$$V_{\text{excess air}} = \left(7'400 \frac{\text{Nm}^3}{\text{h}}\right) \times \frac{4.75\%}{21\% - 4.75\%} \sim 2'200 \frac{\text{Nm}^3}{\text{h}} \quad (4.12a)$$

Based on the above equations, the air volume of about 7'000  $\text{Nm}^3/\text{h}$  received from the clinker kiln would increase due to water evaporation, dehydroxilation, combustion and false air intake. The gas volume increases by about 4'100  $\text{Nm}^3/\text{h}$  to 11'100  $\text{Nm}^3/\text{h}$  (Equations 4.13 and 4.13a).

$$V_{\text{to clinker kiln}} = V_{\text{from combustion}} + V_{\text{from H}_2\text{O}} + V_{\text{excess air}} \quad (4.13)$$

$$V_{\text{to clinker kiln}} = 7'400 \frac{\text{Nm}^3}{\text{h}} + 1'500 \frac{\text{Nm}^3}{\text{h}} + 2'200 \frac{\text{Nm}^3}{\text{h}} = 11'100 \frac{\text{Nm}^3}{\text{h}} \quad (4.13a)$$

The additional gas volume must be absorbed by the integrated clinker kiln process.

Converting the nominal air flow, which is based on normal conditions of  $T_N = 0^\circ\text{C}$  (273K) and  $p_N = 1'013 \text{ mbar}$  to actual conditions, with about  $T_A = 850^\circ\text{C}$  (1123K) and an actual ambient pressure of about  $p_A = 1'015 \text{ mbar}$ , results in an air flow of about  $V_{\text{act}} = 45'000 \text{ Am}^3/\text{h}$  (Equation 4.14) exiting the calciner:

$$V_{\text{act}} = V_{\text{to clinker kiln}} \left(\frac{p_N}{p_A}\right) \times \left(\frac{T_A}{T_N}\right) \quad (4.14)$$

$$V_{\text{act}} = 11'100 \frac{\text{Nm}^3}{\text{h}} \left(\frac{1'013 \text{ mbar}}{1'015 \text{ mbar}}\right) \times \left(\frac{1123 \text{ K}}{273 \text{ K}}\right) \sim 45'000 \frac{\text{Am}^3}{\text{h}} \quad (4.14a)$$

#### 4.2.4.5 Impact on clinker kiln line

One objective is that the integrated rotary calciner must be designed in a way that the production rate of the clinker kiln is not – or not significantly – impacted by the additional gas volume derived from the clay calciner. Usually, due to safety margins in the preheater, including the fan, additional gas volumes of about 10 % of the clinker kiln system flue gas can be accepted without a reduction of the clinker kiln production rate. Because of the additional volume of flue gases returning to the cement clinker kiln, the thermal energy balance of the kiln will be slightly

affected and preliminary simulations have shown that additional 300 kJ per kg calcined product (approx. 30 kJ per kg clinker) will be required in the connected kiln system to maintain cement clinker capacity. If the clinker kiln cannot absorb the additional gas volume, a potential modification or replacement of the existing ventilation must be considered.

#### 4.2.4.6 Impact of calcite on the gas balance

In cases where calcite is present, additional heat for decarbonization is required. In addition, the volume of exhaust gases increases due to the additional presence of CO<sub>2</sub> from the decarbonization.

Depending on the content of CaCO<sub>3</sub> in the raw material, additional energy for decarbonization of about 1'780 kJ/kg CaCO<sub>3</sub> should be considered.

Additionally, higher exhaust gas volumes due to the formation of CO<sub>2</sub> during the reaction of CaCO<sub>3</sub> to CaO and CO<sub>2</sub> should be considered, at 440 kgCO<sub>2</sub> per ton of CaCO<sub>3</sub>.

Overall, where calcite is present, a separate theoretical calculation is required.

#### 4.2.5 Calciner design

Based on the above theoretical assumptions regarding the mass and gas flows, the calciner system was designed using the parameters shown in Figure 4-8. The design pertains to an integrated rotary calciner.

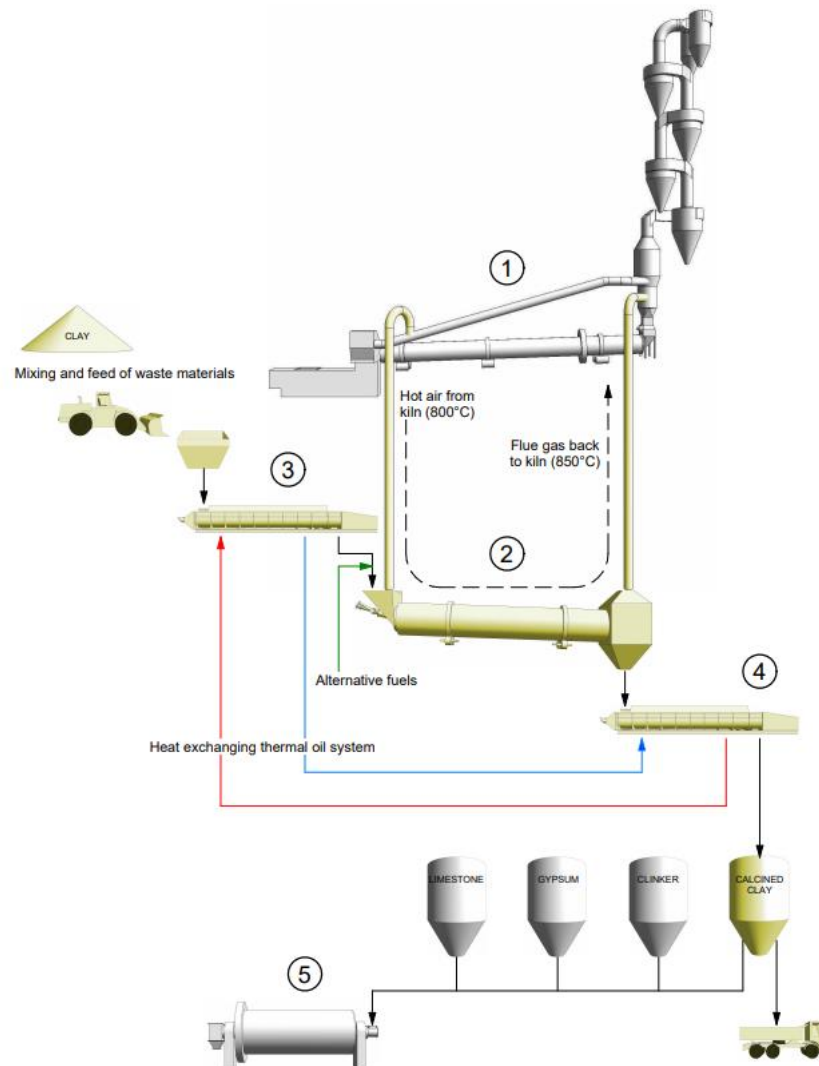


Figure 4-8: Summary of design parameters of heat-exchanging and calciner system

#### 4.2.6 Colour control

Although several oxides can influence the colour, hematite ( $\text{Fe}_2\text{O}_3$ ) is the most critical for the final colour of the product. It causes a reddish colour in the cement, which is undesirable mainly for marketing and acceptance reasons. The colour can be influenced by altering the conditions during calcination and cooling of the material.

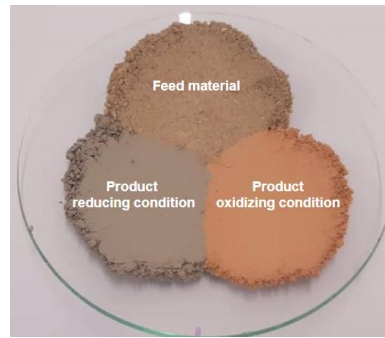
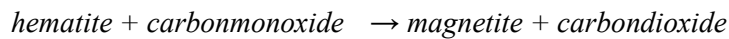
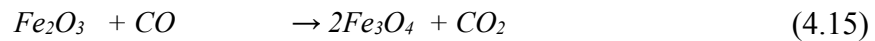
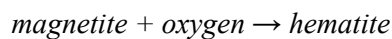


Figure 4-9: Influencing product colour by controlling the oxygen level during calcining and cooling

Due to combustion reactions in the rotary calciner and the presence of CO, at temperatures higher than 650 °C, mainly magnetite ( $Fe_3O_4$ ) is formed during the calcination process (Equation 4.15). The formation of magnetite is enhanced by a reducing atmosphere inside the calciner and the resulting excess of CO.



Magnetite causes a more desired black colour in the final product. It is best to avoid the dissolution of magnetite and its conversion into reddish hematite, which is caused by the oxidation of  $Fe^{2+}$  to  $Fe^{3+}$  during the cooling process (Equation 4.16).



Given the above scenario, it is desirable either to enforce rapid cooling or to maintain reducing conditions during the cooling stage until the temperature falls below 300 °C. At that point, no more oxidation reactions are expected. As explained earlier in Chapter 3, existing technologies – namely the flash calciner or rotary calciner – require the injection of environmentally critical, expensive fuel oil to obtain a reducing atmosphere during cooling. This injection prevents the conversion of magnetite to hematite.

Using the proposed cooling screws, cooling under the absence of oxygen can be more easily achieved. An airlock system, comprising a rotary valve or double flap valve, is installed after the cooling screw to avoid oxygen intake (Figure 4-10).

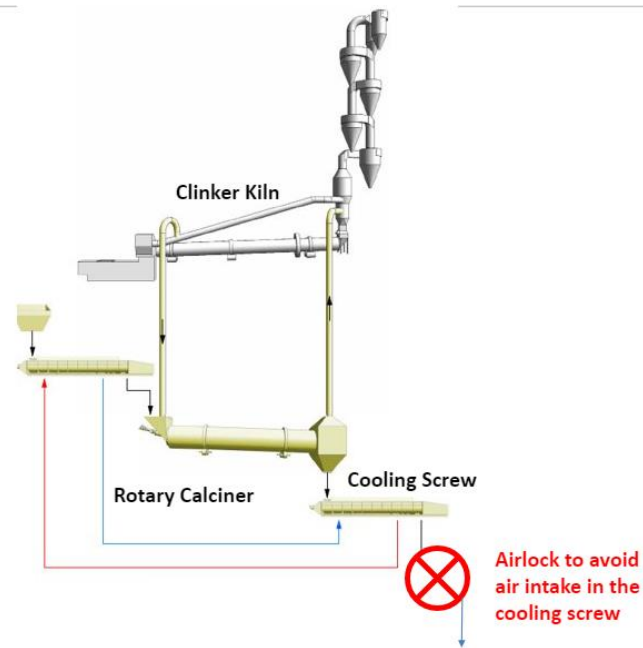


Figure 4-10: Colour control by preventing oxygen intake into the cooling screw

#### 4.2.7 Emission prediction

The origin of the desired materials – such as AWS, RCS and DCG – means that the variety and quantity of critical volatile elements might be large. Therefore, applying conventional calcining technologies, such as an independent rotary or flash calciner, might be critical. The reason is that the material is gradually heated in counter-current flow and volatile elements are leaving the calciner untreated and are emitted as exhaust.

The integrated rotary calciner creates little additional emissions at the main stack of the cement clinker kiln. That is because the combustion gases leaving the rotary calciner enter the clinker kiln calciner and therefore undergo additional combustion at about 850-1000 °C. Other volatile elements combine with CaO inside the clinker kiln calciner and are discharged with the clinker in solid form. The design of the clinker kiln system means that the same stack is used and no additional emission source is created (Figure 4-11).



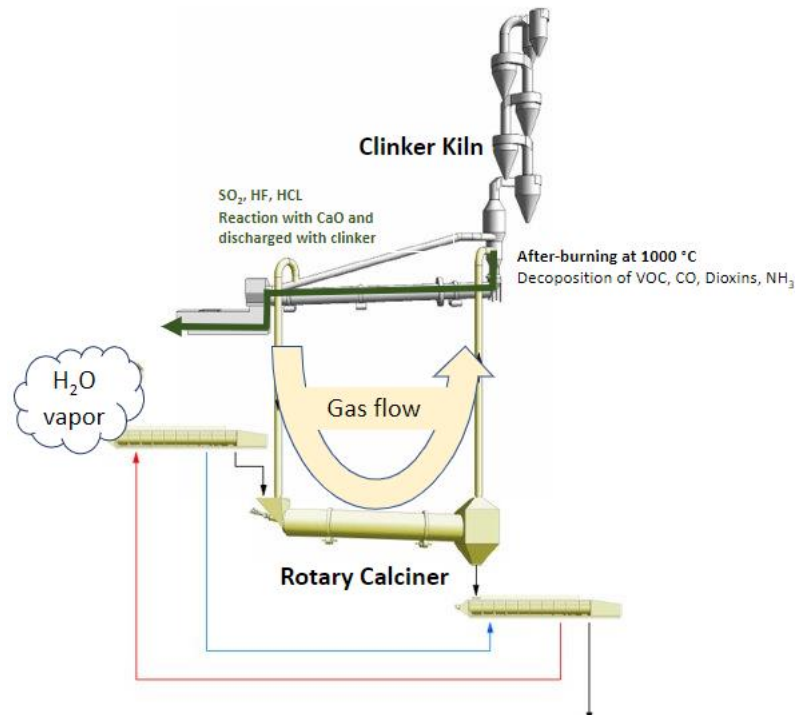


Figure 4-11: Emission behaviour of integrated rotary calciner

#### 4.2.7.1 Emission during drying

Heating and drying of the feed material is anticipated to occur at temperatures of 100–120 °C., Therefore, only water vapor is expected during the drying step. The anticipated volume of water vapor is roughly 3 tph, as calculated earlier in this chapter. Materials containing organic components in solid form, such as paper or wood, do not create any emissions at that temperature. In the case of volatile liquids such as solvents, oil or gasoline, they would emit VOC in the drying step, leading to VOC emissions. Therefore, either volatile liquids should be avoided inside the feed material or secondary gas cleaning should be considered.

#### 4.2.7.2 Emission during calcination

Emissions that develop due to combustion and reactions of the feed material inside the rotary calciner leave the system at temperatures of about 850 °C. They are transported to the clinker kiln, where they are exposed to about 850-1000 °C whereby a gas residence time of 5 to 10 seconds at typically close to 900 °C is usual for the operation of a calciner including the lowest cyclone stage of a cement clinker preheater.

**Water vapour:** uncritical water vapour is expected due to drying and dehydroxilation. The vapour passes through the clinker kiln preheater system and exits via the main stack.

**VOC, CO and dioxins:** All VOC emissions released in the rotary calciner undergo a post combustion in the cement clinker kiln because of the significantly high temperatures. This concept also allows operating the clay calciner under partly reducing conditions. The reason is that VOC compounds and CO from incomplete combustion are completely after-burned in the cement kiln.

**NH<sub>3</sub>:** NH<sub>3</sub> thermally degrades inside the cement clinker kiln and therefore does not contribute to additional NH<sub>3</sub> emissions.

**SO<sub>2</sub>:** SO<sub>2</sub> emission is a common challenge for many clay deposits, mainly because of volatile pyritic sulphur in the clay. In the case of an integrated calciner system, SO<sub>2</sub> is captured in the lowest cyclone stages by suspended CaO particles. The CaO reacts with the SO<sub>2</sub> to produce CaSO<sub>3</sub> which is discharged with the product.

**Acid gases (HF, HCl):** Like SO<sub>2</sub>, after entering the clinker kiln calciner, acid gases such as HF and HCl come into intense contact with suspended CaO particles. These particles react and are discharged with the product as CaCl<sub>2</sub> or CaF<sub>2</sub>.

**Heavy metals:** Mercury (Hg) in the raw material or fuel of the rotary kiln becomes volatile. If it exceeds the regulatory limits, this needs to be considered for secondary abatement measures in the clinker kiln exhaust. Exceeding the limits for Hg could be especially problematic for the calcination of RCS and would require secondary exhaust gas cleaning measures. All other heavy metals are discharged with the calciner product in the form of dust.

**CO<sub>2</sub>:** The impact of the rotary calciner system on CO<sub>2</sub> is analysed in the following subsection.

#### 4.2.8 CO<sub>2</sub> footprint of produced material

An important driver to investigate alternative SCM is the reduction of CO<sub>2</sub> in the cement. Reduced CO<sub>2</sub> is in turn associated with a reduction of calcite and fuel as the only contributors. The selection of material and production process can influence the CO<sub>2</sub> release. This point is illustrated by comparing the CO<sub>2</sub> impact of clinker production with that of calcined clay using different manufacturing methods.

In a clinker kiln, CO<sub>2</sub> is released due to chemical processes during the decomposition of minerals, such as calcite, and the burning of organic fuels. Approximately 55 % of the CO<sub>2</sub> development is associated with the decarbonization of calcium carbonate (calcite) (Equation 4.17) at temperatures above 700 °C. The remaining 45 % of CO<sub>2</sub> is associated with burning fuels and electrical energy required to produce clinker.



*Calcite* → *Calciumoxide* + *Carbondioxide*

Based on the molar weight of CaO (56 g/mol) and CO<sub>2</sub> (44 g/mol), 1 ton of calcite (CaCO<sub>3</sub>) releases 440 kg CO<sub>2</sub>/t and 560 kg CaO/t when heated.

To produce clinker, a CaO content of about 65 % is required. Based on a contribution of about 0.785 t of CO<sub>2</sub> per t of CaO (44 g/mol CO<sub>2</sub> / 56 g/mol CaO), on average about 510 kg of CO<sub>2</sub> per t of clinker is produced during the decarbonization of calcite.

When calcite is absent, as is the case with many clays, the main CO<sub>2</sub> contributor is diminished. Additionally, the thermal activation of clay occurs at significantly lower temperatures, namely about 700–850 °C (compared to 1'400 °C for clinker). Furthermore, a significantly higher thermal energy consumption of clinker compared to calcined clay is attributed to the heat of formation which is for the decarbonization 1'780 kJ/kg CaCO<sub>3</sub> compared to about 50 % less heat of formation for the calcination of clay with a required 900 kJ/kg calcined clay.

Table 4-6 shows the net CO<sub>2</sub> contribution depending on the product (clinker or calcined clay) and the manufacturing method of calcined clay. Regarding the proposed calcination method, 100 % of the biomass (wood chips) can be used with 0 % of net CO<sub>2</sub> contribution. Only additional CO<sub>2</sub> from Fuels relates to a slightly higher fuel consumption of the cement clinker kiln contributing to approximately 30 kg CO<sub>2</sub> per ton of calcined material.

As explained in Chapter 3, other conventional calcining methods cannot operate with 100 % biomass. In the flash calciner, the low retention time of a few seconds inside the combustion area and low combustion temperature means that only noble fuels with high volatility – such as coal – can be used for direct firing. The higher combustion temperature inside a conventional rotary calciner would allow for a higher content of alternative fuels such as biomass. Therefore, the calculation of the CO<sub>2</sub> contribution of a conventional rotary calciner considers a fuel mix

of about 50 % biomass and 50 % of easily combustible noble fuel, such as coal. In Table 4-6, it is assumed that the clay is free of calcite or dolomite. If calcite or dolomite are present in the clay, CO<sub>2</sub> from decarbonization can be expected and would add to the CO<sub>2</sub> contribution. This would be especially true for the thermal treatment of some AWS or RCS.

In all cases, the contribution of CO<sub>2</sub> related to the consumption of electrical energy is limited. The average carbon intensity of electrical energy in Europe ranges from 55 gCO<sub>2</sub> per kWh in France to 724 gCO<sub>2</sub> per kWh in Poland. The CO<sub>2</sub> contribution from electrical energy shown in Table 4-5 reflects an average carbon intensity of electricity of 300 gCO<sub>2</sub> per kWh, such as for Germany (Ember, 2020).

Table 4-5: Net CO<sub>2</sub> contribution depending on product (clinker or calcined clay) and the manufacturing method of calcined clay

	Clinker production	Calcined clay production		
		conventional rotary calciner	conventional flash calciner	new method with integrated calciner
CO <sub>2</sub> from decarbonization of calcite	530 kg CO <sub>2</sub> /t clinker	0 kg CO <sub>2</sub> /t calcined clay <sup>2)</sup>	0 kg CO <sub>2</sub> /t calcined clay <sup>2)</sup>	0 kg CO <sub>2</sub> /t calcined clay <sup>2)</sup>
CO <sub>2</sub> from Fuel <i>(based on an average of 95 kg CO<sub>2</sub> / GJ for coal and 0 kg CO<sub>2</sub> / GJ for biogenic fuels)</i>	275 kg CO <sub>2</sub> /t clinker <sup>4)</sup> <i>(3200 kJ/kg clinker)</i>	119 kg CO <sub>2</sub> / t calcined clay <sup>3)</sup> <i>(2500 kJ/kg calcined clay)</i>	170 kg CO <sub>2</sub> / t calcined clay <sup>4)</sup> <i>(2000 kJ/kg calcined clay)</i>	30 kg CO <sub>2</sub> /t calcined clay <sup>5)</sup> <i>(1700 kJ/kg calcined clay)</i>
CO <sub>2</sub> from electrical energy <i>(based on 300 kg CO<sub>2</sub> / MWh)</i>	18 kg CO <sub>2</sub> /t clinker <i>(60 MWh/t clinker)</i>	12 kg CO <sub>2</sub> /t calcined clay <i>(40 MWh/t calcined clay)</i>	18 kg CO <sub>2</sub> /t calcined clay <i>(60 MWh/t calcined clay)</i>	15 kg CO <sub>2</sub> /t calcined clay <i>(50 MWh/t calcined clay)</i>
<b>Total</b>	<b>823 kg CO<sub>2</sub>/t clinker</b>	<b>131 kg CO<sub>2</sub>/t calcined clay</b>	<b>188 kg CO<sub>2</sub>/t calcined clay</b>	<b>45 kg CO<sub>2</sub>/t calcined clay</b>

<sup>1)</sup> assumed 67 % lime in the clinker, <sup>2)</sup> assumed absence of calcite and dolomite, <sup>3)</sup> assumed 50 % coal and 50 % biomass (i.e. wood chips), <sup>4)</sup> assumed 90 % coal or similar and 10 % biogenic fuel, <sup>5)</sup> assumed 100 % biomass (i.e. wood chips) and 30 kg CO<sub>2</sub>/t calcined clay for cement clinker kiln impact

The difference between the CO<sub>2</sub> contribution of calcined clay (45–131 kg CO<sub>2</sub>/t) and clinker (823 kg CO<sub>2</sub>/t) is substantial; this point alone makes the extended use of calcined clay attractive for the cement industry. The benefit of the new method using an integrated calciner yields even greater advantages than the existing calcining methods, such as flash and rotary calciners (Table 4-5). The production of calcined clay would emit only 45 kg CO<sub>2</sub> for every ton of calcined clay.

Based on the anticipated production volume of 100'000 tons per year clinker or calcined clay, the new method could save more than 75'000 tons CO<sub>2</sub> per year, compared to clinker. Apart from the environmental benefits of producing calcined clay rather than clinker, in monetary terms (and assuming a future CO<sub>2</sub> tax of EUR 100 per ton of CO<sub>2</sub>), savings of around EUR 7.5 million per year could be feasible (Table 4-6).

Table 4-6: *Impact of material and calcining method on the CO<sub>2</sub> production and potential CO<sub>2</sub> taxes*

	Clinker production	Calcined clay production		
		conventional rotary calciner	conventional flash calciner	new method with integrated calciner
CO <sub>2</sub> produced per year based on 100'000 tons production per year	82'300 t CO <sub>2</sub> /year	13'100 t CO <sub>2</sub> /year	18'800 t CO <sub>2</sub> /year	4'500 t CO <sub>2</sub> /year
Total CO <sub>2</sub> tax based on EUR 100 /t CO <sub>2</sub>	8.23 Mio EUR/year	1.31 Mio EUR/year	1.88 Mio EUR/year	0.45 Mio EUR/year

#### 4.2.9 Grinding requirements

This section discusses the grinding requirements for calcined clay. Whether calcined clay needs to be ground depends on the cement type and required particle size. Generally, it is assumed that grinding is required.

The material composition is important for grinding, since the feed material consists of a wide range of materials with different properties. It includes both soft and easily grindable clay and quartz that is hard, abrasive and difficult to grind. The behaviour of the materials needs to be investigated in specific tests to avoid potential problems such as

- overgrinding of clay
- coating of clay to the grinding media (balls, rollers, liners)
- high electrical energy consumption due to grinding of quartz
- high wear due to quartz

### 4.3 Summary of Chapter 4

SCMs with hydraulic, latent hydraulic or pozzolanic reaction behaviours, or a mixture thereof, can be produced through thermal activation at temperatures below 850 °C. These SCMs should fulfil the cement norms, mainly in terms of composition and strength development.

The newly patented methodology can dry and thermally activate various materials, using about 20 % less thermal energy than conventional methods. Its integration with an existing clinker kiln system means that thermal energy can be reduced. Emissions are significantly lower in the case of processing difficult, contaminated materials.

In the presence of hematite ( $\text{Fe}_2\text{O}_3$ ) in the raw material, the patented screw heat-exchanging system can be operated in an optimized way to avoid further oxidation of magnetite ( $\text{Fe}_3\text{O}_4$ ) and its conversion into reddish hematite. The red colour is not desired for marketing reasons. A system to produce about 100'000 tons per year SCMs was modelled and can be integrated into an existing clinker kiln with minimal impact on its operation. The reduction of  $\text{CO}_2$  compared to clinker could be significant, at about 70'000 tons  $\text{CO}_2$  per year. Tests to prove the described theoretical assumptions were conducted and are described in the following chapters.

## Chapter 5: Experimental tests and proof of concept

*Chapter 5 describes tests that were conducted to demonstrate the theoretical assumptions regarding the proposed design. The main assumption was that alternative SCM can be produced from materials sourced from the circular economy, and that the proposed new technology can be used to thermally activate the materials.*

### 5.1 Introduction

To demonstrate that suitable alternative SCMs can be produced by the proposed process, a testing programme was developed. The goal was to investigate waste materials that were locally available and to simulate the various steps of the process in the new activation technology. Due to the proximity of two cement plants, the following material samples were collected:

1. Kaolinitic AWS from the Rennes region in France
2. Non-kaolinitic AWS, RCS and DCG from the Geneva region in Switzerland

The samples were collected from the corresponding source in the presence of a geologist. The objective was to obtain materials that were sufficiently representative for further testing. Regarding the sample from Switzerland, the received materials (AWS, RCS and DCG) were proportioned and mixed by the laboratory to obtain the desired chemical and mineralogical composition.

For both locations, large bags of about 1.5 t were prepared to conduct the following testing steps. The steps are described in more detail in the paragraphs below.

- |                                       |  |
|---------------------------------------|--|
| 1. Material characterization          | Holcim test centre, Switzerland and France       |
| 2. Crushing                           | Bedeschi test centre, Italy                      |
| 3. Drying with heat-exchanging screws | Koelmann test centre, Germany                    |
| 4. Calcination                        | IBU-tec test centre and TKIS Testcenter, Germany |
| 5. Grinding                           | Verein Deutscher Zementwerke VDZ, Germany        |
| 6. Concrete testing                   | Holcim test centre, Switzerland and France       |

## 5.2 Sampling and characterization

### 5.2.1 Kaolinitic AWS from France

Samples from a potential AWS pond at an aggregate washing facility near Rennes, France were collected and further studied. As evident from the picture in Figure 5-1, such mud ponds are a fundamental problem for nature, because for decades the area remains inaccessible and re-cultivation is impossible. In addition, for safety reasons, the ponds need to be well protected to avoid people entering.

If successfully tested, this and similar deposits could be a perfect local material source to be used in the cement industry in the future. Such use would also relieve the environment and improve its safety.



Figure 5-1: Sampling at AWS pond near Rennes, France

Representative bulk samples were collected from four ponds (No. 3, 4, 5 and 6), whereas at the largest pond, No. 5, five samples were collected by an excavator at the rim of the pond. At the other three smaller deposits, only two to three samples were taken. All samples were analysed in the laboratory for moisture, particle size distribution and material characteristics.



Table 5-1: Moisture of samples from AWS deposit near Rennes, France

Sample	Sample Number	Moisture (%) 100 % related to wet according to EN12880
3A	Geo-19-03900-P	38.3
3B	Geo-19-03901-P	40.2
4A	Geo-19-03902-P	40.7
4B	Geo-19-03903-P	39.8
5A	Geo-19-03904-P	47.0
5B	Geo-19-03905-P	44.6
5C	Geo-19-03906-P	39.3
5D	Geo-19-03907-P	32.5
5E	Geo-19-03908-P	34.5
6A	Geo-19-03909-P	51.9
6B	Geo-19-03910-P	53.7
6C	Geo-19-03911-P	54.2

Materials discharged from the aggregate washing process generally have moisture content of about 70–80 %. These materials are pumped into the ponds, where they settle, and the water content is thus reduced to 30–55 % (Table 5-1). Some ponds, like pond No. 3, are not refilled with slurry for at least a decade but still contain a moisture of about 40 %.

For the anticipated calcining process, moistures of <20 % are required. Therefore, natural dewatering inside the pond is not sufficient to achieve the desired moisture levels and mechanical dewatering in centrifuges or filter presses or natural drying must be considered.

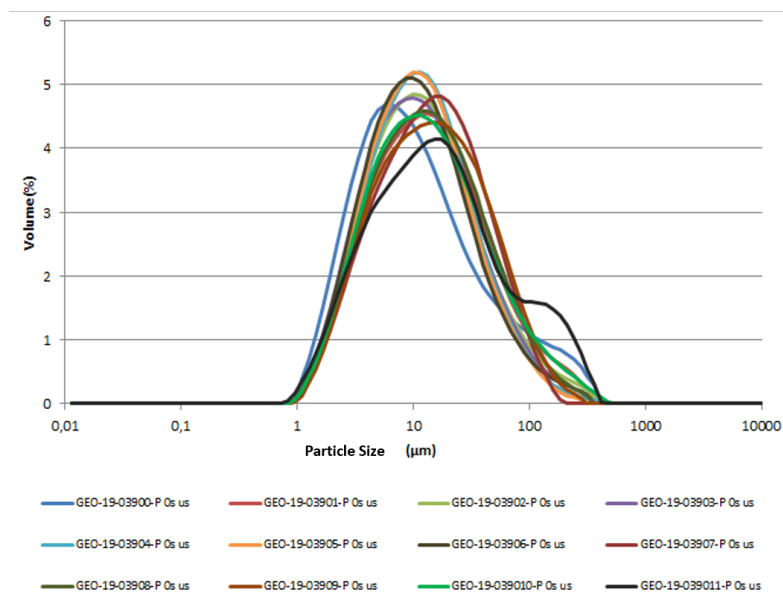


Figure 5-2: Particle size distribution of AWS deposit near Rennes, France

Especially interesting is the exceptionally fine particle size distribution (PSD) (Figure 5-2). To a large extent, such material is ready to be used in cement without further grinding, once it has been properly thermally activated.

Other indicators of the material were as follows:

- Bulk density: 1.13 t/m<sup>3</sup>
- Organic matter content: 8.33 % of dry matter

The content of organic matter in the samples was rather high and this could indicate some vegetation on top of the sludge basins. It could also be the result of organic-based flocculants that are used to improve the aggregate washing process. In any case, the elevated content of organics would become critical if the material is later thermally treated in a conventional rotary or flash calciner.

For further chemical, mineralogical and mortar analysis, selected samples were prepared. The chemical analysis was carried out by X-ray fluorescence analyser (XRF) and the mineralogical analysis by X-ray diffraction analyser (XRD). Table 5-2 and Table 5-3 display the chemical and mineralogical composition of the prepared samples.

Table 5-2: Chemical composition of kaolinitic AWS sample, Rennes (France) according to XRF

Material	Average Chemical Composition
	<b>Content in %</b>
% LOI	9.30
% SiO <sub>2</sub>	57.70
% Al <sub>2</sub> O <sub>3</sub>	21.30
% TiO <sub>2</sub>	0.52
% Fe <sub>2</sub> O <sub>3</sub>	8.12
% Mn <sub>2</sub> O <sub>3</sub>	0.04
% CaO	0.28
% MgO	0.47
Total S as % SO <sub>3</sub>	0.11
% P <sub>2</sub> O <sub>5</sub>	0.23
<b>% Sum</b>	<b>98.07</b>

Table 5-3: Mineralogical composition of kaolinitic AWS sample, Rennes (France) according to XRD

Phase	Notation/Formula	Raw Feed Content in %
Quartz	$SiO_2$	22.8
Muscovite	$KAl_2AlSi_3O_8(OH)_2$	6.4
Illite	$(K,H_3O)(Al,Mg,Fe)_2(Si,Al)_4O_{10}[(OH)_2 \cdot (H_2O)]$	9.6
Chlorite	$(Mg,Fe)_3Al(Si_3Al)O_{10}(OH)_8$	4.3
Kaolinite	$Al_2Si_2O_5(OH)_4$	47.4
Calcite	$CaCO_3$	0.2
Dolomite	$MgCa(CO_3)_2$	0.1
Hematite	$Fe_2O_3$	1.1
Goethite	$FeOOH$	*
Microcline	$KAlSi_3O_8$	2.9
Albite	$NaAlSi_3O_8$	0.5
Sanidine	$K(AlSi_3O_8)$	2.3
Siderite	$FeCO_3$	0.4
Alunite	$KAl_3(SO_4)_2(OH)^6$	1.1
Anatase	$TiO_2$	0.5
<b>% Sum</b>		<b>99.6</b>

\* some percentage of goethite, not quantified by XRD, is present and affects the quantification of product phases

In addition to the elevated kaolinite content, other types of clay – such as illite and muscovite – were present. Once these are thermally activated, they could additionally contribute to the performance of the produced SCM.

The elevated amount of  $Fe_2O_3$  – namely 8.12 % – in the chemical composition can impact the undesirable reddish colour of the thermally activated SCM. Special precautions should be considered, especially during the calcining and cooling phase, as described earlier in Chapter 4.

In addition, a thermogravimetric (TG) analysis was performed using a Mettler Toledo TGA DSC1. The sample was heated to 1'000 °C at a heating rate of 10 K/min under atmospheric conditions. The results are shown in Figure 5-3. The first peak reflects the evaporation of the physically bound water, which is present in all materials. After that, a peak from 250–300 °C indicates the decomposition of goethite. As early as 450 °C, dehydroxylation of kaolinite occurred. The formation of the desired metakaolin is expected to be completed at about 850 °C which will be the target temperature for the semi-industrial testing. At temperatures around 950

°C, further structural changes occurred, which were caused by the transformation from metakaolin to spinel. At this temperature the desired pozzolanic reaction of the metakaolin will be destroyed.

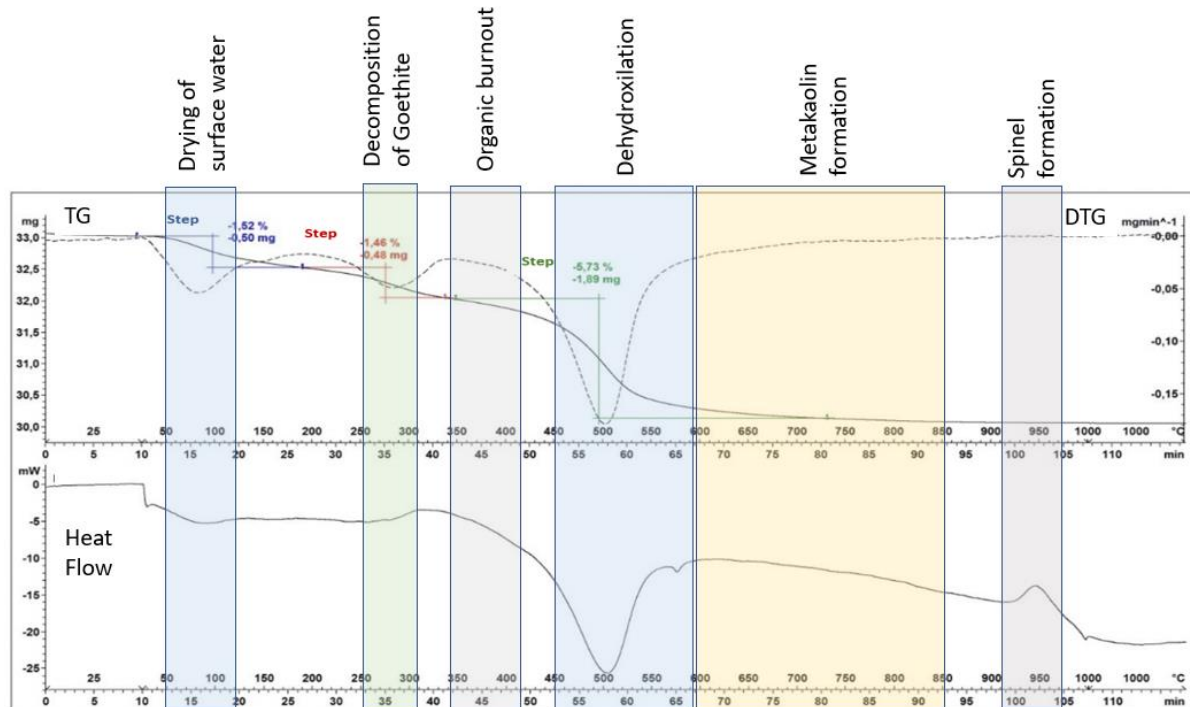


Figure 5-3: TG, DTG and Heat Flow analysis of kaolinitic AWS, Rennes, France

### 5.2.2 Non-kaolinitic AWS from Switzerland

In continuation of the above investigation, AWS from Switzerland was analysed. It was found to have a significantly lower kaolinite content inside the sludge, or none at all. Therefore, the AWS of six aggregate and sand quarries was analysed. The sample was received in a laboratory at Holcim Switzerland, and similar tests were conducted to those performed for the AWS from France. For the sake of simplicity, only three of the samples are described below (Figure 5-4).

The sample as received had a moisture content of 19–22 %. This figure is close to that which can be expected after mechanical water removal in a filter press for AWS with a limited clay content. The density in all cases was roughly  $1.4 \text{ t/m}^3$  (Table 5-4).

Table 5-4: Average moisture and density of selected non-kaolinitic AWS samples, Switzerland

Material	MTD120081 Oberdorf Filter cake AWS	MTD120113 Kirchberg Filter cake AWS	MTD120083 Bretonnieres Filter cake AWS
	<b>Content in %</b>		
% Moisture	21.9	20.4	19.6
Density (t/m <sup>3</sup> )	1.357	1.330	1.338

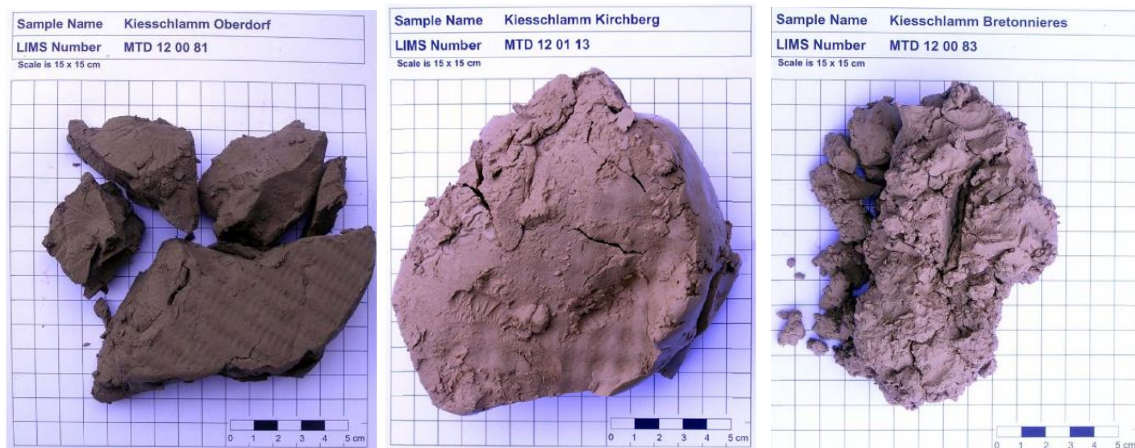


Figure 5-4: Images of received AWS sample as delivered

The received AWS showed a very fine PSD, with most of the material being below 100  $\mu\text{m}$  (Figure 5-5).

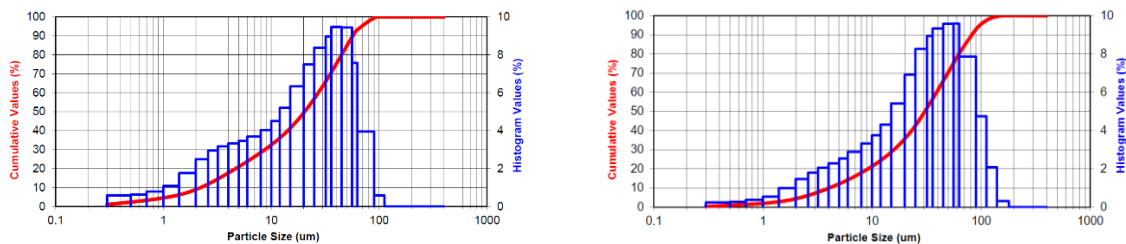


Figure 5-5: PSD in tested non-kaolinitic AWS sample from Kirchberg (left) and Bretonnieres (right), Switzerland

The chemical analysis was performed using XRF and the mineralogical analysis by XRD. The results are shown in Tables 5-5 and 5-6.

Table 5-5: Chemical composition of selected non-kaolinitic AWS sample, Switzerland, according to XRF

Material	MTD120081 Oberdorf Filter cake AWS	MTD120113 Kirchberg Filter cake AWS	MTD120083 Bretonnieres Filter cake AWS
	Content in %		
% LOI	23.99	27.31	32.05
% SiO <sub>2</sub>	31.42	31.65	19.42
% Al <sub>2</sub> O <sub>3</sub>	9.37	5.67	4.68
% TiO <sub>2</sub>	0.45	0.31	0.21
% Fe <sub>2</sub> O <sub>3</sub>	3.92	2.36	2.20
% Mn <sub>2</sub> O <sub>3</sub>	0.07	0.08	0.06
% CaO	25.99	24.85	38.26
% MgO	1.82	6.36	1.41
% Na <sub>2</sub> O	0.46	0.33	0.41
Mn <sub>2</sub> O <sub>3</sub>	0.07	0.08	0.06
SrO	0.04	0.03	0
Total S as % SO <sub>3</sub>	0.05	0.05	0.05
% P <sub>2</sub> O <sub>5</sub>	0.11	0.07	0.08
<b>% Sum</b>	<b>97.76</b>	<b>99.15</b>	<b>98.89</b>

Table 5-6: Mineralogical composition of non-kaolinitic AWS sample, Switzerland, according to XRD

Phase	Notation/Formula	MTD120081 Oberdorf Filter cake AWS	MTD120113 Kirchberg Filter cake AWS	MTD120083 Bretonnieres Filter cake AWS
		Content in %		
Quartz	SiO <sub>2</sub>	20	24	13
Muscovite	KAl <sub>2</sub> AlSi <sub>3</sub> O <sub>8</sub> (OH) <sub>2</sub>	17	7	6
Illite	(K,H <sub>3</sub> O)(Al,Mg,Fe) <sub>2</sub> (Si,Al) <sub>4</sub> O <sub>10</sub> [(OH) <sub>2</sub> ·(H <sub>2</sub> O)]	0	0	0
Chlorite	(Mg,Fe) <sub>3</sub> Al(Si <sub>3</sub> Al)O <sub>10</sub> (OH) <sub>8</sub>	3	6	2
Kaolinite	Al <sub>2</sub> Si <sub>2</sub> O <sub>5</sub> (OH) <sub>4</sub>	0	0	0
Smectite	Al <sub>2</sub> [(OH)2Si <sub>4</sub> O <sub>10</sub> ]·nH <sub>2</sub> O	0	0	0
Calcite	CaCO <sub>3</sub>	52	33	72
Dolomite	MgCa(CO <sub>3</sub> ) <sub>2</sub>	4	25	2
Microcline	KAlSi <sub>3</sub> O <sub>8</sub>	0	2	2
Anatase	TiO <sub>2</sub>	0	0	0
Albite	NaAlSi <sub>3</sub> O <sub>8</sub>	1	3	3
Orthoclase	KAlSi <sub>3</sub> O <sub>8</sub>	0	0	0
<b>% Sum</b>		<b>100</b>	<b>100</b>	<b>100</b>

Compared to the sample from France, the AWS from Switzerland were characterized by no kaolinitic content and a high – but widely ranging – amount of calcite and dolomite. Other clays, mainly muscovite, were present. However, according to literature (Fernandez et al., 2011)

these are not expected to contribute significantly to the strength development of cement. The content of iron oxide was in the range of 2–4 %.

The sulphur and TOC content of the sample were determined with infrared absorption at various temperatures. The values were 0.05 % SO<sub>3</sub> and 0.12 % TOC, which are quite low and uncritical for thermal activation. In addition, thermogravimetric analysis (TGA) was performed. The samples were heated to 1'000 °C at a rate of 10 K/min under atmospheric conditions. The results are shown in Figure 5-6.

Weight loss started at about 700 °C and reached its maximum at 850 °C, which is a clear sign of the expected decarbonization of calcite and dolomite and the dehydroxilation of the remaining clays and an indication of the target temperature for the semi-industrial testing.

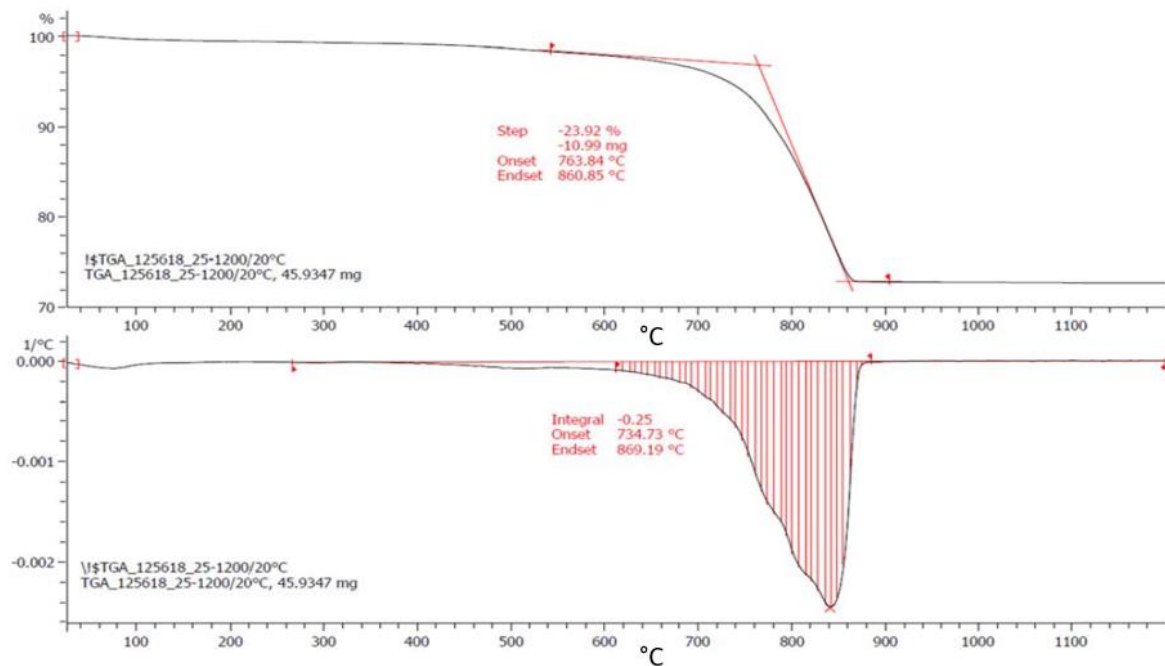


Figure 5-6: TG analysis of AWS sample from Kirchberg, Switzerland

### 5.2.3 Road cleaning sludges from Switzerland

To identify possible usage of RCS to be potentially combined with other materials to form a SCM, 26 samples from one RCS collector were analysed over a few weeks (Figure 5-7).



Figure 5-7: Investigated Road Cleaning Sludge

The conducted tests were mainly focused on moisture, chemical composition and environmental critical elements. Tables 5-7 and 5-8 present a summary of the test results.

Table 5-7: Chemical composition of investigated RCS Switzerland, according to XRF

	Avg.	Min.	Max.
<b>% SiO<sub>2</sub></b>	<b>45.2</b>	42.2	49.4
<b>% Al<sub>2</sub>O<sub>3</sub></b>	<b>6.1</b>	5.5	6.8
<b>% Fe<sub>2</sub>O<sub>3</sub></b>	<b>3.8</b>	3.4	4.2
<b>% CaO</b>	<b>13.9</b>	11.7	17
<b>% MgO</b>	<b>1.5</b>	1.2	1.8
<b>% SO<sub>3</sub></b>	<b>0.7</b>	0.5	0.8
<b>% K<sub>2</sub>O</b>	<b>1.4</b>	1.2	1.6
<b>% Na<sub>2</sub>O</b>	<b>0.7</b>	0.6	1
<b>% TiO<sub>2</sub></b>	<b>0.4</b>	0.3	0.4
<b>% Mn<sub>2</sub>O<sub>3</sub></b>	<b>0.1</b>	0.1	0.1
<b>% P<sub>2</sub>O<sub>5</sub></b>	<b>0.4</b>	0.3	0.7
<b>% Cr<sub>2</sub>O<sub>3</sub></b>	<b>0</b>	0	0
<b>% SrO</b>	<b>0</b>	0	0
<b>% ZnO</b>	<b>0.1</b>	0.1	0.1
<b>% Sum</b>	<b>98.9</b>		



Table 5-8: Environmentally relevant characteristics of investigated RCS

		Avg.	Min.	Max.
<i>Organics</i>				
<i>TOC</i>	%	<b>6.36</b>	4.96	8.15
<i>PCB</i>	ppm	<b>0.22</b>	0.1	0.4
<i>Selected Heavy Metals</i>				
<i>Cr</i>	ppm	<b>153</b>	108	237
<i>Hg</i>	ppm	<b>0.24</b>	0.07	0.76
<i>Pb</i>	ppm	<b>66</b>	34	99
SO <sub>3</sub>				
<i>SO<sub>3</sub></i>	%	<b>0.66</b>	0.51	0.91

As expected, the collected RCS showed a high content of silica and was heavily polluted with organic matter and heavy metals.

Table 5-9: Moisture of investigated RCS

		Avg.	Min.	Max.
<i>Moisture</i>	%	<b>41.5</b>	38.3	45.4

The moisture content was high. It would require significant thermal energy, unless the water is mechanically removed before the thermal activation process (Table 5-9).

#### 5.2.4 Deconstruction gypsum from Switzerland

In the frame of this study, a construction waste processing plant near Zurich, Switzerland was visited. Samples were taken and analysed (Figure 5-8).



Figure 5-8: Receiving and storage of pre-sorted gypsum boards

The testing strategy for the DCG had to be adapted from the AWS or RCS process because there were other expected challenges, such as:

- Oversized material
- Contamination with organics, metals and construction waste
- Conditions at the sorting plant

Large DCG boards were shredded to 100 % < 100mm and delivered to the Holcim test centre. Table 5-10 shows the fractions of the PSD after shredding.

Table 5-10: DCG particle size distribution

	PSD				
	>100 mm	> 20 mm	5–20 mm	< 5 mm	
<b>Sample P.1894</b> DCG after shredding	0 %	29 %	36 %	35 %	

Especially important was the evaluation of the degree of contamination. Contamination can influence both the preparation process and the quality of the product. Hence, first the metallic fraction was removed manually. The coarse non-metallic fraction (>20 mm) of the delivered material was then closely analysed for its composition. The reason for removing the metallic fraction was to simulate a processing plant at which metallic contamination could be removed by magnetic separators or eddy current separation. Other contamination, such as combustibles, ceramics and insulation materials, are more difficult and costly to remove. Table 5-11 shows the material composition of the sampled DCG excluding metals.

Table 5-11: Material composition of DCG excluding metals

				
P.1894 >20mm Whole fraction w/o metals	P.1894 >20mm Combustibles	P.1894 >20mm Ceramics	P.1894 >20mm Isolation	P.1894 >20mm Gypsum
100 %	17 %	12 %	9 %	62 %

It was rather surprising that only 62 % of the DCG consisted of gypsum itself; the remaining part comprised combustibles, isolation and ceramic contamination. The analysis of the actual gypsum showed the following mineralogical composition (Table 5-12).

Table 5-12: Mineralogical composition of gypsum part of DCG after removal of solid contaminants, according to XRD

Phase	Notation/Formula	P.1894
		Content in %
Quartz	$SiO_2$	1
Gypsum incl. Hemihydrate and Anhydrite	$CaSO_4$	84
Calcite	$CaCO_3$	2
Dolomite	$MgCa(CO_3)_2$	12
<b>% Sum</b>		<b>100.0</b>

The moisture level of the samples was, as expected, usually below 5 %.

### 5.2.5 Sample preparation and shipping

The two samples were prepared and numbered for further testing, namely:

- kaolinitic AWS from Rennes region, France (SL-2020-06-CH)
- mixture of non-kaolinitic AWS, RCS and DCG from Geneva region, Switzerland (EC-2020-06-SYM)

The goal was to collect a sample that was as representative as possible of the deposits in terms of their mineralogical content and moisture.

#### **Kaolinitic AWS from Rennes region, France SL-2020-06-CH**

A sample of 1'000 kg was collected from several locations of the kaolinitic AWS deposit near Rennes, France. The material was deliberately not mechanically pre-dried, since the behaviour of the equipment regarding materials having moisture of about 40 % needed to be tested. Additional smaller samples were also prepared and shipped for further testing of the material handling and crushing.

#### **Mixture of non-kaolinitic AWS, RCS and DCG in Switzerland (EC-2020-06-SYM)**

AWS was collected at several aggregate washing plants in Switzerland and mixed. DCG was obtained from a pre-sorting facility near Zurich. About 1'000 kg of the following mixture of materials was prepared, properly mixed inside a concrete mixer and crushed to <30 mm at the Holcim laboratory in Switzerland:

- Aggregate washing sludge (AWS) 77 %

- Road cleaning sludge (RCS) 8 %
- Deconstruction gypsum (DCG) 15 %

The resulting mix is called “alternative non-kaolinitic SCM”. The mineralogy of the mixed sample is shown in Table 5-13.

Table 5-13: Mineralogical composition of mix of AWS, RCS and DCG according to XRD

Phase	Notation/Formula	EC-2020-06-SYM P.1848
		Content in %
Quartz	$SiO_2$	35.6
Illite	$(K,H_3O)(Al,Mg,Fe)_2(Si,Al)_4O_{10}[(OH)_2 \cdot (H_2O)]$	0
Muscovite	$KAl_2AlSi_3O_8(OH)_2$	1.4
Chlorite	$(Mg,Fe)_3Al(Si_3Al)O_{10}(OH)_8$	5.0
Kaolinite	$Al_2Si_2O_5(OH)_4$	0
Smectite	$Al_2[(OH)_2Si_4O_{10}] \cdot nH_2O$	0
Calcite	$CaCO_3$	27.6
Dolomite	$MgCa(CO_3)_2$	6.2
Hematite	$Fe_2O_3$	0.2
Gypsum	$CaSO_4 \cdot 2H_2O$	12.6
Anhydrite	$CaSO_4$	1.6
Microcline	$KAlSi_3O_8$	0
Anatase	$TiO_2$	0
Albite	$NaAlSi_3O_8$	5.7
Sanidine	$K(AlSi_3O_8)$	3.0
Hornblende	<i>complex</i>	1.1
<b>% Sum</b>		<b>100</b>

The samples from France and Switzerland were placed in large bags and shipped to the drying screw testing centre of the company Koellmann in Adenau, Germany (Figure 5-9). Additionally, two smaller and uncrushed samples of 10 kg were shipped to the Bedeschi test centre in Italy for the crushing investigation.



Figure 5-9: left: Mix of AWS, RCS, DCG from Switzerland, Right: Kaolinitic AWS, Rennes, France

### 5.3 Drying screw conveyor testing

Drying screw tests were performed at the facilities of Koellermann in Adenau, Germany (Figure 5-10). The tests proceeded according to a trial plan that was prepared beforehand and partly adjusted according to the first results during the trial.

The aims of the test were 1) to simulate the drying part of the heat-exchanging process, 2) confirm the suitability and design assumptions and 3) define the sizing parameters that were required to design a suitable industrial-scale heat-exchanging screw with a thermal oil system. Additionally, the behaviour of the screw with occasional difficult and sticky material was to be tested.



Figure 5-10: Koellermann testing facility with drying screw



The tests were carried out using a double-shaft screw heat exchanger made by Koelmann, with the following design characteristics:

- Arrangement horizontal
- Diameter of hollow flights 320 mm
- Conveying length 2'175 mm
- Weight without bulk material ca. 3'000 kg

The heat transfer medium was a thermal oil with the following characteristics:

- Type Therminol 66
- Spec. thermal capacity @ 260 °C 2.42 kJ/kg.K
- Density @ 260 °C 0.84 t/m<sup>3</sup>

A thermal oil electric heating system was capable of heating about 3.6 m<sup>3</sup>/h thermal oil to an inlet oil temperature of up to 300 °C. The same system transported the oil through the housing, flights and shafts of the screw (Figure 5-11).

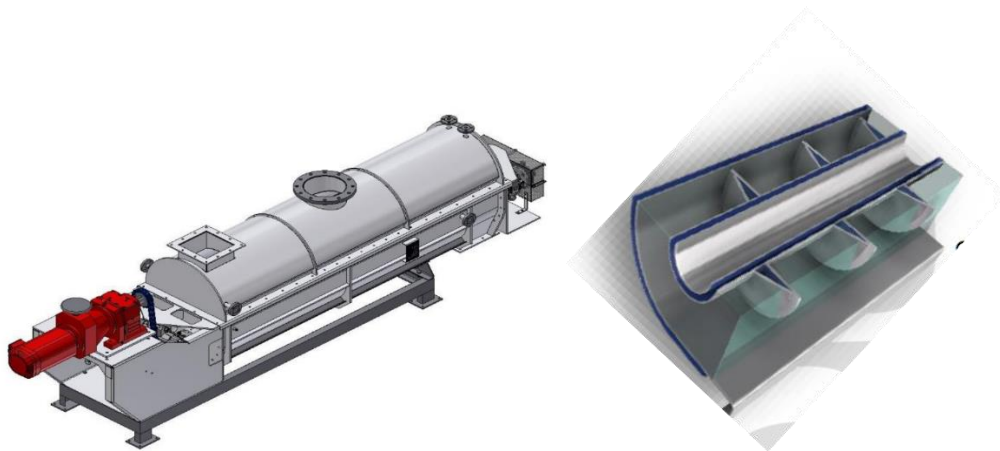


Figure 5-11: Schematic picture of Koelmann heat-exchanging screw conveyor (Köllemann, 2020)

The feed and product moisture were measured by a moisture meter (Sartorius MA 35) before and after the test. The screws operated with a feed rate of 130–170 kg per h and transferred the heat via a total surface of 7.2 m<sup>2</sup>, based on a 100 % filling level. This specification is important to define the size of the industrial heat exchangers.

Numerous tests with different retention times were conducted.

To simulate conditions as anticipated for the industrial application, the set point of the thermal oil temperature leaving the heater was initially defined as about 300 °C. However, this temperature could not be maintained due to insufficient capacity of the electrical heater. The test was therefore conducted at a somewhat lower oil temperature. However, the crucial difference between the two temperatures (IN and OUT) was successfully maintained for all tests at about 20°C (Figure 5-12).

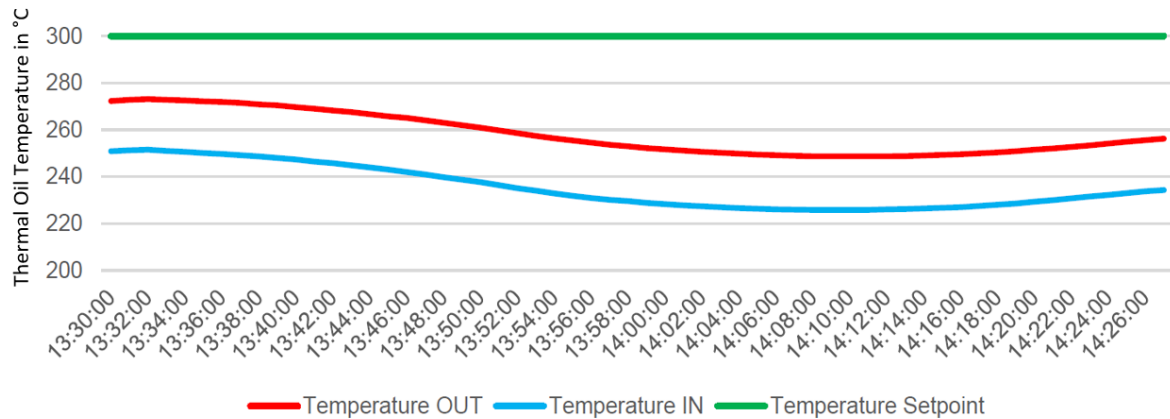


Figure 5-12: Thermal oil temperature progression with EC-2020-06-SYM

The heat introduced from the thermal oil system into the drying screw was calculated based on the volume flow and temperature difference as well as the thermal oil's specific heat capacity and density. This heat value was similar across all tests and was in the region of 146 MJ/h (Table 5-14).

Table 5-14: Calculated heat from thermal oil heating system

1. HEAT AVAILABLE FOR DRYING		
Thermal Oil Flow (V oil)	m <sup>3</sup> /h	3.6
Heat capacity (cp) @260 °C	kJ/(kg*K)	2.42
Density @ 260 °C	kg/m <sup>3</sup>	0.84
Temperature difference (IN) and (OUT)	K	20
<b>Heat available from thermal Oil System</b>	<b>MJ/h</b>	<b>146</b>

The results were generally as expected. However, the heat required to heat the material and evaporate the water did not fully match the heat input and varied by about 20 %. The discrepancy was mainly due to heat losses, variation of feed rate and expected inaccuracies in measurements due to the nature of the temporary semi-industrial testing facility (Table 5-15).

Table 5-15: Heat from thermal oil heating system

		Test No:1 with EC- 2020-06	Test No:2 with EC- 2020-06	Test No:3 with SL-2020- CH	Test No:4 with SL-2020-CH
<b>Feeding conditions</b>					
Moisture of wet feed material	%	18	18	43.8	29.4
Remaining moisture after dryer	%	4.9	3.8	29.4	3.63
Moist material feed	kg	159	167	191	134
Material product	kg	138	143	163	99
Testing time	min	25	40	45	45
Evaporated water in drying step	tph	0.050	0.036	0.037	0.046
Material temperature in	°C	18.5	18.5	18.2	41
Material temperature out	°C	97.5	79	74	82
<b>2. Heat requirement for drying</b>					
Heating up of:					
Feed material	MJ/h	30	15	14	7
Water inside the feed material	MJ/h	17	9	9	8
Evaporation energy of water	MJ/h	113	80	83	104
Heat losses	MJ/h	15	15	15	15
<b>Total heat requirement for drying</b>	<b>MJ/h</b>	<b>174</b>	<b>119</b>	<b>120</b>	<b>134</b>
<b>Balance error</b>		<b>-28</b>	<b>27</b>	<b>26</b>	<b>12</b>

The testing results showed that the surface area required for heat transfer was between 24 MJ/h/m<sup>2</sup> and 35 MJ/h/m<sup>2</sup>. These figures are an important indicator for the sizing of an industrial screw heat-exchanging system (Table 5-16).

Table 5-16: Calculation of specific heat transfer area

<b>Calculation of Heat Transfer Coefficient</b>					
Total heat requirement for drying	MJ/h	174	119	120	134
Heat-exchanging surface (100 % filling)	m <sup>2</sup>			7.2	
Filling level during test	%			70	
Effective surface in contact with material	m <sup>2</sup>			5.04	
<b>Specific heat transfer area</b>	<b>MJ/h/m<sup>2</sup></b>	<b>35</b>	<b>24</b>	<b>24</b>	<b>27</b>

An additional objective was to test the behaviour of the material inside the drying screws. During test EC-2020-06-SYM with about 18 % feed moisture, the material was well conveyable within the drying screws. Existing lumps were reduced or completely turned into fine particles and dust through the moisture loss (Figure 5-13). The remaining lumps contained more moisture than the fine part of the material.





Figure 5-13: Mixture of AWS, RCS and DCG before (left) and after (right) drying (test EC-2020-06-SYM)

The highly cohesive sample of SL-2020-06-CH, with a moisture of almost 44 %, was difficult to feed; nonetheless, it was conveyed well through the drying screw without coating the flights or significant formation of lumps (Figure 5-14).



Figure 5-14: Kaolinitic AWS (SL-2020-06-CH) before (left) and after drying (right)

In the case of the industrial drying application, heating of the thermal oil occurs with a cooling screw, which cools down the material from about 800 °C to about 250 °C; the screw also heats up the heat-exchanging thermal oil to about 290 °C. The cooling screw test could not be performed directly in the semi-industrial test facility. However, sufficient industrial applications exist that confirm the suitability of the cooling screw to adequately cool the material from the temperature level of 800 °C (or higher) to 250 °C.

#### 5.4 Calcination testing

Calcination tests were performed at the facilities of IBU-tec in Weimar, Germany. The tests proceeded according to a trial plan that was prepared beforehand and partly adjusted according to the first results during the trial. The results provided an indication of the feasibility of thermal

activation and the production of an alternative SCM with the pre-dried samples of EC-2020-06-SYM and SL-2020-06-CH. The objectives of the calcination testing were to assess

1. Dehydration of clay and/or production of first clinker phases at different temperatures and retention times, using a rotary calciner
2. Operation during oxidizing and reducing conditions
3. Production of large quantities of activated material for further grinding, transport and concrete testing.

#### Process parameters

- Temperature: 700–850 °C
- Residence time: approx. 45 min (hot zone), counter-current flow
- Atmosphere: oxidizing and reducing
- Raw material feed: approx. 40–50 kg/h

The samples were calcined in an indirectly fired kiln with the specifications listed in Table 5-16.

Table 5-17: *Technical Parameters of IBU-tec kiln*

<b>Kiln</b>	<b>IDO3</b>
Material of rotary kiln tube	metallic
Heating	Indirectly, natural gas, 6 burners
Dimensions	Diameter 0.5 m, heated length 4 m, overall length 8.5 m
Temperature range	150–1'100 °C Actual range used: 700–850 °C
Inclination	1.0°
Rotation speed	1.6 rpm

The raw material was fed into the gravimetric dosing unit by a screw via a big-bag feeding station directly into the kiln tube. The kiln was prepared for continuous thermal treatment in counter-current flow and was indirectly heated by six natural gas burners (Figure 5-15).

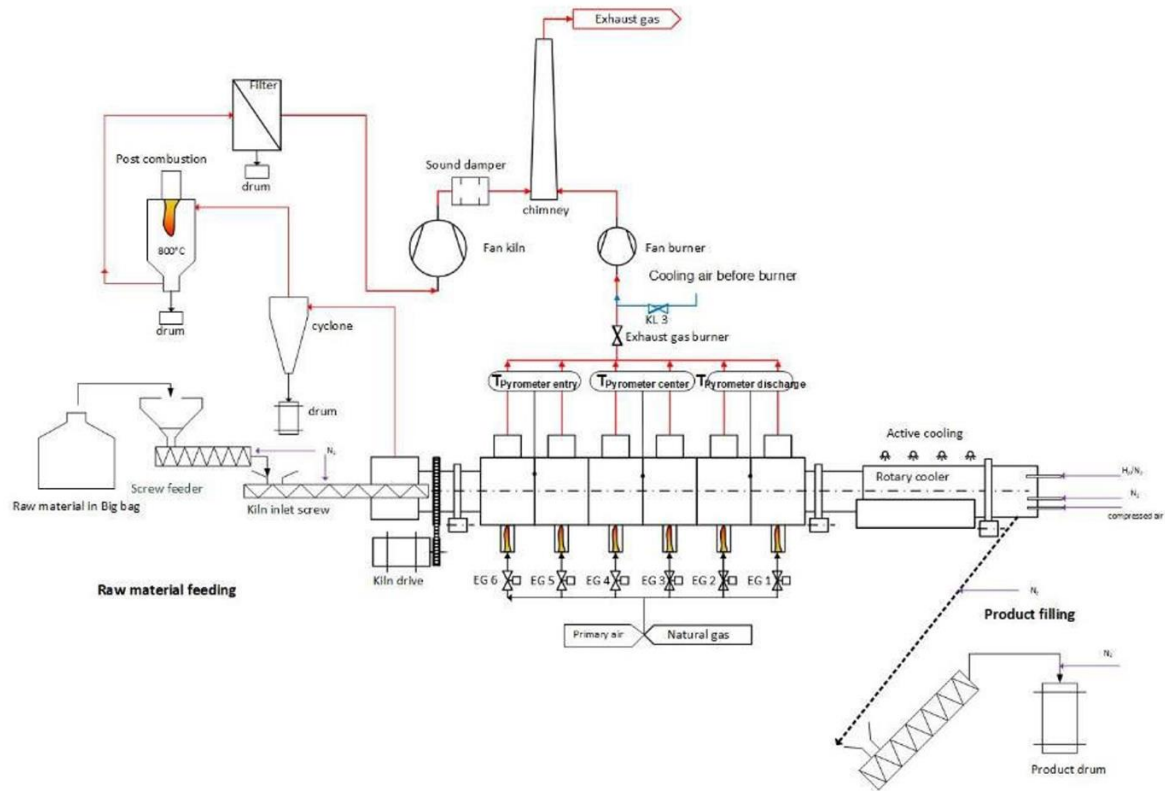


Figure 5-15: Flowsheet of IBU-tec kiln testing facility (IBU-tec, 2020)

The treated material was discharged via a rotary cooler into a product screw (Figure 5-16). It was then packed into drums and prepared for shipment to other testing facilities. The measured loss of ignition (LOI) was used to analyse the achieved quality for different activation temperatures.



Figure 5-16: IBU-tec testing kiln installation (IBU-tec, 2020)

## 5.4.1 Mineralogy of activated products

### 5.4.1.1 Non-kaolinitic SCM

Tests were conducted at 750 °C, 800 °C and 850 °C. As mentioned, limited portions of clay were present in the raw mix. The main focus was on the behaviour of calcite and free lime, which gradually reduced between 750 °C and 850 °C, indicating the production of amorphous phases. The amorphous phases increased to 38 % at 850 °C (Table 5-18) and were expected to contain some reactive phases, such as poorly crystalized belite, or phases of reactive calcium sulpho-aluminate, which result from the reaction between gypsum or anhydrite with calcite and dolomite.

Table 5-18: Mineralogical composition of product of non-kaolinitic SCM sample at different temperatures, according to XRD

Phase	Notation/Formula	Raw feed after mixing	Oxidizing condition @ ~750 °C	Oxidizing condition @ ~800 °C	Oxidizing condition @ ~850 °C
			Content in %	Content in %	Content in %
Quartz	$SiO_2$	35.6	27.9	31.2	29.3
Calcite	$CaCO_3$	27.6	14.1	7.2	7.1
Dolomite	$MgCa(CO_3)_2$	6.2	0	0	0
Muscovite	$KAl_2AlSi_3O_8(OH)_2$	1.4	0.4	0.4	0.3
Illite	$(K,H_3O)(Al,Mg,Fe)_2(Si,Al)_4O_{10}[(OH)_2 \cdot (H_2O)]$	0	0	0	0
Kaolinite	$Al_2Si_2O_5(OH)_4$	0	0	0	0
Chlorite	$(Mg,Fe)_5Al(Si_2Al)O_{10}(OH)_8$	5.0	0	0	0
Pyrite	$FeS_2$	0	0	0	0
Hematite	$Fe_2O_3$	0.2	0	0	0
Magnetite	$Fe_3O_4$	0	0	0	0
Anatase	$TiO_2$	0	0	0	0
Orthoklas	$KAlSi_3O_8$	0	0	0	0
Gypsum	$CaSO_4 \cdot 2H_2O$	12.6	0	0	0
Anhydrite	$CaSO_4$	1.6	6.1	7.3	7.4
Albite	$NaAlSi_3O_8$	5.7	6.0	6.9	6.0
Sanidine	$K(AlSi_3O_8)$	3.0	3.4	3.5	2.7
Hornblende	<i>complex</i>	1.1	2.9	3.7	2.8
Periclase	$MgO$	0	0.9	1.2	1.1
Free Lime	$CaO$	0	2.1	5.6	4.8
Amorph/microcrystalline		0	36.1	32.9	38.3
<b>% Sum</b>		<b>100</b>	<b>99.9</b>	<b>99.9</b>	<b>99.8</b>

#### 5.4.1.2 Kaolinitic AWS from France

At temperatures of about 800 °C, all kaolinite and illite clay minerals were transformed in amorphous phases, which could contribute to the performance of the produced SCM. The amorphous content increased to about 45 %. A significant portion of the amorphous content contributed to the conversion of kaolinite to metakaolin. Slightly higher amorphous content was observed during oxidizing conditions; this point was interesting but not relevant for the overall result of the test. Further investigation of this phenomena could be a topic of further studies.

Other clay minerals, such as muscovite, were only partly transformed at those temperatures. Crystalline quartz remained unchanged and can be considered inert, meaning it does not contribute to the cement's performance (Table 5-19).

Table 5-19: Mineralogical composition of product of kaolinitic AWS sample under oxidizing and reducing condition at different temperatures; Rennes, France according to XRD

Phase	Notation/Formula	Raw Feed	Oxidizing condition @ ~710 °C	Oxidizing condition @ ~795 °C	Reducing condition @ ~825 °C
		Content in %			
Quartz	$SiO_2$	22.8	30.5	29.0	30.0
Muscovite	$KAl_2AlSi_3O_8(OH)_2$	6.4	2.6	2.0	11.0
Muscovite dehydrox.		0	5.1	5.3	3.5
Orthoclase	$KAlSi_3O_8$	0	4.9	4.5	5.1
Illite	$(K,H_3O)(Al,Mg,Fe)_2(Si,Al)_4O_{10}[(OH)_2 \cdot (H_2O)]$	9.6	0	0	0
Chlorite	$(Mg,Fe)_5Al(Si_3Al)O_{10}(OH)_8$	4.3	1.9	0	0
Kaolinite	$Al_2Si_2O_5(OH)_4$	47.4	4.1	0	0
Calcite	$CaCO_3$	0.2	0	0	0
Dolomite	$MgCa(CO_3)_2$	0.1	0	0	0
Hematite	$Fe_2O_3$	1.1	4.7	5.0	3.6
Goethite	$FeOOH$	*	0	0	0
Microcline	$KAlSi_3O_8$	2.9	2.1	2.4	3.2
Albite	$NaAlSi_3O_8$	0.5	0.6	0.8	1.1
Sanidine	$K(AlSi_3O_8)$	2.3	0	0	0
Siderite	$FeCO_3$	0.4	0	0	0
Alunite	$KAl_3(SO_4)_2(OH)^6$	1.1	0	0	0
Anatase	$TiO_2$	0.5	0	0	0
Merwinite	$Ca_3Mg(SiO_4)_2$	0	0.2	1.3	0.9
Rutile	$TiO_2$	0	1.3	1.0	0.2
Maghemite	$\gamma-Fe_2O_3$	0	0.1	0.2	0.5
Amorphous/ Microcrystalline		0	41.0	47.7	38.1
<b>% Sum</b>		<b>99.6</b>	<b>99.1</b>	<b>99.1</b>	<b>99.1</b>

\* some % of goethite not quantified by XRD was also present, which affected the quantification of product phases

Under oxidizing conditions, more hematite was present in the product, leading to a stronger reddish colour. The product colour under a reducing atmosphere was dark brown, as described in the next paragraph.

#### 5.4.2 Colour

As noted, the content of iron oxide was high in the kaolinitic AWS sample from Rennes, France (SL-2020-06-CH). Tests under oxidizing and reducing conditions in the calciner and cooler were thus conducted to determine the influence on the colour of the product depending on the oxygen concentration. As described in Chapter 4, the reddish colour of hematite is not desirable

due to poor customer acceptance; the black or grey colour of magnetite is preferred. The results of the tests are outlined in Chapter 6.

## 5.5 Crushing tests

Crushing tests were not directly conducted. However, samples of material were submitted to relevant crusher suppliers. Because of the high moisture and sticky behaviour of the material and the presence of highly abrasive quartz, a double roller mineral sizer with slow rotation speed was selected. The crusher works by pressing material between the rollers so that fine sticky agglomerate passes through the rollers, taking the shape of the channel between them (Figure 5-17). Coarse and oversized stones, including quartz, would be crushed and downsized to the required 95 % of the material being smaller than 30 mm and 100 % being smaller than 35 mm. This is the required maximum size for the upstream drying screw conveyors.

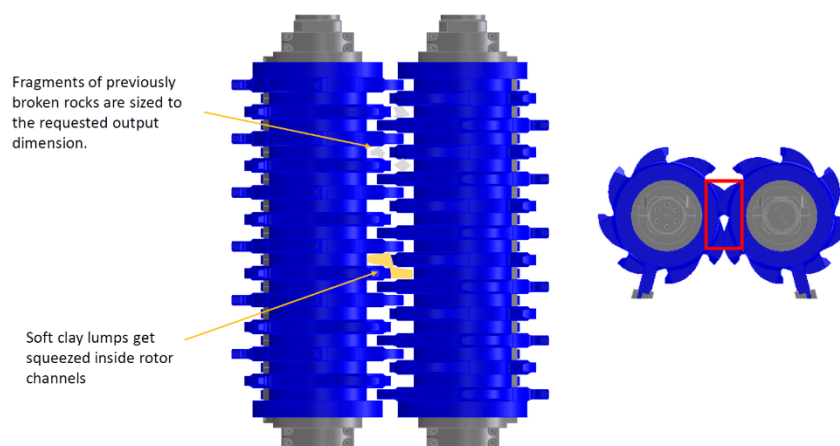


Figure 5-17: Schematic of mineral sizer

## 5.6 Grinding tests

Looking at the particle size distribution of the kaolinitic and none-kaolinitic AWS shown in Figure 5-2 and 5-5, none or only very limited grinding would be required to achieve the target fineness of below 100  $\mu\text{m}$ . In view of an industrial application a flexible grinding system was envisaged which will be capable to grind either AWS or material from a natural deposit or a mixture with DCG and RCS.



A wide range of feed materials was represented by a mixture of several activated materials, which were mixed and shipped to VDZ Technology GmbH, Duesseldorf/Germany. This company was assigned to conduct grinding trials on their ball mill system. For a future industrial application, grindability testing should be conducted using the final choice of materials.

The purpose of the first grinding test was to demonstrate the suitability of a ball mill system. The aim was to produce a product that met the norms, was sufficiently fine to be activated in a cement and provided a well-balanced particle size distribution – which would avoid the over-grinding of soft clay or limestone and the insufficient grinding of hard and difficult to grind quartz.

Mainly due to the quantity of hard and abrasive quartz, a ball mill system was selected. Other grinding systems such as vertical roller mills would also be feasible if they provided sufficient wear protection. Roller presses would probably not be suitable because of the plastic behaviour of clay.

The continuous grinding plant of VDZ is characterized by its capacity to be operated in both a single pass mode and a recirculating mode. The plant is shown in Figure 5-18 with a brief explanation of the individual components. In the single pass operation, only the material feed for defined dosing (1) and the heatable single-chamber ball mill (2) are used. The ball mill is equipped with lifting bars inside the grinding chamber. It has a discharge wall with an adjustable hole width for the discharge opening (Figure 5-18), which has a free area of 10.6 % when fully open. The mill's dimensions are 0.4 m x 1.2 m, with a length-to-diameter ratio (L/D) of 3.0.

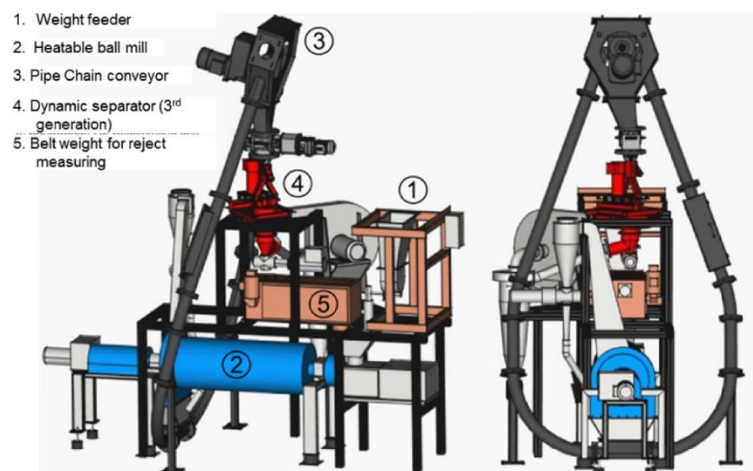


Figure 5-18: VDZ grinding installation (VDZ, 2021)



The mill speed during the test was 48 rpm, which resulted in a critical speed of 72 %. The mill was filled with approximately 95 kg of grinding media, which resulted in a filling degree of 13 %. The ball charge consisted of 50 % of 15-mm and 50 % of 25-mm grinding media.

The weight feeder was equipped with a speed adjustable dosing screw which operates at 10–50 kg/h.

The aim of the grinding trial was to produce ground calcined material with a product fineness of  $D_{90} < 100 \mu\text{m}$ . In other words, 90 % of the product particles are smaller than  $100 \mu\text{m}$ . The particle size distribution of the material was measured by sieving for the coarse range and by laser diffraction in the finer particle size range. Figure 5-19 displays the measured PSD of the fresh feed. The  $D_{50}$  value of the material was determined at approximately  $100 \mu\text{m}$ , and the  $D_{90}$  value was measured at about  $1'500 \mu\text{m}$ .

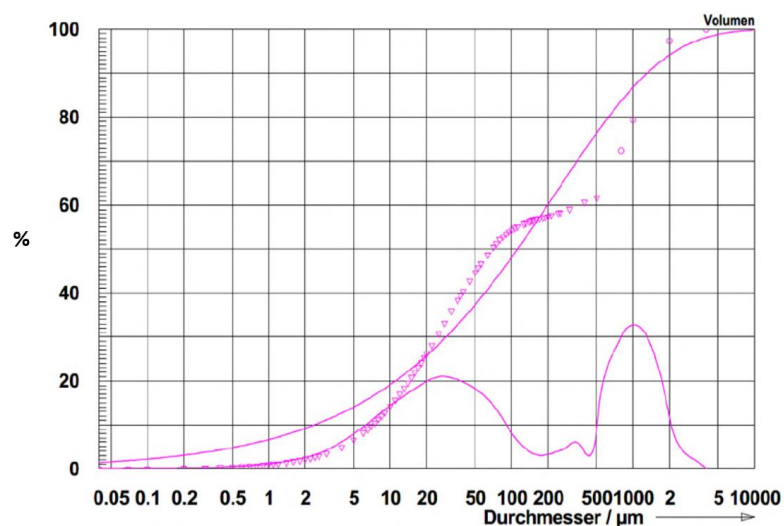


Figure 5-19: PSD of fresh feed without particles above 4 mm

To closely simulate the possible expected conditions under the new method of activation, the material was preheated in the oven to about  $100 \text{ }^\circ\text{C}$ . Three trials were then conducted with different feed rates and a stable mill ventilation of 1 m/s. To obtain a stable grinding operation, a ramp-up time of 15–20 minutes with the desired feed rate was employed. After this period, the test was started. The materials of the cyclone and the mill outlet were collected separately. After the test, the mill was opened and photographs were taken to obtain information about coating of the mill internals and the filling degree.

The test was conducted with different feed rates of 32, 40 and 50 kg/h. The duration of the test was about 30–50 minutes. The capacities of material collected at the mill and cyclone outlet

were measured. At the end of the trial, a crash stop was performed and the mill was opened. As shown in Figure 5-20, the mill was properly filled. No major coating was visible at the lining and the outlet wall in any of the three tests. The grinding media was also not coated, providing efficient grinding conditions.



Figure 5-20: View inside the testing ball mill (Trial 1)

To investigate the possible segregation of fine and coarse material, the mill outlet and the cyclone materials were separately collected and homogenized. Samples were taken and analysed with laser diffraction. As shown in Figure 5-21, the cyclone product was slightly finer than that of the mill outlet. Similar results were achieved for all three trials. These results indicate that fine clay was not predominantly picked up in the air flow and did not accumulate in the cyclone.

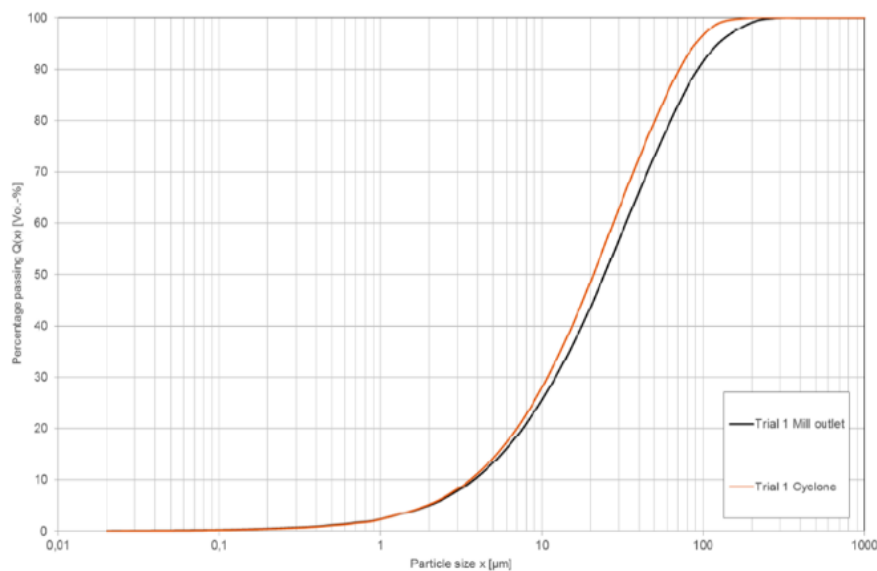


Figure 5-21: PSD of mill and cyclone product with Trial 1 with 40 kg/h feed

Table 5-20: PSD parameters of grinding trials

Trial	Feed rate in kg/h	D 50 in $\mu\text{m}$	D 90 in $\mu\text{m}$
Trial 1 mill	40	24.5	92.8
Trial 1 cyclone	40	20.8	71.3
Trial 2 mill	50	24.9	99.2
Trial 2 cyclone	50	25.2	83.0
Trial 3 mill	32	23.1	81.2
Trial 3 cyclone	32	23.2	73.5
<i>Trial 1 weighted</i>	40	23.3	85.7
<i>Trial 2 weighted</i>	50	25.0	94.7
<i>Trial 3 weighted</i>	32	23.1	78.7

During the test, several machine parameters were recorded. Most important for this test was the power consumption of the mill. Data was recorded every 10 seconds and an average was calculated; the results are shown in Table 5-20. From experience it is known that the mill shows approximately 20 % higher power consumption than a larger industrial ball mill. Therefore, a corrected value is indicated in Table 5-21 as an estimation.

Table 5-21: Power consumption of the different trials

Trial	Feed rate in kg/h	Mill motor power in kW	Specific mill motor power consumption in kWh/t	Corrected specific mill motor power consumption in kWh/t
Trial 1	40	0.5491	13.7	10.9
Trial 2	50	0.5493	11.0	8.8
Trial 3	32	0.5494	17.2	13.8

In Figure 5-22, the D50 and D90 values from the weighted PSDs (Table 5-17) are shown in correlation to the corrected specific power input. The table shows a clear influence of the power input on the D90 value but not on the D50 value. It can be assumed that some of the less grindable particles remained in the coarser fraction of the material, whereas the finer fraction consisted mainly of material that was easily grindable.

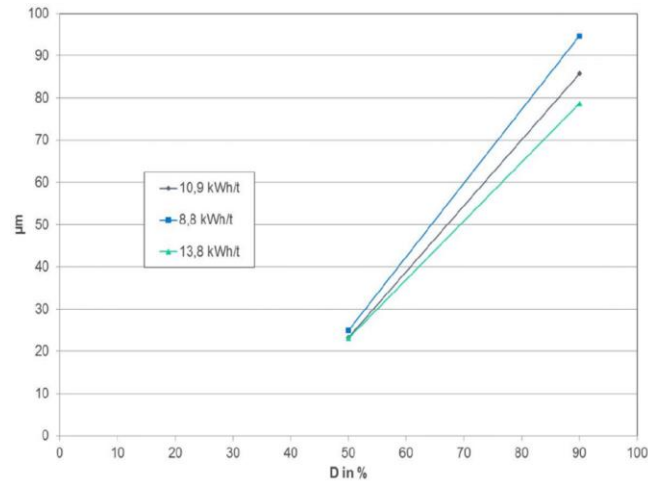


Figure 5-22:  $D_{50}$  and  $D_{90}$  value in correlation to power input

The next investigation focused on whether high air velocities inside the mill would cause clay to be discharged with the mill vent air, thus avoiding overgrinding. Trials were conducted with velocities slightly above 1.0 m/s. During the first tests, it became clear that high air velocities lead relatively quickly to insufficient residence time in the mill and to the presence of too much material in the cyclone of the mill dedusting. The material filling in the mill was low and resulted in a theoretical loss of grinding energy (Figure 5-23). The test was interrupted due to the insufficient calcined material that remained. In conclusion, for industrial applications, wider flexibility in the air velocity should be allowed to make the most use of the grinding efficiency and avoid overgrinding, especially of the clay.



Figure 5-23: Empty mill during pre-trials with air velocities of  $> 1\text{ m/s}$  above the ball filling

In summary, the test results showed that grinding of the preheated activated material was feasible. Potential risks that could harm the grinding efficiency, such as coating of the clay on balls and liners, was not observed. Although not conclusively demonstrated by the test, it appeared that overgrinding could potentially be prevented by a flexible aeration system to extract soft

and sufficiently ground material via the mill vents. The grindability ranged widely, between 9 kWh/t and 14 kWh/t, depending partly on the mill operation. In real life, once the final location of an industrial application is selected, detailed tests must be conducted with specific materials to determine the final grindability.

### **5.7 Mortar compressive strength testing**

Testing was performed on mortar prisms with a standard dimension of 40 mm x 40 mm x 160 mm according to EN 196-1. The mortar was prepared by mixing the desired cement composition with norm sand and water to obtain a mixture with a plastic composition, inside an automatic mixer. Each mortar cube consisted of (450 +/- 2) g cement, (1'350 +/- 5) g sand and (225 +/- 1) g water. The prepared cubes were stored for the first 24 h in storage with a humidity level of at least 90 % and a temperature of 20 °C. After 24 h, the cubes were stored in water at 20 °C for further curing. A compressive strength test was then performed at the following time intervals.

- 48 h (+/- 30 min)
- 7 d (+/- 2h)
- 28 d (+/- 8h)

For the testing of compressive strength, pressure was equally applied to the complete surface of the cube and was then increased by (2'400 +/- 200) N/s until the cube broke. The tests were repeated three times and the arithmetic average of each of the three results was calculated.

### **5.8 Water demand testing**

Cement paste, from mixture of the cement with water, has a certain resistance to the penetration of a standard needle according to EN-196-3. The amount of water required to achieve the standard stiffness was determined on the basis of several penetration attempts on cement with different levels of water content.

## **5.9 Summary of Chapter 5**

The various tests conducted to validate the new manufacturing technology did not reveal any surprises. The results demonstrated that drying in a heat-exchanging screw as well as calcining, grinding and colour control were feasible and technologically manageable.

Mortar and water demand testing were conducted according to the European Norm EN 196-1.

The impact of the thermally activated products and the results of the semi-industrial testing on the dimensioning of the new calcining method are described in the following chapter.

## Chapter 6: Experimental results

*Chapter 6 focuses on the test results and suitability of the tested materials to serve as SCMs. The results presented here include the performances of thermally treated and produced alternative SCMs and their influence on the strength of the produced cement. The chapter also evaluates the results of several semi-industrial tests conducted to validate the theoretical assumptions underlying the heat exchange (drying/cooling), calcination, material handling and grinding processes.*

### 6.1 Characteristics of activated materials

Not all minerals develop cementitious properties after thermal activation. Therefore, the study aimed to investigate minerals with suitable compositions to produce an alternative SCM. The selected materials contain blends of waste streams currently mainly deposited in quarries or landfills, comprising mainly the following:

- limestone;
- clay;
- quartz and feldspar
- calcium sulphates.

Due to the proximity of two cement plants, the following waste materials, which are locally available in sufficient quantities, were investigated and thermally activated:

1. Kaolinitic AWS from the Rennes region in France;
2. Non-kaolinitic alternative SCM comprising 77% AWS, 15% RCS and 8% DCG from the Geneva region in Switzerland.

In both cases, a suitable mineral composition was achieved, and the thermally activated materials developed latent hydraulic and pozzolanic properties required for the strength development of cement (Figure 6-1).

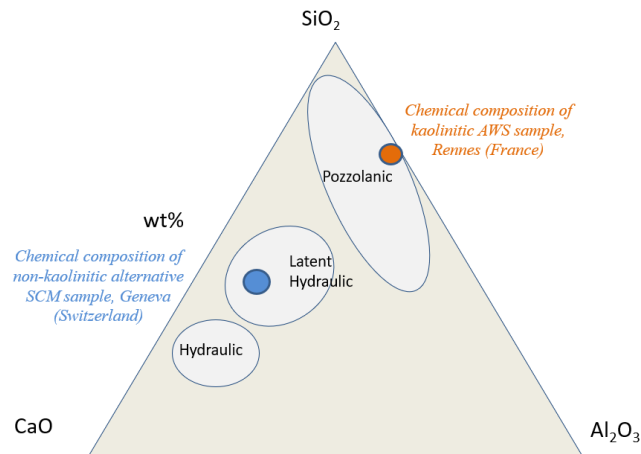


Figure 6-1: Reaction behaviour of investigated kaolinitic AWS and none-kaolinitic alternative SCM shown in a ternary CAS phase diagram

The benefit of 8 % RCS in the non-kaolinitic alternative SCM sample from Switzerland was considered from ecological and financial viewpoints. The highly contaminated RCSs were especially evaluated due to the high prices of CHF 200 (EUR 180) per ton in Switzerland, which can be obtained for appropriate thermal treatment. Due to the low quantity of RCS in the mixture, the potential impact on the cement reaction is negligible.

DCG was considered mainly regarding processing an anthropogenic material and the formation of calcium sulphate (anhydrite) and subsequently the substitution of natural gypsum in the final cement product. Additionally, especially in latent hydraulic systems, the calcium sulphate acts as a reaction activator, enhancing the reactivity. Consequently, the concrete performance and reaction behaviour of the none kaolinitic alternative SCM was better than expected for a theoretically latent hydraulic reacting SCM as outlined in chapter 6.2.

The thermal treatment of the DCG above 400°C is essential. Tests were conducted with untreated gypsum boards to replace natural gypsum in cement, showing a significant reduction in the cement compressive strength, attributed to the high content of organics, including paraffin waxes and silicones. Mortar tests with the thermally treated DCG showed the same strength development as geogenic gypsum from a natural deposit (Kruspan, Bier & Weihrauch, 2022).

Theoretically, DCG or RCS could also have been used in the kaolinitic AWS. However, these were not available close to the cement plant in France.



## 6.2 Concrete performance and colour

### 6.2.1 Thermally activated kaolinitic AWS from France

The thermally activated kaolinitic AWS from the facility near Rennes, France, was mixed with CEM I 52.5N and ground limestone to obtain cements with the following composition:

- 50% CEM I 52.5N from a Lafarge plant at Saint Pierre LaCour, France with 90% clinker, 5% limestone and 5% gypsum;
- 25% activated kaolinitic AWS;
- 25% limestone.

For comparison reasons, additional mortars were prepared with the following compositions:

- 100% CEM I 52.5N from a Lafarge plant at Saint Pierre LaCour, France;
- 50% CEM I 52.5N from a Lafarge plant at Saint Pierre LaCour, France + 50% limestone.

The compressive strength was measured after 2 and 28 days. The results are shown in Figures 6-2 and 6-3.

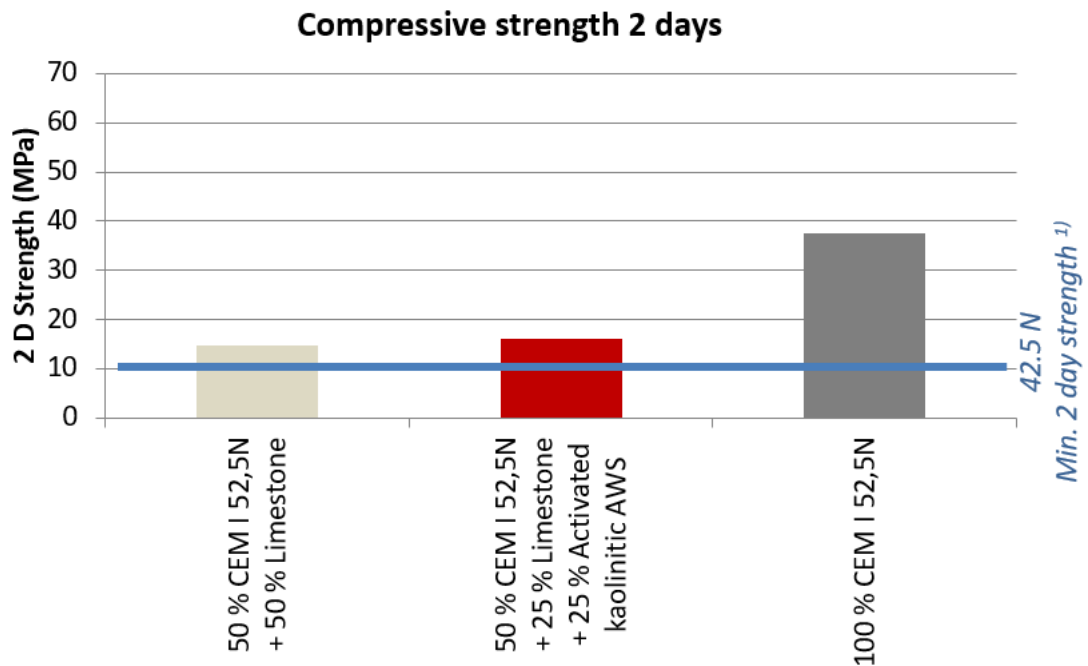


Figure 6-2: 2-Day compressive strength of different mortars (<sup>1)</sup>According to EN196-1)

After 2 days, the mortar prepared with 25% activated kaolinitic AWS and 25% limestone showed similar strength development to that of the mortar with 50% inert limestone. This result confirmed that activated kaolinitic AWS did not contribute to the early strength of concrete. The desired strength class of 42.5 N with a minimum early strength of 10 MPa was obtained for the cement mixture with calcined kaolinitic AWS. If an increased early strength is required, further optimization regarding the fineness or increased content of CEM I 52.5N should be considered for industrial applications.

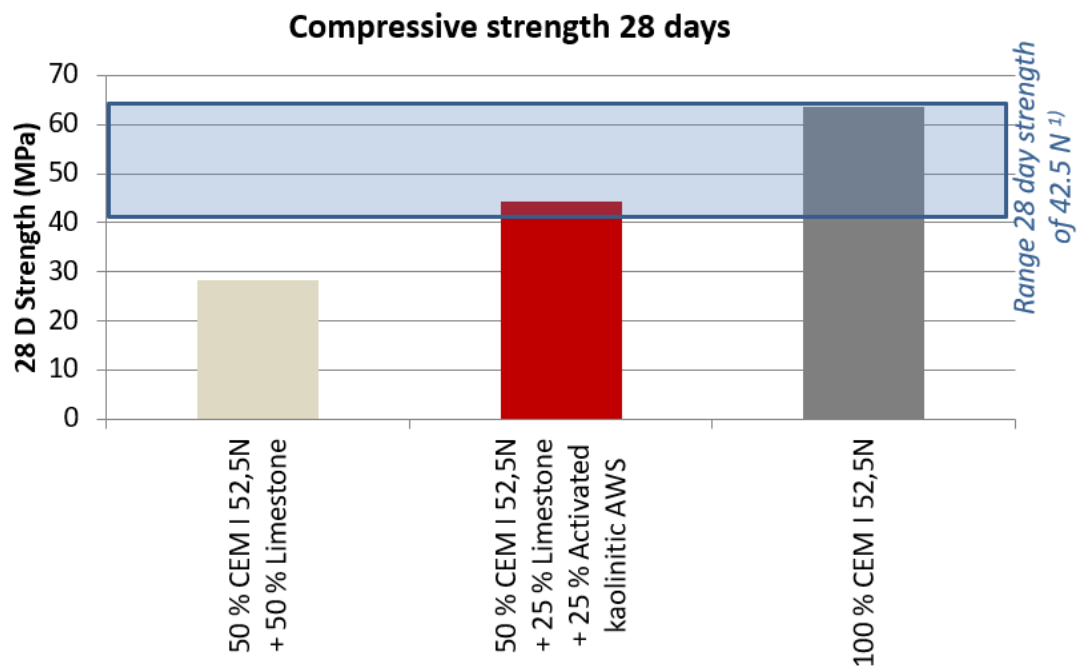


Figure 6-3: 28-Day compressive strength of different mortars (<sup>1)</sup>According to EN196-1)

The performance differed at 28 days, with the activated kaolinitic AWS contributing substantially to the compressive strength development (more so than the mortar with 50% limestone). The desired minimum strength of 42.5 MPa was achieved but at the lower limit. With an increase in the content or fineness of CEM I 52.5N, the desired strength required to produce a 42.5-MPa cement according to EN196-1 would be achievable in an industrial application.

The content of activated kaolinitic AWS deteriorates the rheology. With a water-to-cement ratio of 0.5 for all mortar mixes, the activated kaolinitic AWS mortar showed a significantly reduced mortar spread of only about 200 mm (Figure 6-4). A water-to-cement ratio of about 0.6 would be required to achieve the same spread as the 100% CEM I or the 50% limestone mortar. However, this would decrease the mortar strength. Therefore, admixtures would be required to

achieve a similar water-to-cement ratio and the same mortar spread. During testing, approximately 0.2% of the admixture Econex 395S was required to achieve the desired mortar spread of approximately 260 mm.

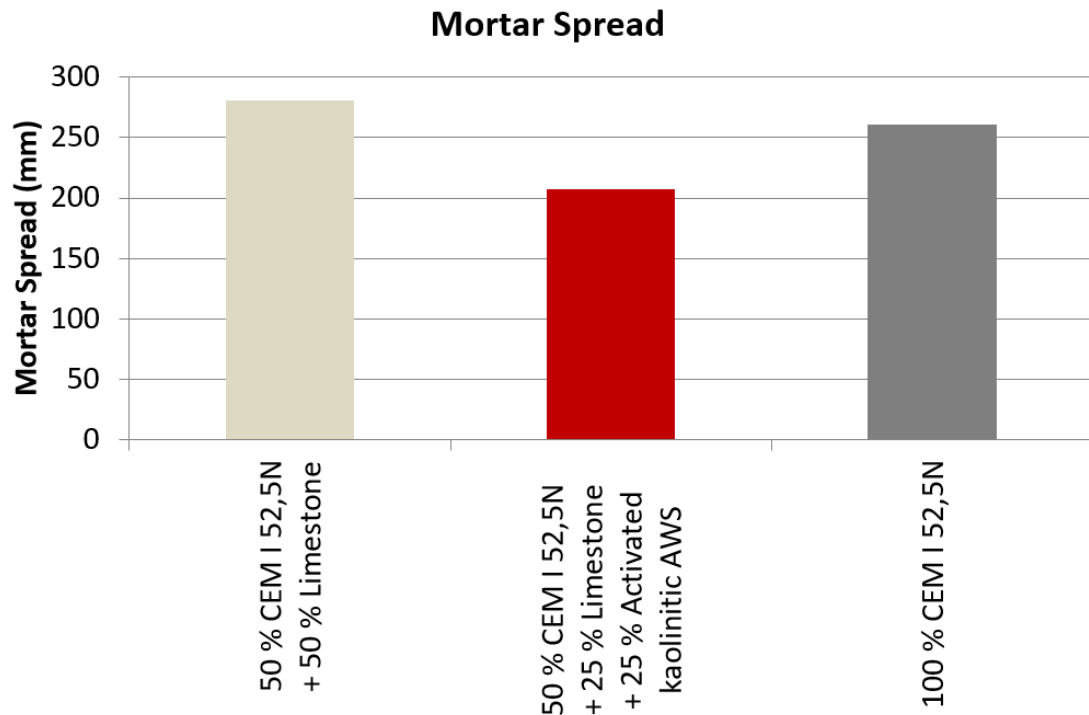


Figure 6-4: Mortar spread of different mixtures

An important contributor to the water demand is the fineness of the clay. If clay is ground together with the cement, overgrinding can occur due to the significant difference in grindability. Therefore, separate grinding of the calcined clay should be considered.

Like many clays, the tested kaolinitic AWS had a significant content of around 8% of iron oxide in the feed material. As outlined in Chapter 4, the presence of haematite ( $\text{Fe}_2\text{O}_3$ ) is critical as it causes an unwanted reddish colour in the product and the final cement. The atmosphere in the calciner was changed during the test from oxidizing to reducing conditions to influence the colour of the resulting product. This was achieved by injecting  $\text{CO}_2$  into the calciner and cooler, allowing a sub-stoichiometric operation and the creation of excess CO.

Due to the reducing gas atmosphere, dark grey to dark brown magnetite ( $\text{Fe}_3\text{O}_4$ ) was formed at temperatures of approximately 800 °C. Furthermore, as a simulation of the future production

process, the reducing conditions were maintained at the cooling stage before reaching temperatures of approximately 300 °C.



Figure 6-5: Influencing the product colour by varying the calcination conditions of the kaolinitic AWS sample from Rennes/France (SL-2020-06-CH)

Controlling the atmosphere influenced the product colour, impacting the cement and concrete colour (Figures 6-5 and 6-6).



Figure 6-6: Examples of concrete colour in calcined clay cements. Left, calcination under oxidizing conditions; right, calcination under reducing conditions

### 6.2.2 Thermally activated non-kaolinitic alternative SCM from Switzerland

The thermally activated mixture of non-kaolinitic AWS, RCS and DCG from Switzerland is hereafter called “non-kaolinitic alternative SCM”. In this study, it was mixed with CEM I 42.5N to obtain a cement with the following composition:

- 85% CEM I 42.5N from a Holcim plant at Siggenthal with 90% clinker, 5% limestone and 5% gypsum;
- 15% mixture of thermally activated non-kaolinitic alternative SCM from Switzerland.

For comparison reasons, additional mortars were prepared with the following compositions:

- 100% CEM I 42.5N from a Holcim plant at Siggenthal, Switzerland;
- 85% CEM I 42.5N from a Holcim plant at Siggenthal, Switzerland + 15% burnt oil shale from Dotternhausen, Germany.

The compressive strength was measured after 2 and 28 days, and the results are shown in Figures 6-7 and 6-8. The comparison with the BOS was necessary because one of the objectives was the potential replacement of BOS by activated non-kaolinitic alternative SCM. Compared to the tests with activated kaolinitic AWS, a lower substitution rate of CEM I 42.5N was considered, namely 15%.

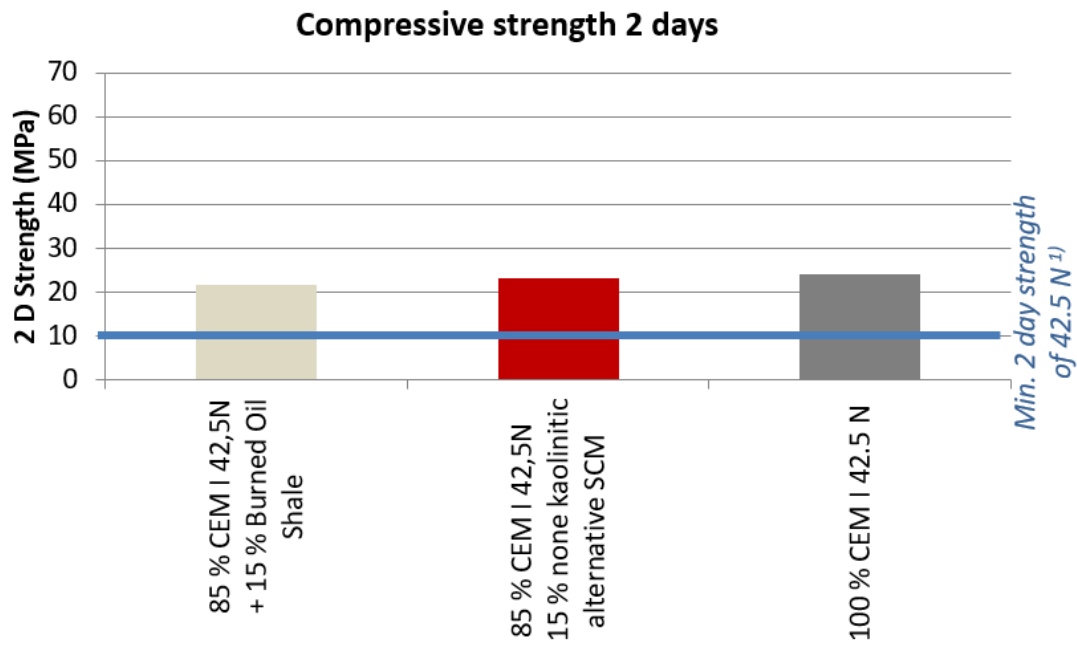


Figure 6-7: 2 Day compressive strength of different mortars (<sup>1)</sup>According to EN196-1)

After 2 days, the prepared mortar with 15% activated non-kaolinitic alternative SCM showed a similar strength development to CEM I 42.5 N. It also offered a better contribution than BOS, indicating that hydraulic reactions occurred and contributed to the early strength (Figure 6-7). The desired early strength of 10 MPa, required for the strength class 42.5 N according to EN196-1, was achieved for the cement mixture.

On day 28, the mortar with an activated non-kaolinitic mixture contributed similarly to the compressive strength development of CEM 42.5.

The performance of the mixture with BOS was significantly better than that of the non-kaolinitic SCM. This was due to strong pozzolanic reactions.

The desired strength of at least 42.5 MPa was achieved in all three test cases. Hence, a possible increase in the content of activated non-kaolinitic alternative SCM can be considered for industrial application (Figure 6-8).

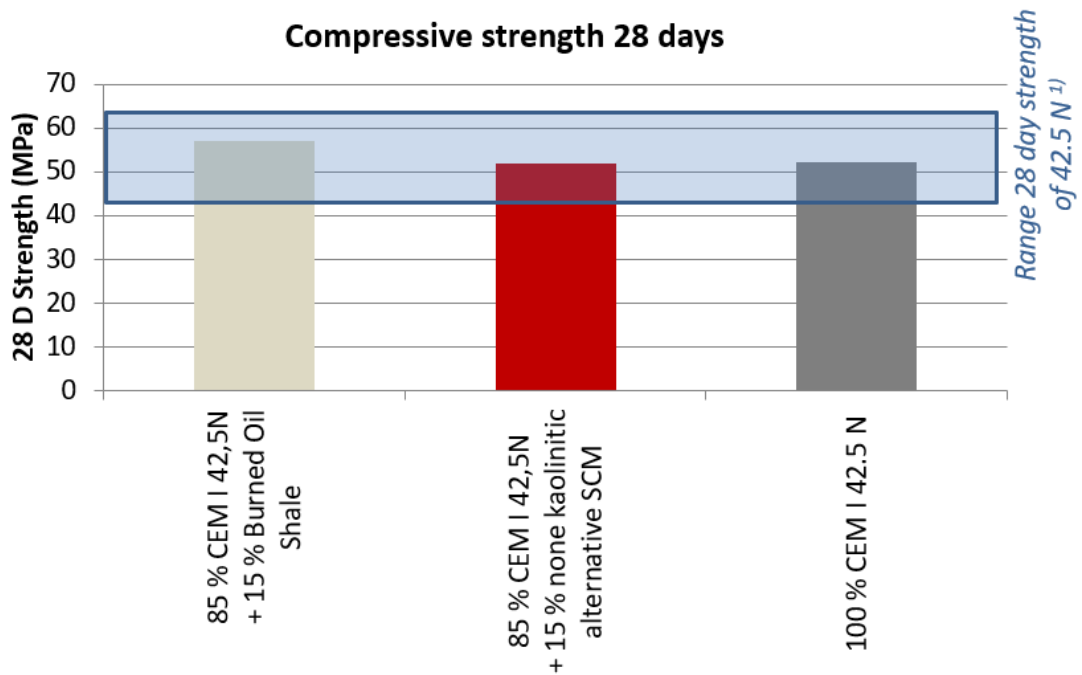


Figure 6-8: 28 Day compressive strength of different mortars (<sup>1)</sup>According to EN196-1)

Despite the relatively low iron oxide content in the non-kaolinitic alternative SCM, in the range of 2%–4%, the impact on the colour remained significant. Figure 6-9 shows the colours of the following cement mixtures:

- Ordinary Portland cement (CEM 42.5 N);
- Non-kaolinitic alternative SCM produced under oxidizing conditions;
- Non-kaolinitic alternative SCM produced under reducing conditions;
- Burnt oil shale;
- Ground limestone.

The new calcination technology can operate under reducing conditions to manage the colour expectations. This point is explained in previous chapters.

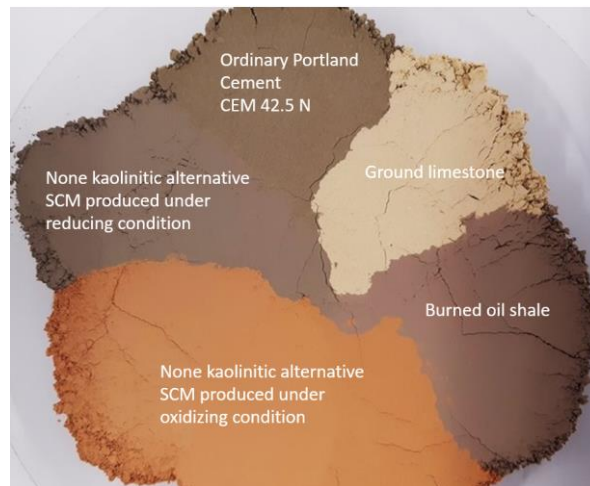


Figure 6-9: Colours of products

### 6.3 Equipment dimensioning

The theoretical considerations (Chapter 4) were integrated with the experimental results (Chapter 5). Based on the outlined industrial-scale capacity of 100'000 tons per year, the overall system was then dimensioned and designed within the framework of this study.

#### 6.3.1 Process mass flow

A simplified overall mass flow diagram was prepared based on the earlier process calculations and experimental results of Chapters 4 and 5. The diagram is shown in Figure 6-10. For simplicity, the following paragraphs mainly focus on the following key equipment dimensioning:

- Heat-exchanging screws and thermal oil system;
- Rotary calciner;
- Ball mill.

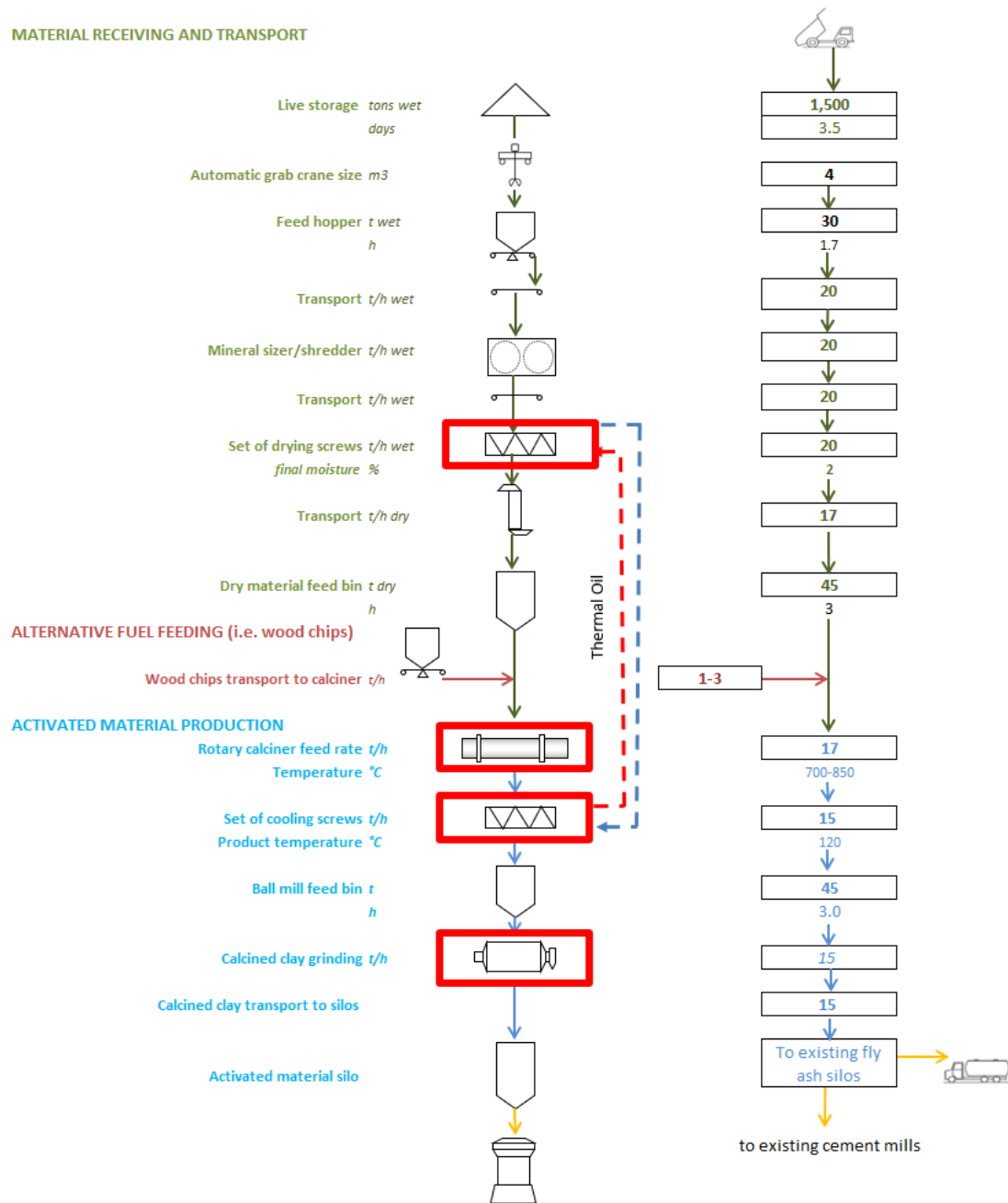


Figure 6-10: Simplified overall massflow diagram of calcining process

### 6.3.2 Heat-exchanging screws and thermal oil system

#### Quantity and size of drying screws

Tests with the Koelmann drying screw indicated that a minimum specific heat transfer area of  $a_{\text{spec}} = 24 \text{ MJ/h/m}^2$  (Table 5-14) is required for the drying screw size. A similar range was expected by the supplier, based on prior tests with similar materials.



During the cooling process of the alternative SCM, from 800 °C to 250 °C, thermal energy of about  $Q_{usable} = 10'204$  MJ/h is released (Equation 4.7c). It is transferred to the drying screws via a heat-exchanging thermal oil system. The surface of the industrial drying screw arrangement should be no less than  $A=425$  m<sup>2</sup> of active heat-exchanging area, calculated with Equation 6.1:

$$A = \frac{Q_{usable}}{a_{spec}} \quad (6.1)$$

$$A = \frac{10'204 \frac{MJ}{h}}{24 \frac{MJ}{h \times m^2}} = 425 \text{ m}^2 \quad (6.1a)$$

Based on the supplier's proposal, three drying screws with four flights each, with a total surface area of screws and housing of 193 m<sup>2</sup> each, were considered. They provided a total area having three screws and 75 % filling of 435 m<sup>2</sup>, which is slightly larger than the minimum requirement of 425 m<sup>2</sup>.

#### Thermal oil requirement and flow rate

As the heat transfer medium, a thermal oil with the following characteristics was selected:

- Type Therminol 66
- Spec. Thermal capacity @ 280 °C 2.49 MJ/t K
- Density @ 280 °C 0.825 t/m<sup>3</sup>

It is assumed that the thermal oil enters the drying system at a temperature of 290 °C and is discharged at about 270 °C. Heat required to be transferred was calculated at 10'204 MJ/h.

$$m = \frac{Q_{usable}}{cp \times \Delta T} \quad (6.2)$$

$$m = \frac{10'204 \frac{MJ}{h}}{2.49 \frac{MJ}{t K} \times (290^\circ C - 270^\circ C) K} \sim 205 \frac{t}{h} \quad (6.2a)$$

$$V = \frac{m}{\rho} \quad (6.3)$$

$$V = \frac{205 \frac{t}{h}}{0.825 \frac{t}{m^3}} \sim 250 \frac{m^3}{h} \quad (6.3a)$$

For the recovered heat of 10'204 MJ/h to be conveyed from the cooling to the heating screw, the volume of thermal oil exchanged must be at least 250 m<sup>3</sup>/h (Equation 6.3).

For industrial application, a slightly higher than required thermal oil volume of 270 m<sup>3</sup>/h was selected (Table 6-1).

Table 6-1: Selected thermal oil volume of heat-exchanging screws

	Selected Thermal Oil Volume
Shaft and Flights	3 x 72 m <sup>3</sup> /h = 216 m <sup>3</sup> /h
Housing	3 x 18 m <sup>3</sup> /h = 54 m <sup>3</sup> /h
<b>Total</b>	<b>270 m<sup>3</sup>/h</b>

### Cooling screw design limitations

Cooling screws could not be tested in a semi-industrial test. Therefore, CFD simulations were performed to ensure that overheating of the specified thermal oil was avoided. According to the supplier's thermal specifications, temperatures of 569 °C are critical for the oil to decompose, and temperatures above 399 °C should be avoided to prevent auto-ignition in the case of leakage. Several design changes were performed, especially regarding the design of the screw flights, to avoid these critical conditions (Figure 6-11).

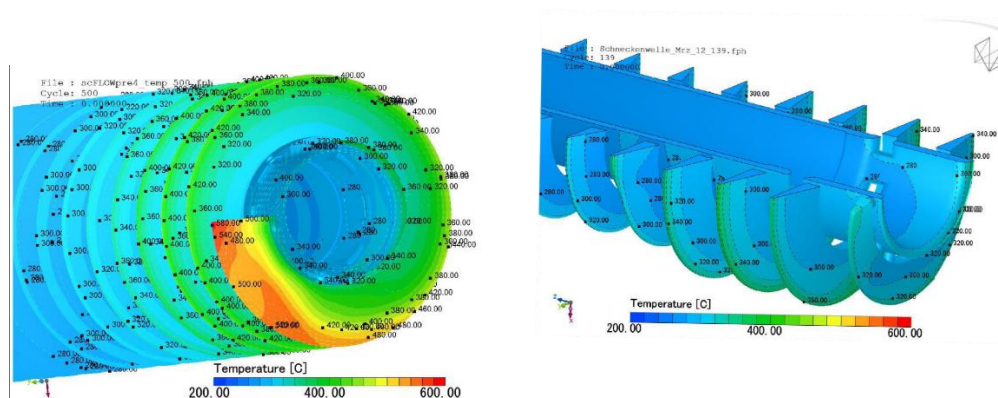


Figure 6-11: Critical oil temperature before (left) and after design modification (right) of the cooling screw.

### 6.3.3 Rotary calciner dimensioning

Raw material, fuel and air or combustion gases travel through the rotary calciner in co-current flows. The purpose is to expose the mixture of material and fuel entering the calciner to hot air (800–900 °C) from the clinker kiln.

The rotary kiln has lifting elements in the first 40 % (approximately) of its cylindrical portion. The intention is to expose the material and fuel intensively to the hot air from the clinker kiln, dry it completely, and simultaneously start ignition of the fuels and heat transfer to the material in order to start the thermal activation process.

A low gas velocity of 2–3 m/s enables the separation of the material from the flue gases to a large extent.

Combustion is not required to be fast. Rather coarse fuel with a moderate NCV is preferred to avoid local overheating.

Based on the expected actual air flow passing the calciner to the clinker kiln ( $V_{act}$ ) of 45'000 Am<sup>3</sup>/h, as calculated in Chapter 4 (Equation 4.13), the calciner diameter ( $D$ ) should be about 2.5 m inside the refractory. This would achieve a gas velocity ( $v$ ) of 2.5 m/s (Equation 6.4).

$$D (m) = \sqrt{\frac{4 \times V_{act} \left(\frac{Am^3}{h}\right)}{\pi \times v \left(\frac{m}{s}\right) \times 3'600 \frac{s}{h}}} \quad (6.4)$$

$$D (m) = \sqrt{\frac{4 \times 45'000 \frac{Am^3}{h}}{\pi \times 2.5 \times 3600 \frac{s}{h}}} = 2,5 m \quad (6.4a)$$

Considering a refractory thickness of 152 mm, the resulting kiln shell would have an inside shell diameter of 2.8 m.

The rotary calciner must provide sufficient time for the complete burnout of the fuel and the thermal activation of the material. A flexible residence time of 30–90 min, with an average of about 60 min, was considered in the test case. However, it is adjustable with a flexible kiln speed.

Based on Equation 6.5, for the dimensioning of rotary kilns (Duda, 1985), a rotary calciner with the parameters shown in Table 6-2 was selected.

$$t = \frac{1.77 \times L \times \sqrt{\theta}}{v \times (D - 2 \times \text{Lining}) \times \text{rpm}} \times F \quad (6.5)$$

Table 6-2: Design parameters of rotary calciner

	Symbol	Rotary calciner
Calciner length	L	18.5 m
Diameter inside shell	D	2.8 m
Refractory thickness	Lining	2 x 152 mm
Material residence time	T	30 – 90 min
Angle of repose of material	Θ	35-40°
Calciner slope	Y	1.15 °
Velocity	rpm	0.5 - 2.0 (1 rpm for 60 min average)
Factor (which equals 1 if kiln has a constant diameter)	F	1

The main process control parameter for the energy input is the temperature of the flue gases at the exit of the rotary calciner. This temperature must be maintained at about 850 °C.

### 6.3.4 Ball mill dimensioning

The objective of the first installation was to dimension a grinding system with sufficient flexibility to process numerous locally available materials.

The results of the grinding test (described in Chapter 5) confirmed that a ball mill is capable of sufficiently grinding the product to a desired particle size of  $D_{90} < 100 \mu\text{m}$  (i.e. 90 % of the product is smaller than  $100 \mu\text{m}$ ). The specific power consumption ranged up to 14 kWh/t at the mill motor. It is expected that most of the grinding energy is absorbed by the hard-to-grind quartz. The soft calcined limestone, clay or gypsum consumes significantly less energy to achieve the desired fineness.

Based on a desired capacity of 15 tph and a grindability of 14 kWh/t at the motor, the installed motor power of the industrial application must not be less than 210 kW. To allow for sufficient flexibility in the first installation, a mill with an installed power of 250 kW and the parameters shown in Table 6-3 was selected.

Table 6-3: Design parameters of ball mill

	Symbol	Ball Mill
Mill motor power	P	250 kW
Mill length (grinding path)	L	3.8 m
Mill diameter (inside shell)	$D_i$	2.1 m
Mill diameter (inside liners)		1.8 m
No of compartments		1
Ball filling level	%	28-31 %
Ball charge	t	14
Mill speed	rpm	average 23.5 rpm (75 % $n_{critical}$ ) - variable

The mill is aerated with a dedicated filter and fan system. The aeration is adjustable from 0.5 m/s to 1.5 m/s air speed above the ball charge; this feature provides sufficient flexibility to discharge fine particles from the mill and avoid overgrinding. The mill fan is therefore equipped with a variable speed drive. The mill system is also equipped with a highly efficient separator to separate the product from coarse material; the latter is returned to the grinding system.

#### 6.4 CO<sub>2</sub> reduction

This section examines the CO<sub>2</sub> emissions associated with the activated products and the new technology. Based on the theoretical background and the comparison of the CO<sub>2</sub> contribution of available calcining technologies (see Chapter 4), Table 6-3 describes the specific CO<sub>2</sub> footprint of the materials tested from France and Switzerland using the new calcining technology.

Table 6-3: Net CO<sub>2</sub> contribution related to materials tested with the new calcining technology

	<b>Clinker production</b>	<b>Kaolinitic AWS from France</b>	<b>Non-kaolinitic alternative SCM from Switzerland</b>
CO <sub>2</sub> from decarbonization of calcite	530 kg CO <sub>2</sub> /t clinker <sup>1)</sup>	~1 kg CO <sub>2</sub> /t product (0.2 % calcite)	176 kg CO <sub>2</sub> /t product (~40 % calcite @ 440 kg CO <sub>2</sub> /t)
CO <sub>2</sub> from decarbonization of dolomite	0 kg CO <sub>2</sub> /t	~0 kg CO <sub>2</sub> /t product (0.1 % dolomite)	24 kg CO <sub>2</sub> /t product (~5 % dolomite @ 480 kg CO <sub>2</sub> /t)
CO <sub>2</sub> from Fuel (clinker kiln) <i>(based on an average of 95 kg CO<sub>2</sub> / GJ for coal and 0 kg CO<sub>2</sub> / GJ for biogenic fuels)</i>	275 kg CO <sub>2</sub> /t clinker <sup>2)</sup> <i>(3200 kJ/kg clinker)</i>	30 kg CO <sub>2</sub> /t SCM <sup>2)</sup> <i>(300 kJ/kg SCM)</i>	60 kg CO <sub>2</sub> /t SCM <sup>2)</sup> <i>(300 kJ/kg SCM)</i>
CO <sub>2</sub> from Fuel (integrated calciner) <i>0 kg CO<sub>2</sub> / GJ for biogenic fuels</i>	not required	0 kg CO <sub>2</sub> /t SCM <sup>3)</sup>	0 kg CO <sub>2</sub> /t SCM <sup>3)</sup>
CO <sub>2</sub> from electrical energy <i>(based on 300 kg CO<sub>2</sub> / MWh)</i>	18 kg CO <sub>2</sub> /t clinker <i>(60 MWh/t clinker)</i>	15 kg CO <sub>2</sub> /t product <i>(50 MWh/t product)</i>	15 kg CO <sub>2</sub> /t product <i>(50 MWh/t product)</i>
<b>Total</b>	<b>823 kg CO<sub>2</sub>/t clinker</b>	<b>46 kg CO<sub>2</sub>/t product</b>	<b>275 kg CO<sub>2</sub>/t product</b>

<sup>1)</sup> assumed 67 % lime in the clinker, <sup>2)</sup> assumed 90 % coal or similar and 10 % biogenic fuel, <sup>3)</sup> assumed 100 % of biomass (i.e. wood chips)

The production of clinker released the largest quantity of CO<sub>2</sub> (823 kg CO<sub>2</sub>/t clinker). The main factors leading to the different CO<sub>2</sub> footprints of the two new products were the composition and – especially – the content of calcite and dolomite. Due to the very low quantity of calcite and dolomite in the kaolinitic AWS from France, the main CO<sub>2</sub> contributor was diminished. The calcite and dolomite content of the alternative SCM from Switzerland ranged widely depending on the source but was high in all cases.

The thermal energy consumption of the alternative non-kaolinitic SCM was expected to be high due to the decarbonization of calcite, which consumes more heat (1'780 kJ/kg CaCO<sub>3</sub>) than the dehydroxylation of clay (900 kJ/kg clay). However, there was no impact on the CO<sub>2</sub> footprint of the rotary calciner. This is attributed to the use of 100 % biogenic woodchips, with zero net CO<sub>2</sub> contribution. The CO<sub>2</sub> input due to electrical energy consumption of the system was comparably low in all cases.

Compared to the produced cement mixture, the benefits of kaolinitic AWS could be profound. This could lead to a highly competitive cement with a notably low CO<sub>2</sub> contribution that is more than 50 % less than that of Portland cement (Table 6-4).

Table 6-4: Composition and net CO<sub>2</sub> contribution of the produced cement

Portland cement	Cement with kaolinitic AWS from France	Cement with alternative non-kaolinitic SCM from Switzerland
<p>■ Clinker   ■ Gypsum   ■ Limestone   ■ Kaolinitic AWS from France   ■ None kaolinitic SCM from Switzerland</p>		
<b>740 kg CO<sub>2</sub>/t Cement</b>	<b>340 kg CO<sub>2</sub>/t Cement</b>	<b>658 kg CO<sub>2</sub>/t Cement</b>

As described in Chapter 4, in Europe the norms do not currently allow high substitution rates. Hence, the use of a high content of activated kaolinitic AWS and limestone remains theoretical in nature. Other standards, such as the North American ASTM, are more flexible regarding the composition and content of SCMs. For instance, ASTM- C618 permits unlimited calcined pozzolana content (ASTM International, 2019). A new European standard (EN-197-5) allowing for higher substitution rates is currently in the approval phase and is expected for release in 2022.

## 6.5 Summary of Chapter 6

Two products were tested: AWS from France and a non-kaolinitic alternative SCM from Switzerland. They both fulfilled the cement norms in terms of early (2-d) and late (28-d) strength. Therefore, they can be considered as a potential new SCM. They might offer a good alternative to replace depleting sources of SCM such as fly ash or granulated blast furnace slag with a locally produced product from the circular economy. A few adjustments would be required in the mixture of kaolinitic AWS from France to meet the current European cement norms. Nonetheless, the potential to replace substantial amounts of clinker is considerable.

The potential to reduce the CO<sub>2</sub> footprint is significantly stronger for the kaolinitic AWS from France; this alternative could allow for the production of a cement with 50 % and above lower CO<sub>2</sub> emission than OPC. The results of the semi-industrial testing confirmed the suitability of

---

the heat-exchanging screws and the potential to design an energy-efficient and compact calcining and grinding system.



## Chapter 7: Conclusion and outlook

### 7.1 Conclusions

This thesis studies locally available waste materials currently deposited in landfills with the aim of transforming them into circular economy-based SCMs. Additionally, a new calcination methodology to thermally activate these materials was introduced and tested. The following observations and conclusions are presented in this thesis:

1. Many AWSs have suitable mineralogy and chemistry; these materials can be thermally activated to develop hydraulic, semi-hydraulic or pozzolanic (or a mixture) reaction behaviour. Within the framework of this thesis, the following SCMs were investigated:
  - a. Kaolinitic AWS with a kaolinite content of 47%;
  - b. A mixture of 77 % non-kaolinitic AWSs with a high content of calcite, 15 % DCG and 8 % RCS.
2. The tested and activated kaolinitic AWS had the highest potential to substitute substantial amounts of cement clinker. Within the framework of this research, 60% of the cement clinker was substituted by a combination of activated kaolinitic AWS, limestone and gypsum. Despite the high proportion of substitution, the compressive strength development contributed significantly to the 28-day strength performance of the prepared mortars. However, the contribution of activated kaolinitic AWS to the early compressive strength measured after 2 days was relatively weak. The early strength development was mainly supported by the cement clinker and not by the content of calcined kaolinitic AWS. Although European cement norms (EN-197-1) do not yet allow cement clinker substitution rates above 35% (CEM II/B), the tested mortars fulfilled the European Norms (EN 196-1) for strength class 42.5N, even with a 60% substitution of cement clinker.
3. A thermally activated mixture of non-kaolinitic AWSs, DCG and RCS offered less potential for substituting cement clinker than activated kaolinitic AWS. Combined with limestone and gypsum, 25% of the cement clinker was substituted. European Norms for mortar strength class 42.5R were fulfilled. The prepared mixture can be considered an SCM, and it has the advantage of converting highly contaminated materials, such as RCS and DCG, into a circular economy product. The benefit of 8% RCS and 15% DCG

in the mixture is considered from ecological and financial viewpoints. RCSs have especially been evaluated due to the high prices of CHF 200 (EUR 180) per ton in Switzerland, which can be obtained for appropriate disposal. DCG was considered mainly based on the formation of calcium sulphate (anhydrite) and the substitution of natural gypsum in the final cement product. Additionally, the calcium sulphate acts as a reaction activator, especially in latent hydraulic systems.

4. Existing state-of-the-art calcining technologies are unsuitable for drying, grinding or thermally activating materials in an ecologically friendly way, especially contaminated materials. The study has modelled and tested a new calcination methodology, with the following outcomes:
  - a. A unique screw conveyor heat exchange system was invented, which allows cooling of the newly calcined product from approximately 800 °C to approximately 250 °C. The modelled industrial application recovers approximately 10'000 MJ/h in thermal energy from cooling screws and conveys the heat via a thermal oil system to a set of drying screws. The drying screws can dry up to 17% of the moisture autonomously without adding extra heat. Semi-industrial trials have demonstrated the suitability of the equipment. Based on the results, an industrial application has been designed within this study.
  - b. A rotary calciner was designed, which was connected to an existing cement clinker kiln. The study outlines the advantages of receiving hot air (of 800°C–900°C) from the clinker kiln system, passing the air to the calciner and returning the flue gases to the cement clinker kiln system. The modelled system operates in co-current flow. The temperature of gases and material passing the kiln is maintained at approximately 800°C–850°C, and temperature peaks, which would destroy the structure of calcined clays such as metakaolin, are avoided, enhancing the product quality. The study demonstrated that the new calciner would minimally impact the overall emission of a cement factory, even when thermally processing contaminated materials. Organic emissions leaving the calciner (e.g. VOC, CO or dioxins) undergo post-combustion inside the cement clinker kiln at 850°C–1'000°C. Other potential emissions (e.g. SO<sub>2</sub>, HF and HCl) would combine with the CaO in the cement clinker kiln and are discharged via the clinker product.

- c. A ball mill grinding system was tested. The test results showed that grinding the preheated activated material was feasible. Grinding the material achieved the desired fineness of  $D_{90} < 100 \mu\text{m}$ . Potential risks of reducing the grinding efficiency, such as coating of the clay on balls and liners, were not observed. During the test, the difficult-to-grind quartz was intended to remain in the mill for complete grinding. Although the test did not conclusively demonstrate this point, it appeared that overgrinding of soft clay or lime might be preventable by a flexible aeration system to extract sufficiently ground material via the mill aeration. However, the semi-industrial tests did not confirm this dynamic, and the quartz was unintentionally evacuated as part of the aerating air flow.
5. The produced SCMs (kaolinitic and non-kaolinitic) contained iron oxide; thus, the product showed an undesired reddish colour. The colour is caused by haematite formation during calcination – and especially cooling of the product – occurring under excess oxygen. In this study, the new calcination methodology was designed to prevent haematite formation by preventing oxygen from entering the cooling screws. Furthermore, the rotary calcining system was modelled with sufficient flexibility to allow operation under either oxidizing or reducing conditions.
6. The potential to reduce the CO<sub>2</sub> footprint was strongest for the composite cement produced from kaolinitic AWS. This SCM could enable cement production with more than 50% less CO<sub>2</sub> emission than OPC. For an industrial application producing 100'000 tons per year, the CO<sub>2</sub> savings would be roughly 75'000 tons per year compared to clinker.

## 7.2 Outlook

In Germany alone, approximately 15 million tons of AWSs are deposited annually. The volume estimated for central Europe is roughly 50 million tons (in solids). Given these substantial quantities, thermally activated AWS could become a prime source of SCM. Careful mapping of the location, mineralogy and chemistry of AWS should be performed, and high-potential deposits should be identified.

Substitution rates exceeding 60% of cement clinker are feasible especially with pozzolanic AWSs and can achieve the mandatory cement strength. Further optimization potential could involve influencing the reactivity of the produced SCM by adjusting the mineral composition to achieve a well-balanced pozzolanic and hydraulic/latent hydraulic reaction. Especially the

calcination of calcite together with a sulphate component like DCG seemed to improve the reactivity of the produced SCM. Consequently, the tested none kaolinitic SCM has performed in the concrete more like a hydraulic SCM than the expected slower and less reactive latent hydraulic SCM, which could be a distinct advantage and should be investigated further.

Concerning the outlook of the investigated new method to thermally activate materials, the detailed engineering phase for a pilot installation will soon be complete. An order has been placed for construction of the pilot plant (Figure 7-1). The plant is expected to start commercial operation in the first quarter of 2023. Given the new method's potential compared to existing technologies, several projects are planned. These are expected to be realized once the pilot facility has been successfully commissioned.

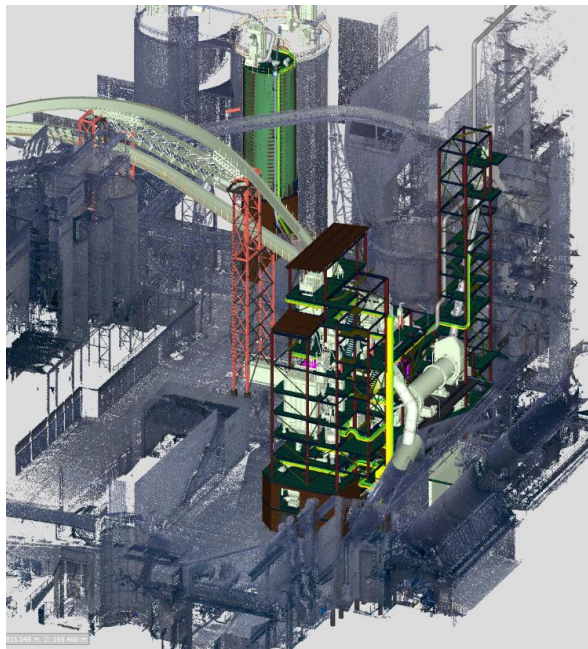


*Figure 7-1: 3D view of the pilot installation*

The full potential of the new system has not yet been exhaustively studied. The system has high flexibility for further optimizing the production capacity of SCM and clinker production. This could be interesting, especially when achieving higher rates of clinker substitution.

In terms of waste materials, AWS, DCG and RCS have been investigated in this study. Other locally available materials could be overburden from mining operations or contaminated earth. The study also only considered wood chips as fuel. Other fuels could also be investigated, such as by-products from the chemical industry, agriculture or selected municipal wastes.

Concrete will remain one of the most important construction materials. Given the increasing global demand for concrete driven by the ever-growing population and increase in living standards, the cement industry must find faster solutions to significantly reduce the emission of greenhouse gases and stop the overexploitation and depletion of natural resources. This thesis presents one solution to positively impact the ecological footprint of cement production. However, the future goal should be completely carbon neutral production, with a significant reduction in exploiting natural resources such as limestone and clay, increased recycling and a return to a circular economy of available anthropogenic material stocks (Kruspan, Bier & Weihrauch, 2022).

## Literature

- Abu El-Rub, Z., Kujawa, J., Albarahmieh, E., Al-Rifai, N., Qaimari, F., & Al-Gharabli, S. (2019). High Throughput Screening and Characterization Methods of Jordanian Oil Shale as a Case Study. *Energies*, *12*(16), 3148
- Ahmed, R., Jaafar, M. S., Bareq, M., Hejazi, F., & Rashid, R. S. (2019). Effect of supplementary cementitious material on chemical resistance of concrete. *IOP Conference Series: Earth and Environmental Science*, *357*(1), 012016. <https://doi.org/10.1088/1755-1315/357/1/012016>
- Al-Naffakh, J., & Jafar, I. (2020). Process and Impact of Combustion on Cement Oxide Minerals: An Experimental Study. *International Journal of Environment, Engineering and Education*, *2*(2), 1–8.
- Alberici, S., De Beer, J., Van Der Hoorn, I., & Staats, M. (2017). *Fly ash and blast furnace slag for cement manufacturing*. Retrieved from <https://www.econstor.eu/bitstream/10419/196207/1/2017-19-fly-ash-blast-furnace-slag-cement-manufacturing.pdf>
- Andrew, R. M. (2018). Global CO<sub>2</sub> emissions from cement production. *Earth System Science Data*, *10*(1), 195–217. <https://doi.org/10.5194/essd-10-195-2018>
- Antoni, M. (2013). *Investigation of cement substitution by blends of calcined clays and limestone*. Retrieved from [https://os.zhdk.cloud.switch.ch/tind-tmp-epfl/38f4aea1-d5a0-4e7a-b5a5-14911e741e78?response-content-disposition=attachment%3B%20filename%2A%3DUTF-8%27%27EPFL\\_TH6001.pdf&response-content-type=application%2Fpdf&AWSAccessKeyId=ded3589a13b4450889b2f728d54861a6&Expires=1641649268&Signature=chIDWQHawLnVK1FkuRIp2tqagg%3D](https://os.zhdk.cloud.switch.ch/tind-tmp-epfl/38f4aea1-d5a0-4e7a-b5a5-14911e741e78?response-content-disposition=attachment%3B%20filename%2A%3DUTF-8%27%27EPFL_TH6001.pdf&response-content-type=application%2Fpdf&AWSAccessKeyId=ded3589a13b4450889b2f728d54861a6&Expires=1641649268&Signature=chIDWQHawLnVK1FkuRIp2tqagg%3D)
- ASTM International. (2019). *The 2021–2026 World Outlook for Normal ASTM Type I Portland Hydraulic Cement*. Brisbane, Australia: ICON Group International.
- Beiser, V. (2019, November 18). Why the world is running out of sand. *BBC*. Retrieved from <https://www.bbc.com/future/article/20191108-why-the-world-is-running-out-of-sand>
- Bernal, S. A., Juenger, M. C. G., Ke, X., Matthes, W., Lothenbach, B., De Belie, N., & Provis, J. L. (2016). Characterization of supplementary cementitious materials by thermal analysis. *Materials and Structures*, *50*(1), 1–13. <https://doi.org/10.1617/s11527-016-0909-2>

- Beton.wiki. (2021). Latent-hydraulisch. Retrieved from <https://www.beton.wiki/index.php?title=Latent-hydraulisch>
- Bizzozero, J., & Scrivener, K. L. (2015). Limestone reaction in calcium aluminate cement–calcium sulfate systems. *Cement and Concrete Research*, 76(1), 159–169. <https://doi.org/10.1016/j.cemconres.2015.05.019>
- Businesswire. (2017). Global supplementary cementitious materials market by material. Retrieved from <https://www.businesswire.com/news/home/20170504006555/en/Global-Supplementary-Cementitious-Materials-Market-Projected-to-be-Worth-USD-100.6-Billion-by-2021-Technavio>
- Cahans, C. (2017). Entleeren und Wiederbefüllen der Strassenschächte. *Umwelttechnik*, 4–5.
- CEMBureau. (2020). Cementing Europe’s Future - Building the Green Deal. Retrieved from <https://cembureau.eu/events/cementing-europe-s-future-building-the-green-deal/>
- Cement. (n.d.). In *Wikipedia*. Retrieved from <https://en.wikipedia.org/wiki/Cement>
- Clay. (2020, December 27). In *Wikipedia*. Retrieved from <https://en.wikipedia.org/wiki/Clay>
- Concrete. (2021b, March 11). In *Wikipedia*. Retrieved from <https://en.wikipedia.org/wiki/Concrete>
- Criado, J. M., Ortega, A., Real, C., & De Torres, E. T. (1984). Re-examination of the kinetics of the thermal dehydroxylation of kaolinite. *Clay Minerals*, 19(4), 653–661. <https://doi.org/10.1180/claymin.1984.019.4.11>
- Daou, I., Lecomte-Nana, G., Tessier-Doyen, N., Peyratout, C., Gonon, M., & Guinebretiere, R. (2020). Probing the Dehydroxylation of Kaolinite and Halloysite by In Situ High Temperature X-ray Diffraction. *Minerals*, 10(5), 480. <https://doi.org/10.3390/min10050480>
- Díaz, A. A., Reyes, R. S. A., Carratalá, F. A., García, L. A. P., Rodríguez, C. A. L., & Hernández, J. F. M. (2020). The Experience of Cuba TRC on the Survey of Kaolinitic Clay Deposits as Source of SCMs—Main Outcomes and Learned Lessons. In S. Bishnoi (Ed.), *Calcined Clays for Sustainable Concrete* (pp. 1-8). Singapore, Singapore: Springer.
- Duda, W. H. (1985). *Cement-Data-Book*. Gütersloh, Germany: Bauverlag.

- Elmqvist, T., Bai, X., Frantzeskaki, N., Griffith, C., Maddox, D., McPhearson, T., ... Watkins, M. (2018). *Urban Planet*. Cambridge, United Kingdom: Cambridge University Press.
- Ember. (n.d.). Global Electricity. Retrieved from <https://ember-climate.org/data/global-electricity/>
- European Commission. (2019a). A European Green Deal. Retrieved from [https://ec.europa.eu/info/strategy/priorities-2019-2024/european-green-deal\\_en](https://ec.europa.eu/info/strategy/priorities-2019-2024/european-green-deal_en)
- European Commission. (2019b). *Methodology for the free allocation of emission allowance in the EU ETS post 2012*. Retrieved from [https://ec.europa.eu/clima/sites/clima/files/ets/allowances/docs/bm\\_study-cement\\_en.pdf](https://ec.europa.eu/clima/sites/clima/files/ets/allowances/docs/bm_study-cement_en.pdf)
- European Committee For Standardization. (2011). *Cement - Part 1: Composition, specifications and conformity criteria for common cements*. Retrieved from [http://www.punto-focal.gov.ar/notific\\_otros\\_miembros/mwi40\\_t.pdf](http://www.punto-focal.gov.ar/notific_otros_miembros/mwi40_t.pdf)
- Faheem, A., Rizwan, S. A., & Bier, T. A. (2021). Properties of self-compacting mortars using blends of limestone powder, fly ash, and zeolite powder. *Construction and Building Materials*, 286(1), 122788. <https://doi.org/10.1016/j.conbuildmat.2021.122788>
- Fernandez, R., Martirena, F., & Scrivener, K. L. (2011). The origin of the pozzolanic activity of calcined clay minerals: A comparison between kaolinite, illite and montmorillonite. *Cement and Concrete Research*, 41(1), 113–122. <https://doi.org/10.1016/j.cemconres.2010.09.013>
- Gallego, H., Toro, E., & Rojas, R. (2020). State of the Art: Process of Pozzolan Formation from Ash and its Applications. *Revista Ingeniería de Construcción*, 35(2), 119–125.
- Global Cement and Concrete Association. (n.d.). Burnt shale. Retrieved from <https://gccassociation.org/cement-and-concrete-innovation/clinker-substitutes/burnt-shale/>
- Ground granulated blast-furnace slag. (2021, January 22). In *Wikipedia*. Retrieved from [https://en.wikipedia.org/wiki/Ground\\_granulated\\_blast-furnace\\_slag](https://en.wikipedia.org/wiki/Ground_granulated_blast-furnace_slag)
- Gruskovnjak, A. (2006). *Hydration mechanisms of activated blast furnace slag*. Bern, Schweiz: Universität Bern.
- Hewlett, P., & Liska, M. (2019). *Lea's Chemistry of Cement and Concrete* (5<sup>th</sup> ed.). Rotterdam, Netherlands: Butterworth-Heinemann.



- IBU-tec. (2020, August). *Calcination of Clay mixtures* (2020.30.2084). Weimar, Germany: IBU-tec and Holcim.
- Ilic, B., Mitrovic, A., & Milicic, L. (2010). Thermal treatment of kaolin clay to obtain metakaolin. *Chemical Industry*, 64(4), 351–356. <https://doi.org/10.2298/hemind100322014i>
- Illustration. (2021). *VDZ*. Abgerufen von <https://www.vdz-online.de/en/services/process-technology/mechanical-process-technology>
- International Energy Agency, Cement Sustainability Initiative, & World Business Council for Sustainable Development. (2018). *Technology Roadmap Low-Carbon Transition in the Cement Industry*. Retrieved from <https://webstore.iea.org/download/direct/1008>
- Kanton Luzern. (2013). *Entsorgung von Strassenwischgut*. Retrieved from [https://uwe.lu.ch/-/media/UWE/Dokumente/publikationen/Publikationen\\_01\\_A\\_bis\\_F/Entsorgung\\_von\\_Strassenwischgut\\_neu.pdf](https://uwe.lu.ch/-/media/UWE/Dokumente/publikationen/Publikationen_01_A_bis_F/Entsorgung_von_Strassenwischgut_neu.pdf)
- Killingley, J. S., & Day, S. J. (1990). Dehydroxylation kinetics of kaolinite and montmorillonite from Queensland Tertiary oil shale deposits. *Fuel*, 69(9), 1145–1149. [https://doi.org/10.1016/0016-2361\(90\)90072-x](https://doi.org/10.1016/0016-2361(90)90072-x)
- Kiseleva, I. A., Orogodova, L. P., Krupskaya, V. V., Melchakova, L. V., Vigasina, M. F., & Luse, I. (2011). Thermodynamics of the kaolinite-group minerals. *Geochemistry International*, 49(8), 793–801. <https://doi.org/10.1134/s001670291106005x>
- Köllemann. (2020). *TEST REPORT „Drying / heating of clay“* (OC-200203). Adenau, Germany: Koellemann and Holcim.
- Konist, A., Neshumayev, D., Baird, Z. S., Anthony, E. J., Maasikmets, M., & Järvi, O. (2020). Mineral and Heavy Metal Composition of Oil Shale Ash from Oxyfuel Combustion. *ACS Omega*, 5(50), 32498–32506. <https://doi.org/10.1021/acsomega.0c04466>
- Kosmatka, S. H., Kerkhoff, B., & Panarese, W. C. (1979). *Design and Control of Concrete Mixtures* (14th ed.). Skokie, Illinois: Portland Cement Association.
- Krakow, L. (2012). *Überschussminerale - Massenabfälle oder Zukunftsrohstoffe?* Retrieved from [https://www.dr-krakow-labor.de/site/assets/files/1121/sdgg\\_heft\\_80-geohannover\\_2012\\_artikel.pdf](https://www.dr-krakow-labor.de/site/assets/files/1121/sdgg_heft_80-geohannover_2012_artikel.pdf)

- Kruspan, P., Bier, T. & Weihrauch, M. (2022). *The necessity for switching to Anthropogenic Cement Constituents ACCs: examples from industry perspective*. München, Deutschland: Thomé-Kozmiensky Verlag GmbH.
- Külaots, I., Goldfarb, J. L., & Suuberg, E. M. (2010). Characterization of Chinese, American and Estonian oil shale semicokes and their sorptive potential. *Fuel*, 89(11), 3300–3306. <https://doi.org/10.1016/j.fuel.2010.05.025>
- LafargeHolcim. (2020). Driving green construction with net zero pledge. Retrieved from <https://connect.lafargeholcim.com/global/net-zero-pledge>
- Lehne, J., & Preston, F. (2018). *Making Concrete Change: Innovation in Low-carbon Cement and Concrete*. Retrieved from <https://www.chathamhouse.org/sites/default/files/publications/research/2018-06-13-making-concrete-change-cement-lehne-preston.pdf>
- Locher, F. W. (2000). *Zement: Grundlagen der Herstellung und Verwendung*. Düsseldorf, Deutschland: Bau + Technik.
- Maheswaran, S., Iyer, N. R., Palani, G. S., Pandi, R. A., Dikar, D. D., & Kalaiselvam, S. (2015). Effect of high temperature on the properties of ternary blended cement pastes and mortars. *Journal of Thermal Analysis and Calorimetry*, 122(2), 775–786. <https://doi.org/10.1007/s10973-015-4817-4>
- Markert, S. (2021). BBC-Podcast covering LC3. Retrieved from <https://lc3.ch/>
- Martirena Hernández, J. F., Almenares-Reyes, R., Zunino, F., Alujas-Diaz, A., & Scrivener, K. L. (2020). Color control in industrial clay calcination. *RILEM Technical Letters*, 5(1), 1–7. <https://doi.org/10.21809/rilemtechlett.2020.107>
- Massazza, F. (1993). Pozzolan cements. *Cement and Concrete Composites*, 15(4), 185–214. [https://doi.org/10.1016/0958-9465\(93\)90023-3](https://doi.org/10.1016/0958-9465(93)90023-3)
- Mathieu, A. (2013). *Investigation of cement substitution by blends of calcined clays and limestone*. Retrieved from [https://os.zhdk.cloud.switch.ch/tind-tmp-epfl/38f4aea1-d5a0-4e7a-b5a5-14911e741e78?response-content-disposition=attachment%3B%20file-name%2A%3DUTF-8%27%27EPFL\\_TH6001.pdf&response-content-type=application%2Fpdf&AWSAccessKeyId=ded3589a13b4450889b2f728d54861a6&Expires=1641914481&Signature=aoyepky6hUv6z55DIJ6dfjqjRDE%3D](https://os.zhdk.cloud.switch.ch/tind-tmp-epfl/38f4aea1-d5a0-4e7a-b5a5-14911e741e78?response-content-disposition=attachment%3B%20file-name%2A%3DUTF-8%27%27EPFL_TH6001.pdf&response-content-type=application%2Fpdf&AWSAccessKeyId=ded3589a13b4450889b2f728d54861a6&Expires=1641914481&Signature=aoyepky6hUv6z55DIJ6dfjqjRDE%3D)

- Nolting, U., Dehn, F., Haist, M., & Link, J. (2018). *Betone der Zukunft - Herausforderungen und Chancen: 14. Symposium Baustoffe und Bauwerkserhaltung*. Karlsruhe, Germany: KIT Scientific Publishing.
- Ptáček, P., Frajkorová, F., Šoukal, F., & Opravil, T. (2014). Kinetics and mechanism of three stages of thermal transformation of kaolinite to metakaolinite. *Powder Technology*, 264(1), 439–445. <https://doi.org/10.1016/j.powtec.2014.05.047>
- Raado, L. M., Tuisk, T., Rosenberg, M., & Hain, T. (2011). Durability behavior of Portland burnt oil shale cement concrete. *Oil Shale*, 28(4), 507-515. <https://doi.org/10.3176/oil.2011.4.04>
- Redfern, S. A. T. (1987). The kinetics of dehydroxylation of kaolinite. *Clay Minerals*, 22(4), 447–456. <https://doi.org/10.1180/claymin.1987.022.4.08>
- Regourd, M. (1986). Microstructure of Cement Blends Including Fly Ash, Silica Fume, Slag and Fillers. *MRS Proceedings*, 86(1), 1. <https://doi.org/10.1557/proc-86-185>
- Rodgers, B. L. (2018). Climate change: The massive CO2 emitter you may not know about. Retrieved from [https://www.bbc.com/news/science-environment-46455844#:~:text=If%20the%20cement%20industry%20were,global%20agriculture%20business%20\(12%25\).&text=To%20do%20this%20C%20annual%20emissions,at%20least%2016%25%20by%202030](https://www.bbc.com/news/science-environment-46455844#:~:text=If%20the%20cement%20industry%20were,global%20agriculture%20business%20(12%25).&text=To%20do%20this%20C%20annual%20emissions,at%20least%2016%25%20by%202030)
- Rowland, R. A. (1952). Differential Thermal Analysis of Clays and Carbonates. *Clays and Clay Minerals*, 1(1), 151–163. <https://doi.org/10.1346/ccmn.1952.0010118>
- Rutkowska, G., Chalecki, M., Wichowski, P., Żwirska, J., & Barszcz, B. (2016). Influence of siliceous and calcareous fly-ashes on properties of cement mortars. *Journal of Ecological Engineering*, 17(4), 280–288. <https://doi.org/10.12911/22998993/64553>
- Sahnoune, F., Saheb, N., Khamel, B., & Takkouk, Z. (2011). Thermal analysis of dehydroxylation of Algerian kaolinite. *Journal of Thermal Analysis and Calorimetry*, 107(3), 1067–1072. <https://doi.org/10.1007/s10973-011-1622-6>
- Sakir, S., Raman, S. N., Safiuddin, M., Kaish, A. B. M. A., & Mutalib, A. A. (2020). Utilization of by-products and wastes as supplementary cementitious materials in structural mortar for sustainable construction. *Sustainability*, 12(9), 3888. <https://doi.org/10.3390/su12093888>

- Scheetz, B. E., & Russel, E. (1998). Utilization of fly ash. *Current Opinion in Solid State and Materials Science*, 3(5), 510–520. [https://doi.org/10.1016/S1359-0286\(98\)80017-X](https://doi.org/10.1016/S1359-0286(98)80017-X)
- Schmitz, M., Röhling, S., & Dohrmann, R. (2011). *In der grobkeramischen Industrie nutzbares Rohstoffpotenzial der bei Gewinnung und Aufbereitung in der deutschen Steine- und Erdenindustrie anfallenden Feinanteile*. Retrieved from [http://www.deutscherohstoffagentur.de/DE/Gemeinsames/Produkte/Downloads/DERA\\_Rohstoffinformationen/rohstoffinformationen-05.pdf?\\_\\_blob=publicationFile&v=14](http://www.deutscherohstoffagentur.de/DE/Gemeinsames/Produkte/Downloads/DERA_Rohstoffinformationen/rohstoffinformationen-05.pdf?__blob=publicationFile&v=14)
- Scrivener, K. L., John, V. M., & Gartner, E. M. (2018). Eco-efficient cements: Potential economically viable solutions for a low-CO<sub>2</sub> cement-based materials industry. *Cement and Concrete Research*, 114(1), 2–26. <https://doi.org/10.1016/j.cemconres.2018.03.015>
- Scrivener, K., Martirena, F., Bishnoi, S., & Maity, S. (2018). Calcined clay limestone cements (LC3). *Cement and Concrete Research*, 114(1), 49–56. <https://doi.org/10.1016/j.cemconres.2017.08.017>
- Scrivener, K., Zunino, F., Avet, F., & Hangpongpun, W. (2018). *LC3: a promising alternative*. Retrieved from <https://lc3.ch/wp-content/uploads/2020/11/ICR30-KEYNOTE-EPFL-Limestone-Clay-cements.pdf>
- Shehu, I., & Awal, A. A. (2012). Mechanical properties of concrete incorporating high volume palm oil fuel ash. *Advanced Materials Research*, 599(1), 537–540. <https://doi.org/10.4028/www.scientific.net/amr.599.537>
- Sluis, M. (2012). Granite. Retrieved from <https://www.slideshare.net/martinyluis/granite-13073987>
- Snellings, R. (2016). Assessing, Understanding and Unlocking Supplementary Cementitious Materials. *RILEM Technical Letters*, 1(1), 50-55. <https://doi.org/10.21809/rilemtechlett.2016.12>
- Snellings, R., Mertens, G., & Elsen, J. (2012). Supplementary Cementitious Materials. *Reviews in Mineralogy and Geochemistry*, 74(1), 211–278. <https://doi.org/10.2138/rmg.2012.74.6>
- Statista. (2021). Gipsplatten - Produktion in Deutschland bis 2020. Retrieved from <https://de.statista.com/statistik/daten/studie/589581/umfrage/produktion-von-gipsplatten-in-deutschland/>

- Stoch, L., & Waclawska, I. (1981). Dehydroxylation of kaolinite group minerals. *Journal of Thermal Analysis*, 20(2), 291–304. <https://doi.org/10.1007/bf01912877>
- U.S. Environmental Protection Agency. (2015). *Emissions Control of Hydrochloric and Fluorhydric Acid in cement Factories from Romania* [Datensatz]. Retrieved from <https://www.epa.gov/stationary-sources-air-pollution/clay-ceramics-manufacturing-national-emission-standards-hazardous>
- USGS. (n.d.). Environmental Characteristics of Clays and Clay Mineral Deposits. Retrieved from <https://pubs.usgs.gov/info/clays/>
- Varga, G. (2007). The structure of kaolinite and metakaolinite. *Epitoanyag - Journal of Silicate Based and Composite Materials*, 59(1), 6–9. <https://doi.org/10.14382/epitoanyag-jsbcm.2007.2>
- Voicu, G., Ciobanu, C., Istrate, I. A., & Tudor, P. (2020). Emissions Control of Hydrochloric and Fluorhydric Acid in cement Factories from Romania. *International Journal of Environmental Research and Public Health*, 17(3), 1–12. <https://doi.org/10.3390/ijerph17031019>
- Wang, H., Li, C., Peng, Z., & Zhang, S. (2011). Characterization and thermal behavior of kaolin. *Journal of Thermal Analysis and Calorimetry*, 105(1), 157–160. <https://doi.org/10.1007/s10973-011-1385-0>
- Wang, Q., Hou, Y., Wu, W., Liu, Q., & Liu, Z. (2018). The structural characteristics of kerogens in oil shale with different density grades. *Fuel*, 219(1), 151–158. <https://doi.org/10.1016/j.fuel.2018.01.079>
- Weihrauch, M., Bucher, E., Kruspan, P., Blum, R., & Spuler, A. (2021). WO2021/124261. Retrieved from <https://patentscope.wipo.int/search/fr/detail.jsf?docId=WO2021124261>
- Weimann, K., Adam, C., Buchert, M., & Sutter, J. (2021). Environmental Evaluation of Gypsum Plasterboard Recycling. *Minerals*, 11(2), 101. <https://doi.org/10.3390/min11020101>
- Wells, L. S., & Carlson, E. T. (1956). Hydration of aluminous cements and its relation to the phase equilibria in the system lime-alumina-water. *Journal of Research of the National Bureau of Standards*, 57(6), 335. <https://doi.org/10.6028/jres.057.037>

- World Cement. (2015). Challenging mercury: Emission limits and measures. Retrieved from <https://www.worldcement.com/europe-cis/13042015/challenging-mercury-emission-limits-and-measures-671/>
- Wright, F. E., & Rankin, G. A. (1915). The ternary system CaO-Al<sub>2</sub>O<sub>3</sub>-SiO<sub>2</sub>. *American Journal of Science*, 229(1), 1–79. <https://doi.org/10.2475/ajs.s4-39.229.1>
- Zareei, S. A., Ameri, F., Dorostkar, F., & Ahmadi, M. (2017). Rice husk ash as a partial replacement of cement in high strength concrete containing micro silica: Evaluating durability and mechanical properties. *Case Studies in Construction Materials*, 7(1), 73–81. <https://doi.org/10.1016/j.cscm.2017.05.001>
- Žemlička, M., Kuzielová, E., Kuliffayová, M., Tkacz, J., & Palou, M. (2015). Study of hydration products in the model systems metakaolin–lime and metakaolin–lime–gypsum. *Ceramics – Silikáty*, 59(4), 283–291.
- Zhou, Y., Liu, Q., Xu, P., Cheng, H., & Liu, Q. (2018). Molecular Structure and Decomposition Kinetics of Kaolinite/Alkylamine Intercalation Compounds. *Frontiers in Chemistry*, 6(1), 310. <https://doi.org/10.3389/fchem.2018.00310>
- Zunino, F., & Scrivener, K. (2021). The reaction between metakaolin and limestone and its effect in porosity refinement and mechanical properties. *Cement and Concrete Research*, 140(1), 106307. <https://doi.org/10.1016/j.cemconres.2020.106307>
- Zuo, X., Wang, D., Zhang, S., Liu, Q., & Yang, H. (2017). Effect of Intercalation Agents on Morphology of Exfoliated Kaolinite. *Minerals*, 7(12), 249. <https://doi.org/10.3390/min7120249>